Tribological Evaluation of Compressor Contacts - Retrofitting and Materials Studies

T. K. Sheiretov and C. Cusano

ACRC TR-46 July 1993

For additional information:

Air Conditioning and Refrigeration Center
University of Illinois
Mechanical & Industrial Engineering Dept.
1206 West Green Street
Urbana, IL 61801

(217) 333-3115

Prepared as part of ACRC Project 4
Compressor--Lubrication, Friction, and Wear
C. Cusano, Principal Investigator

The Air Conditioning and Refrigeration Center was founded in 1988 with a grant from the estate of Richard W. Kritzer, the founder of Peerless of America Inc. A State of Illinois Technology Challenge Grant helped build the laboratory facilities. The ACRC receives continuing support from the Richard W. Kritzer Endowment and the National Science Foundation. The following organizations have also become sponsors of the Center.

Acustar Division of Chrysler
Allied-Signal, Inc.
Amana Refrigeration, Inc.
Carrier Corporation
Caterpillar, Inc.
E. I. du Pont de Nemours & Co.
Electric Power Research Institute
Ford Motor Company
General Electric Company
Harrison Division of GM
ICI Americas, Inc.
Johnson Controls, Inc.
Modine Manufacturing Co.
Peerless of America, Inc.
Environmental Protection Agency
U. S. Army CERL
Whirlpool Corporation

For additional information:

Air Conditioning & Refrigeration Center
Mechanical & Industrial Engineering Dept.
University of Illinois
1206 West Green Street
Urbana IL 61801

217 333 3115

ABSTRACT

The effect of 3-5% R12 and 20% mineral or alkylbenzene oil on the tribological behavior of R134a-polyolester or polyalkylene glycol oil mixtures in conditions simulating critical contact pairs in rolling piston and swash plate compressors is evaluated. The small residual amounts of R12-oil mixture tends to improve the friction and wear results. The improvement is small and is considered negligible.

Various grades of polyimide and poly(amide-imide) polymers are tested in area contact conditions. Tests with various environments, temperatures, contact pressures, sliding velocities and counterface material characteristics are conducted. Pressure and velocity limits for conditions simulating the critical contact in a swash plate compressor are obtained. Data for a broad range of operating conditions are generated. The refrigerant environment did not significantly change the tribological characteristics of the polymers studied. It is shown that the major limiting factor to their application is the temperature rise in the sliding interface.

Tribological characteristics of various surface treatments for M2 tool steel tested in a concentrated contact conditions and R134a-polyolester oil environment are obtained. Gas, ion, and liquid nitrided, as well as boronized, and TiN coated specimens are tested. Significant increase in the wear resistance is observed with the TiN coating only. All the other processes did not seem to offer any tribological advantages over hardened M2 tool steel.

All the tests are performed on a specially designed high pressure tribometer. It is capable of simulating a broad range of operating conditions and contact geometries. A new data acquisition system for the tribometer, capable of continuous monitoring of the test parameters is introduced.

TABLE OF CONTENTS

CHAPTER 1

Introduction

1.1 Overview

Though not rigorously proven, there are numerous studies which indicate that the chlorine containing hydrocarbons are one of the major factors that cause the observed depletion of the ozone layer. International treaties already require that the production of such chemical compounds be radically decreased in the near future. Some of the most common commercial refrigerants (CFC's) belong to this group of compounds. The required decrease in their production has forced the refrigeration and air-conditioning companies to look for replacement refrigerants with thermodynamic properties similar to those of the CFC's.

There are additional requirements for some of the replacement refrigerants. For those intended to operate in small refrigerators and air conditioners, their miscibility with lubricants and their tribological characteristics are among the most important. These characteristics are essential for an extended operational life of the compressor.

The most common refrigerant currently used in home refrigerators and automotive air conditioners is R12 (dichlorodifluoromethane). This refrigerant will be replaced in the very near future by R134a (tetrafluoroethane). R134a is not miscible with the mineral and alkylbenzene oils, lubricants presently used with R12. R134a is miscible, however, with special synthetic lubricants such as the polyolester and polyalkylene glycol oils. The tribological properties of R12-oil mixtures, however, are generally not matched by base polyolester and polyalkylene glycol oils. The reason for this is that R12 is a good lubricant by itself and enhances the performance of the oil, while R134a does not seem to posses any lubricative properties. This effect is even more pronounced for contacts which may be only marginally lubricated, or contacts in which the boundary lubrication regime prevails.

When using R134a, synthetic oils with additive packages and better tribocontact material properties are probably the most promising ways to solve expected tribological problems. The latter constituted the major part of this study. Polymers capable of operating at high interface temperature and possessing self-lubricating properties were evaluated as prospective materials for area contacts. Hard surface coatings for M2 tool steel were also studied in concentrated contact conditions. In addition, the effect of residual amounts of R12/oil mixture on the tribological behavior of R134a/oil mixture was evaluated.

1.2 Scope of Research

This research was conducted as a part of a larger project which involves the study of various tribological problems arising from the replacement of the currently used refrigerants by ozone-safe refrigerants. The project is sponsored by the ACRC, an industry-university cooperative research center which performs research on refrigerant and air conditioning systems. This study is a continuation of a previous work which treated similar problems. Results from previous studies were extensively used throughout this work. A summary of these results is given below.

1.2.1 Summary of Previous Research

The major accomplishments of previous research are as follows:

• An experimental facility has been developed to test the friction and wear characteristics of oil/refrigerant mixtures. A high pressure tribometer has been designed to permit specimen testing in pressurized refrigerant environment of up to 250 psig and in a wide range of temperatures. The high pressure tribometer has been outfitted with various apparatuses for charging, purging, sampling, and continuous tribological data acquisition by a computer controlled system.

• The critical tribo-contacts for rolling piston, swash plate and reciprocating piston compressors have been identified. The appropriate operating conditions of these contacts have been defined and simulated in the high pressure tribometer. The simulation includes the following parameters: refrigerant vapor pressure, interface temperature, contact pressure, sliding velocity and type of motion, contact geometry, contact pair materials and surface characteristics and type of lubricant.

• Baseline data for mineral oils and alkylbenzenes with refrigerant R12 have been obtained. These data have shown that this refrigerant has good lubricative properties by itself. XPS analysis on the worn surfaces shows the formation of metallic chlorides which aid the lubricative process and protect the surfaces.

• Comparative tests for R134a and various polyolester and polyalkylene glycol oils have also been completed for the same contacts and conditions as the baseline tests. In general, these tests show worse wear results than the baseline tests. XPS analysis shows no surface films produced on the surfaces of the specimens. It has been concluded that R134a does not posses any lubricative properties.

• There is no clear relationship between friction and wear, and each property must be evaluated separately. Refrigerant-oil combinations which produced the least amount of wear on the specimens sometimes produced the highest friction coefficient.

1.2.2 Research Outline

The research performed in this work covers specific problems of interest to the project sponsors. The study is divided into three major sections presented in chapters 2, 3, and 4. In addition, information about the data acquisition system used for this study is given in Chapter 5.

Chapter 2 deals with the tribological problems arising in retrofitted compressors. The effect of small residual amounts of the old R12-oil mixture on the substituted R134a-oil mixture for various contacts and test conditions is evaluated.

In Chapter 3, the tribological properties of several grades of high temperature polymers is evaluated. These polymers are viewed as candidate materials for area contact applications.

The tribological evaluation of various surface treatments for M2 tool steel tested in R134a-oil environment is presented in Chapter 4. These surface treatments were expected to provide better wear resistance for heavily loaded concentrated contacts, similar to the critical contact in a rolling piston compressor.

In Chapter 5, the upgrading of the test facility data acquisition system is described.

1.3 Measurement Procedures

Some measurement techniques were extensively used in this study. They followed the same procedures regardless of the particular test conditions and materials of the specimens. These were the surface roughness and hardness measurements, weight loss, and wear scar measurements.

1.3.1 Surface Roughness Measurements

Surface roughness of contacting bodies is one of the important tribological characteristics. Roughness data for various surfaces are presented throughout this study. All the surface roughness measurements followed the procedure given below.

All the measurements were made with the DEKTAK stylus surface profiler. Load of 40 mg and 10 mg on the stylus were used for the metal and the polymer specimens, respectively.

Traces were always taken perpendicular to the characteristic machining marks. Each surface roughness value was obtained as an average of four measurements taken at four locations on the plate, approximately equidistant from each other (Fig. 1.1).

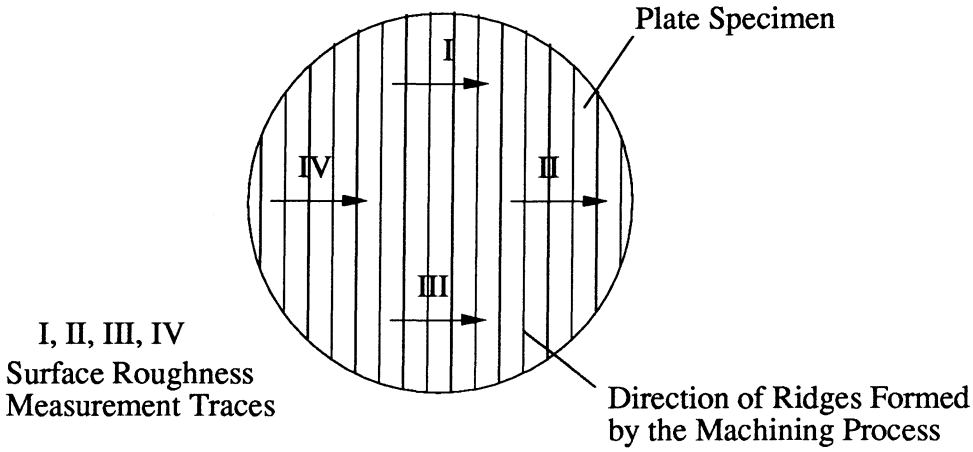

Fig. 1.1 Schematics of the Surface Roughness Measurements

One of the most important parameters that has to be defined when measuring the surface roughness is the cut-off length (trace length). The accuracy of the measurement and the repeatability of results depend strongly on this parameter. It is a common practice to choose a cut-off length one to three times larger than the characteristic peak spacing of the surface in the direction of the traverse. The peak spacing usually produced by common production processes are given in Table 1.1. These data were used to determine the cut-off lengths for the surface roughness measurements.

Table 1.1 - Peak Spacings for some Common Material Removal Processes

Production Process	Average Roughness, μm Ra	Range of Peak Spacing Often Produced, mm				
		0.08	0.25	0.8	2.5	8.0
Super Finishing	0.05 - 0.2	√	√	√		
Lapping	0.05 - 0.4	√	√	√		
Honing	0.1 - 0.8		√	√		
Grinding	0.1 - 1.6		√	√	√	
Diamond Turning	0.1 - 0.4		√	√		
Turning	0.4 - 6.3			√		
Boring	0.4 - 6.3			√	√	√

For most of the cases, the surfaces of the specimens were ground and had surface roughnesses in the range 0.05 - 0.4 μm Ra. Therefore, a cut-off distance of 0.8 mm (800 μm) was used for most of the measurements.

1.3.2 Wear Scar Measurement and Wear Volume Calculations

The width of the wear scar was measured with a Nikon SMZ-2T stereoscopic optical microscope. This width could be obtained with an accuracy of 0.0078 mm, which corresponds to a single division on the measuring scale of the microscope at its highest magnification. The average width of the scar was determined by taking five measurements along the length of the pin.

The geometry shown in Fig. 1.2 was used to calculate the volumetric wear.

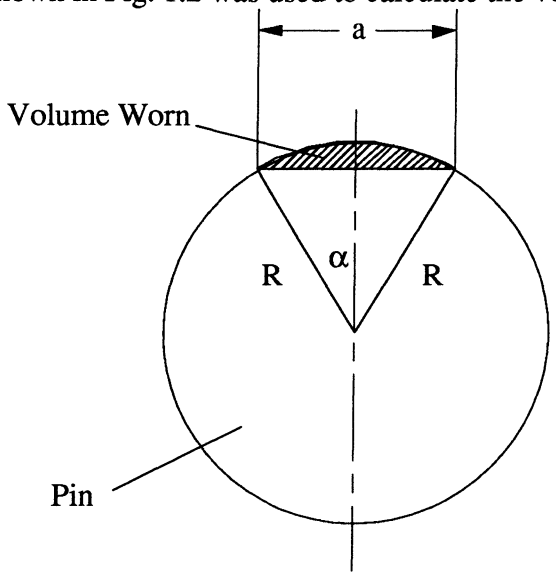

Fig. 1.2 - Geometry Used to Calculate the Volume Worn

The volume worn was calculated according to the following formulae:

$$\alpha = 2\arcsin\frac{a}{2R}, \text{ and}$$

$$V = \frac{1}{2}lR\left(\alpha R - a\cos\frac{\alpha}{2}\right),$$

where l is the length of the pin, V is the volume worn, a is the width of the wear scar and R is the pin radius.

1.3.3 Surface Hardness and Weight Measurements

The surface hardness was measured according to the existing standard procedures. All the surface hardness values presented in this study are average values of three separate measurements.

The weight of the specimens was measured with an analytic balance. The accuracy of the measurements was 0.00001 g. The weight of the specimen was obtained by averaging at least two measurement readings.

CHAPTER 2

Simulative Friction and Wear Study of Retrofitted Swash Plate and Rolling Piston Compressors

2.1 Introduction

The production of dichlorofluoromethane (R12) will cease in the near future. Many air conditioning and refrigeration systems, however, will continue to operate with R12 for many years to come. If the refrigerant in these systems must be changed for reasons such as leakage or maintenance, then the old R12-oil mixture will probably be replaced by a tetrafluoroetane (R134a)-oil mixture. Upon removing the R12-oil mixture, some residual amounts of both the R12 and the oil may remain in the system and may influence the tribological properties of the substituted R134a-oil mixture. Therefore, the goal of this study was to evaluate the tribological properties of small residual amounts of R12-oil mixtures in R134a-oil mixtures.

The tribological properties of the oil-refrigerant mixtures of interest were evaluated by testing specimens in a high pressure tribometer. A complete description of the high pressure tribometer capabilities, the experimental method used, and the test procedures are given in [1] and [2]. For the contacts studied, the operating conditions, materials, and lubricants are also the same as those used in [1] and [2]. The geometry amd materials of the specimens are representative of the geometry and the materials of the critical tribo-contacts found in real compressors. The operating and environmental conditions such as load, speed, pressure, and temperature were also approximately simulated.

Two contact geometries were simulated in this study. One was a vane-piston contact in a rolling piston compressor used in home refrigerators, and the other a shoe-plate contact in a swash plate compressor used in automotive air conditioners. The tribological behavior of pure R134a-oil mixtures were compared to mixtures containing a small amount of residual R12-based mixture. For each contact geometry, tests with both base and formulated versions of the lubricant were conducted. Since, in practice, the tribological contacts of interest have been operated in a R12 environment for a certain period of time, it is expected that some changes of the contact surface properties have occurred. In order to simulate this condition, consecutive tests were conducted on the same materials contact pairs, the first with a R12-oil mixture and the second with a R134a-oil mixture. Note that, in this case, the second test was conducted on an already

worn surface. Tests on a virgin surface were run as well. Higher accuracy of the wear measurements could be achieved when using virgin surfaces.

2.2 Description of the Tests Conducted

2.2.1 Counterformal Contact (Vane-Piston Contact in a Rolling Piston Compressor)

The critical contact in rolling piston compressors is between the vane and the piston. This is a Hertzian contact between two cylindrical surfaces. It is simulated by a contact between a cylindrical pin and a flat disc. The pin has an equivalent diameter such that the contact stresses are the same as in the real vane-piston contact. More information on the pin and disc contact geometry, and pin diameter derivation is given elsewhere [2].

All the test conditions and specimen material properties were kept the same as in our previous studies [1]. The pin, corresponding to the vane in the real compressor, was made from hardened M2 tool steel, while the plate was a hardened gray cast iron. The relevant geometrical and material data for the model are shown in Table 2.1. Test operating conditions are given in Table 2.2. The test duration was chosen such that easily measurable wear could be obtained. The duration of the tests was one hour.

Table 2.1 - Contact Geometries and Materials

Description	Counterformal contact	Area contact
Geometry:		
- Upper specimen	3 in. ∅, Flat disk	3 in. ∅, Flat disk
- Lower specimen	0.25 in. ∅, Pin Length = 0.375 in.	0.2 in. ∅, Flat shoe
Materials:		
- Upper specimen	Gray Cast Iron	Ductile Cast Iron
- Lower specimen	M2 Tool Steel	Si Pb Bronze
Average Hardness:		
- Upper specimen	550 HV (53 RC)	426 HV (38 RC)
- Lower specimen	840 HV (65 RC)	----
Surface topography:		
- Upper specimen	Ground	Ground
- Lower specimen	Ground	Lapped
Average Surface Finish:		
- Upper specimen	0.13 μm Ra	0.13 μm Ra
- Lower specimen	0.28 μm Ra	0.21 μm Ra

Table 2.2 - Operating Conditions

Operating Conditions	Counterformal Contact	Area Contact
Max. Contact Pressure, psi	150,000	18,000
Type of Motion	Oscillatory	Unidirectional
Speed, fpm	± 100 max.	100
Angular Amplitude	± 50°	---
Angular Frequency	5 Hz	---
Env. Pressure, psig	225	25
Env. Temperature, °F	177	245

For the counterformal contact, the oil-refrigerant mixtures under study were:

1) R12 + alkylbenzene oil
2) R134a + base polyolester oil
3) R134a + formulated polyolester oil
4) R134a + base polyolester oil + residual amounts of R12 and alkylbenzene oil.
5) R134a + formulated polyolester oil + residual amounts of R12 and alkylbenzene oil.

Data on the oils used are given in Table 2.3. The polyolester oil is designated as Ester base for the base version, and Ester form for the formulated version. The alkylbenzene oil used was a base oil, designated as Alkylbenz in Table 2.3.

Table 2.3 - Lubricant Data

Oil	Oil Type	Family *	Additives	Viscosity	
				@ 40°C	@ 100°C
Mineral	Mineral Oil	---	No	102	11.12
Alkylbenz	Alkylbenzene	---	No	57	5.8
PAG base	Polyalkylene glycol	Mono	No	135	25
PAG form	Polyalkylene glycol	Mono	Yes	135	25
Ester base	Polyolester	PE	No	23.94	4.88
Ester form	Polyolester	PE	Yes	23.9	4.87
* PE - Pentaerythritol ester; Mono - Monoether					

The R12-oil residue was added to the R134a-oil mixture by the following procedure:

1) A known amount of polyolester oil was supplied to the cup of the tribometer.
2) 20% by weight of alkylbenzene oil was added to the cup.
3) The chamber was charged with R134a refrigerant. The amount of the gas supplied was determined by measuring the weight of the pressure vessel before and after charging.
4) One to five percent by weight of R12 refrigerant was supplied to the chamber from another pressure vessel.

The amount of residual R12 used reflects the fact that almost all of it will escape when the system is refilled. There were some difficulties in supplying such a small quantity of R12 to the chamber. The amount of R134a refrigerant, necessary to maintain a pressure of 225 psi at 177°F in the chamber, was about 200g. Hence, 1% by weight of R12 in the mixture was only 2g. The weight of the pressure vessel itself from which the R12 was supplied was approximately 3000g, i.e. much heavier than the 2g of R12 needed in the chamber. The charging procedure is a dynamic process which makes the monitoring of the weight change difficult. We were able to monitor the weight loss of the vessel with an accuracy of 0.1%, or about 3g. The process of charging continued to the point when approximately 5-6g change in the pressure vessel weight was observed. This corresponded to a range of one to five percent of R12 in R134a. The amount of R12 was double checked by monitoring the change in the chamber pressure. Two hundred grams of R134a at a temperature of 177°F charged in the chamber led to a pressure rise of 220 psig. The additional amount of R12 increased the pressure to the 225 psig at which the tests were conducted.

The amount of alkylbenzene oil used was 20%, since it is expected that a significant quantity of the previously used oil may remain in the system. This amount of oil has been suggested as an extreme but still possible amount of old lubricant that can remain in the system.

Tests were conducted on both virgin materials contact pairs as well as on contact pairs which had already been tested using R12-oil mixtures. The latter tests were conducted to more accurately simulate actual compressor operation, including the possibility of the existence of surface protective films due to a chemical reaction between R12 and the metal surface. These films may continue to protect the surface even after the R12 has been replaced by another refrigerant. For this test series, the first test was conducted with a R12-alkylbenzene oil mixture, which simulated the operation of the compressor before the refill. Next, another test with a R134a-oil mixture, either with or without residual amount of R12-oil mixture, was conducted on the same set of specimens.

Tests conducted on virgin surfaces with R134a-oil mixtures give results that are easier to compare because the initial surface conditions are the same for each test. On the other hand, for tests conducted to simulate retrofitting conditions, i.e. R134a-oil mixture tests following R12-oil mixture tests, the surfaces are already worn when the R134a-oil mixture is tested, and therefore surface topography, as well as contact pressure distribution might be significantly different for the two pairs of tests. Such differences however can also be expected when a compressor is retrofitted with a new refrigerant-oil mixture after being in operation for a long period of time.

All the tests followed the same procedure which is covered more extensively elsewhere [2]. Each test was one hour long, and each test was repeated at least twice with some repeated three times in order to get better reliability of the data. The operating conditions for all the tests were the same.

2.2.2 Area Contact (Shoe-Plate Contact in a Swash Plate Compressor)

The critical contact in the swash plate compressor is that between the shoe and the plate. The equivalent geometry used in each test was the same. The area contact was made up of a bronze shoe, loaded by a steel ball to permit the same degrees of freedom found in the actual compressor, sliding against a flat ductile cast iron plate. Table 2.1 gives the geometry, material and surface conditions used in modeling the area contact. The operating conditions given in Table 2.2 do not completely simulate conditions in the actual compressor. When the area contact was run at pressures equivalent to those in the real compressor, even relatively low speeds caused hydrodynamic liftoff. In order to avoid the liftoff and generate measurable wear, it was necessary to increase the pressure and decrease the speed relative to compressors operation. Hence the contact pressure on the specimen was increased from 1000 psi which is a typical average contact pressure in a real compressor to 18,000 psi, while the sliding velocity was decreased from 2400 to 100 fpm. Hence the contact was operated at a PV = 100,000 psi•fpm instead of the 2,400,000 psi•fpm in the real machine. These conditions, however were more severe from a tribological point of view because in most of the cases, boundary lubrication of the contacts prevailed, while the lubrication regime in the real machine is probably hydrodynamic or mixed most of the time.

For the area contact, the oil-refrigerant mixtures under study were:

1) R12 + mineral oil
2) R134a + base PAG oil
3) R134a + formulated PAG oil
4) R134a + base PAG oil + residual amounts of R12 and mineral oil.
5) R134a + formulated PAG oil + residual amounts of R12 and mineral oil.

PAG (Polyalkaline glycol) oil properties are given in Table 2.3 under the designation PAG base, or PAG form for the base and the formulated versions of the oil, respectively. The oil used as a component of the residual mixture was mineral oil, designated as Mineral in Table 2.3. The mixtures were prepared the same way as for the rolling piston tests.

Most of the tests were run on virgin surfaces. Some tests were run on previously tested specimens lubricated by a R12-mineral oil mixture. However, these specimens tend to mutually polish their mating surfaces to a "mirror finish", and no measurable wear could be obtained in the subsequent tests on the same specimens. Therefore, data from these tests are not presented. Most of the tests were one hour long. Some longer tests were also conducted in order to verify the expected chemical degradation of the PAG oils in the presence of R12. Such degradation could produce HCl (hydrochloric acid) , which would have detrimental effects on the operation of the system. To check for HCl production, a 14 hour test was run, and samples were taken every two hours. Part of the oil sample was shaken with water and the aqueous solution was then studied with pH paper and $AgNO_3$ for the presence of HCl. However, no increase in the acidity was found. Samples were also sent to Caterpillar Oil Testing Laboratory to be tested for their acid numbers, applying a standard ASTM D664 procedure. The results from this test indicated that no acidity change occurred in the PAG base oil. Throughout the test, the acid number remained constant and equal to 0.2. However, it is possible that the duration of these tests was too short to produce oil degradation.

2.3 Data Acquisition

2.3.1 Counterformal Contact (Rolling Piston Compressor)

In addition to the friction coefficient and wear measurements, which were of prime interest, the roughness and hardness of the lower specimen (cast iron plate) were also measured for each test. The last two measurements were conducted in order to check the possibility that some other factors other than type of oil and refrigerant might affect the test results. The data acquisition is described below:

1) The friction coefficient, specimen and chamber temperatures, forces and moments acting on specimens were monitored and recorded continuously throughout the test using a computer data acquisition system (see Chapter 5). The friction coefficient reported was the average value of the friction coefficient data points throughout the test. For this particular contact, the friction coefficient remained almost constant with a slight tendency to decrease as the test proceeded.

2) The amount of wear was evaluated by measuring the width of the wear scar on the upper specimen (M2 tool steel pin) by means of an optical microscope. The accuracy of these measurements was determined by the value of a single division on the microscope measuring

scale at the highest magnification. This value is 0.0078 mm (3.07×10^{-4} in.). The average scar width was about 0.2 mm. Therefore, the width of the wear scar could be measured with an error that did not exceed 3.9%. A typical wear scar appearance is shown in Figure 2.1. The width of the wear scar varied slightly along the length of the specimen by 1-5 divisions (0.0078-0.039 mm) due to speed variations along the pin. The value reported in this case was the mean of five measurements along the length of the specimen. In some cases, the error in these measurements might increase by a few percent due to the irregularity of the wear scar boundaries.

The volume worn can be calculated on the basis of the wear scar width using simple geometry. Since the volume worn is a strongly nonlinear function of the wear scar (cubic), the measurement error may accumulate and reach unacceptable values. Therefore, the reported values for the average volume worn were obtained by processing the average value of the wear scar widths, rather than averaging the wear volumes obtained from each test. This averaging technique works for tests conducted on virgin surfaces only. For the tests run on a previously worn surface, the only way to obtain the volume of the material worn during the second test is to subtract the volume worn during the first test from the total volume worn. Since here we had to work with volumes rather than with wear scar widths, it was expected that the results for the tests conducted on a previously worn surface would be less accurate.

Wear on the mating cast iron plates was observed as well. However, the depth of the wear scar obtained was small and was difficult to measure. Therefore, it was not used for quantitative assessment of the amount of wear.

3) The surface roughness was obtained using a DEKTAK stylus type profilometer.

4) The surface hardness was obtained using the Vickers micro-hardness testing machine.

2.3.2 Area Contact (Swash Plate Compressor)

Friction coefficient, wear, plate hardness and surface roughness of both specimens were obtained. In addition to these measurements, the surface of the bronze shoe specimens was studied for the presence of surface films using XPS (x-ray photoelectron spectroscopy) and SEM (scanning electron microscopy). Since some of our previous studies [1] indicated the formation of protective chlorine-based and fluorine-based films on the metal surfaces when the contact is operated in an R12 environment, the aim of the current analysis was to reveal how these films behave when R12 is replaced by R134a. Three different specimens were analyzed using XPS. The first specimen was tested in a R12-mineral oil mixture. The second and the third specimens were first tested in a R12-mineral oil mixture, and were then tested again in a R134a-PAG oil mixture with and without R12-mineral oil residue.

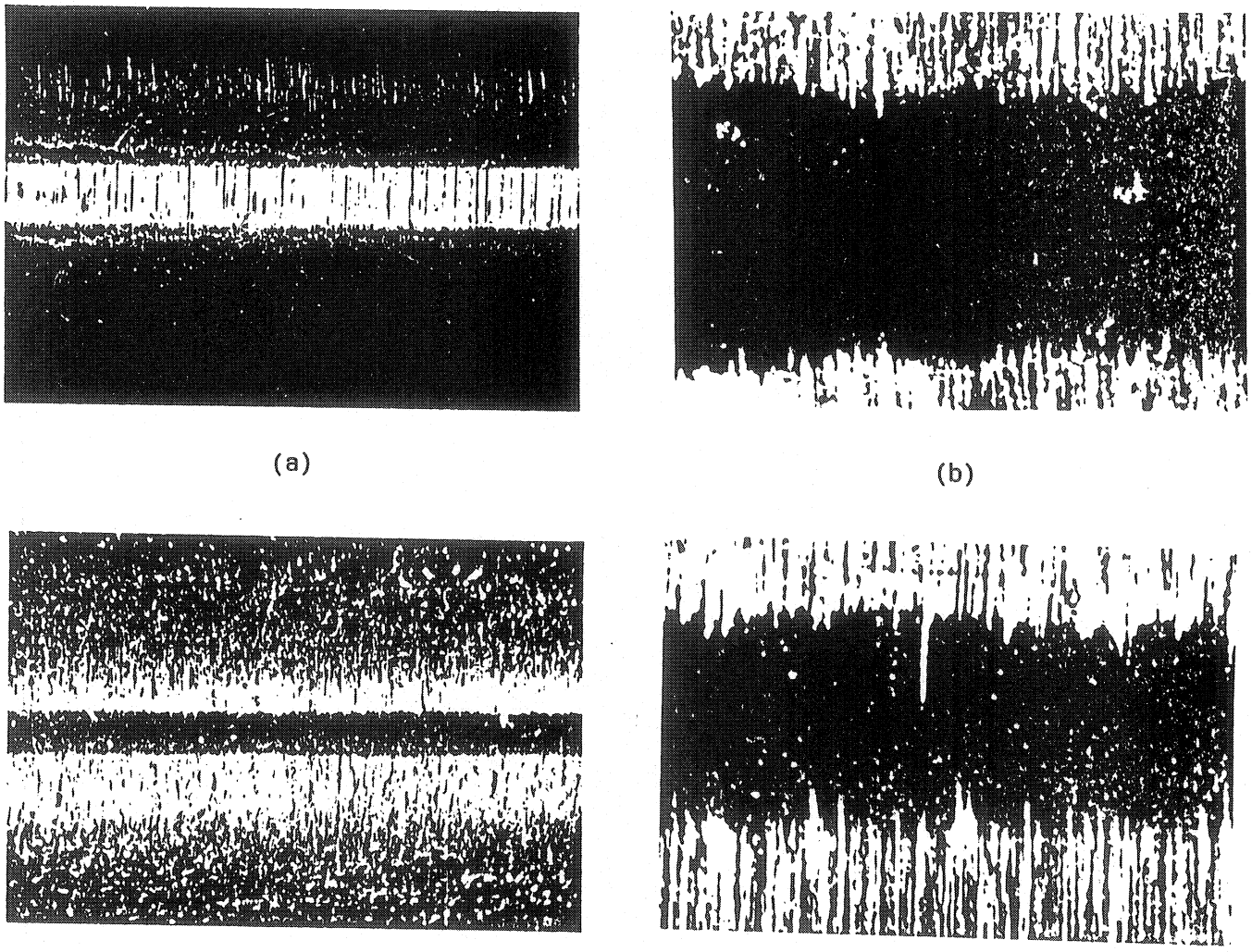

Fig. 2.1-Typical Wear Scars on the M2 Tool Steel Pin:
(a) Test 86RL at Magnification 10x, (b) Test 37RL at Magnification 63x
(c) Test 89RL at Magnification 10x, (c) Test 91RL at Magnification 63x.

The acidity of the oils during the tests involving a mixture of R12 with a PAG oil was also measured. This was done by shaking the oil samples with water and testing the aqueous solution obtained for the presence of HCl. Standard ASTM D664 test for oil acid number was applied as well.

All other measurements were made according to the following procedures:

1) The value for the friction coefficient was obtained in the same way as for the counterformal contact. The records of friction coefficient changes during the test were used not only to compute the mean coefficient of friction value, but also to monitor the type of lubrication regime. In addition, the load on the specimen was monitored by means of the data acquisition system. The load data were used to evaluate the possible effect of dynamic loads on the regime of lubrication.

2) The amount of wear was determined by measuring the weight of the bronze shoe specimens before and after the tests. The reported values for the wear are in mg. The accuracy of the measurements was 0.01 mg. No wear was detected on the mating cast iron plate specimens. On the contrary, some transfer of material from the shoe to the plate was observed.

3) The surface profiles of the bronze shoe specimens were measured using the DEKTAK profilometer.

4) The surface roughness and the hardness of the plates were measured in the same way as for the counterformal contact tests.

2.4 Results and Discussion

2.4.1 Counterformal Contact

The rolling piston tests gave comparatively small scatter of data; therefore, good repeatability of the results was obtained. Table 2.4 gives the results for the rolling piston test conducted on virgin surfaces. The highlighted numbers are the mean values of the data in the column above them. The only exception is the value for the volume worn which is obtained on the basis of the average scar width. The tests designated by an "*" represent data obtained in some previous studies [2]. From the tables, it is evident that the repeatability of the results was good and therefore the reliability was considered to be good as well.

Table 2.5 gives the results for the tests conducted on an already worn surface. The test denoted as "first test" is the one run in a R12-oil mixture environment. The "second test" is the one in which a R134a-oil mixture was used with or without residual amount of R12. Both the first and the second test were one hour long. Since two consecutive tests were run over the same wear scar, data for two wear scar widths and volumes worn are given in Table 2.5.

Table 2.4 - Friction and Wear Data for Counterformal Contact

Duration of Each Test = 1 hour, Tests Run on Virgin Surface

Test #	Refrigerant	Oil	Plate Hardness HV	Frict. Coeff.	Wear Scar mm	Vol. Worn mm^-3
76RL	R134a	Ester base	514	0.105	0.203	2.092
79RL	R134a	Ester base	644	0.086	0.179	1.434
80RL	R134a	Ester base	571	0.106	0.273	5.089
82RL	R134a	Ester base	606	0.095	0.211	2.349
84RL	R134a	Ester base	606	0.090	0.226	2.887
86RL	R134a	Ester base	464	0.090	0.296	6.488
32RL*	R134a	Ester base	-	0.105	0.211	2.349
33RL*	R134a	Ester base	-	0.104	0.242	3.545
				0.098	0.230	3.043
77RL	R134a + R12	Ester base+Alkylbenz	514	0.082	0.203	2.092
78RL	R134a + R12	Ester base+Alkylbenz	626	0.085	0.156	0.949
81RL	R134a + R12	Ester base+Alkylbenz	571	0.106	0.328	8.829
83RL	R134a + R12	Ester base+Alkylbenz	565	0.096	0.211	2.349
85RL	R134a + R12	Ester base+Alkylbenz	606	0.090	0.226	2.887
87RL	R134a + R12	Ester base+Alkylbenz	463	0.090	0.242	3.545
				0.092	0.228	2.964
36RL*	R134a	Ester form	-	0.108	0.218	2.591
37RL*	R134a	Ester form	-	0.106	0.242	3.545
88RL	R134a	Ester form	532	0.113	0.156	0.949
90RL	R134a	Ester form	516	0.115	0.156	0.949
				0.111	0.193	1.798
89RL	R134a + R12	Ester form+Alkylbenz	532	0.095	0.172	1.272
91RL	R134a + R12	Ester form+Alkylbenz	516	0.094	0.195	1.854
				0.094	0.184	1.558

* Tests included in previous studies [2]

Table 2.5a - Friction and Wear Data for Counterformal Contact. Duration of Each Test = 1 hour
First Test Run on Virgin Surfaces in R12-Alkylbenzene Oil Environment.
Second Test Run on Worn Surfaces From the First test in R134a-Ester Base Oil.

Second Test #	Refrigerant	Plate HV	Frict. Coef.	WEAR				
				First Test Wear Scar mm	First Test Volume Worn mm^-3	Second Test Wear Scar mm	Total Volume Worn mm^-3	Second Test Volume Worn mm^-3
73RL	R134a	606	0.085	0.140	0.686	0.250	3.908	3.222
75RL	R134a	606	0.100	0.120	0.432	0.226	2.887	2.455
			0.092		0.559			2.839
49RL*	R134a+R12	582	0.100	0.125	0.488	0.242	3.545	3.057
51RL*	R134a+R12	566	0.085	0.133	0.588	0.222	2.736	2.148
			0.093		0.538			2.603

Table 2.5b - Friction and Wear Data for Counterformal Contact. Duration of Each Test = 1 hour
First Test Run on Virgin Surfaces in R12-Alkylbenzene Oil Environment.
Second Test Run on Worn Surfaces From the First test in R134a-Ester Formulated Oil.

Second Test #	Refrigerant	Plate HV	Frict. Coef.	WEAR				
				First Test Wear Scar mm	First Test Volume Worn mm^-3	Second Test Wear Scar mm	Total Volume Worn mm^-3	Second Test Volume Worn mm^-3
69RL	R134a	464	0.100	0.120	0.432	0.250	3.908	3.476
71RL	R134a	464	0.107	0.125	0.488	0.195	1.854	1.366
94RL	R134a	582	0.096	0.125	0.488	0.211	2.349	1.861
			0.101		0.469			2.234
53RL*	R134a+R12	566	0.901	0.125	0.488	0.226	2.887	2.399
55RL*	R134a+R12	516	0.080	0.120	0.432	0.211	2.349	1.917
57RL*	R134a+R12	516	0.078	0.140	0.686	0.234	3.205	2.520
95RL*	R134a+R12	582	0.086	0.120	0.432	0.195	1.854	1.422
			0.286		0.510			2.065

Friction coefficients are given for the second test only. The surface hardness of the plate is also given. The wear during the second test is obtained by subtracting the volume worn during the first test from the total volume worn. These values can, therefore, be compared to the amount of volume worn on a virgin surface since both tests lasted one hour. The highlighted values in this table represent the mean values for the data in the column above them.

Since the first tests given in Table 2.5 were run on a virgin surface, the value for the volume worn can be compared to the values of the volume worn in Table 2.4. From this comparison it is evident that the R12-alkylbenzene oil-refrigerant mixture is much better from a tribological point of view than any of the R134a-oil combinations. This confirms the results from our studies reported before. Data from Table 2.4 and Table 2.5 are the basis for the plots on Figure 2.2 and Figure 2.3.

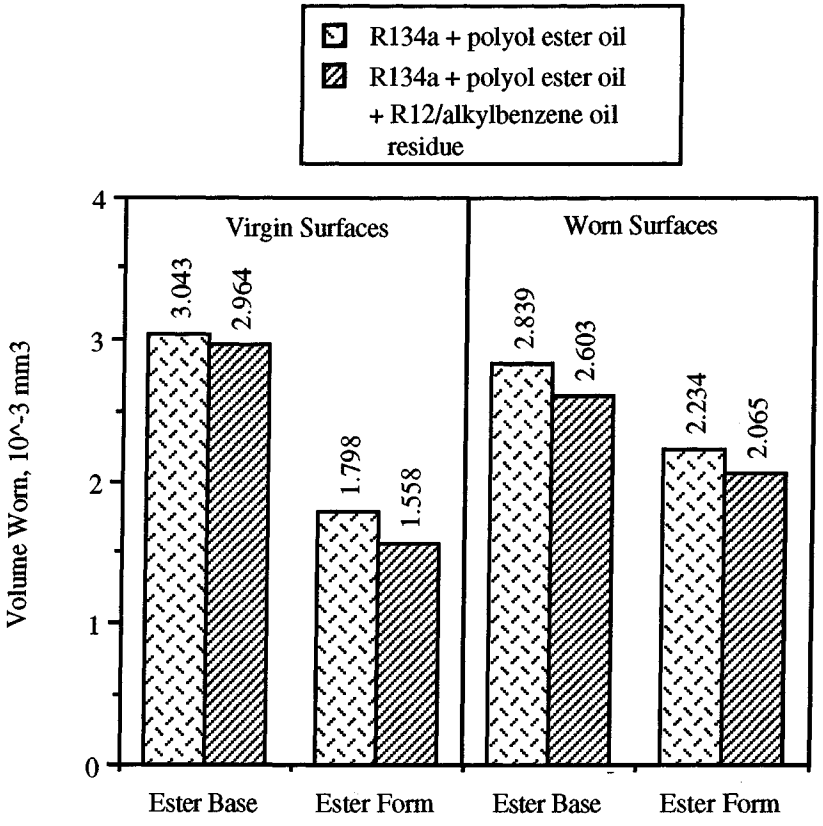

Figure 2.2 - Wear Results for Counterformal Contact
Duration of Each Test = 1 hour

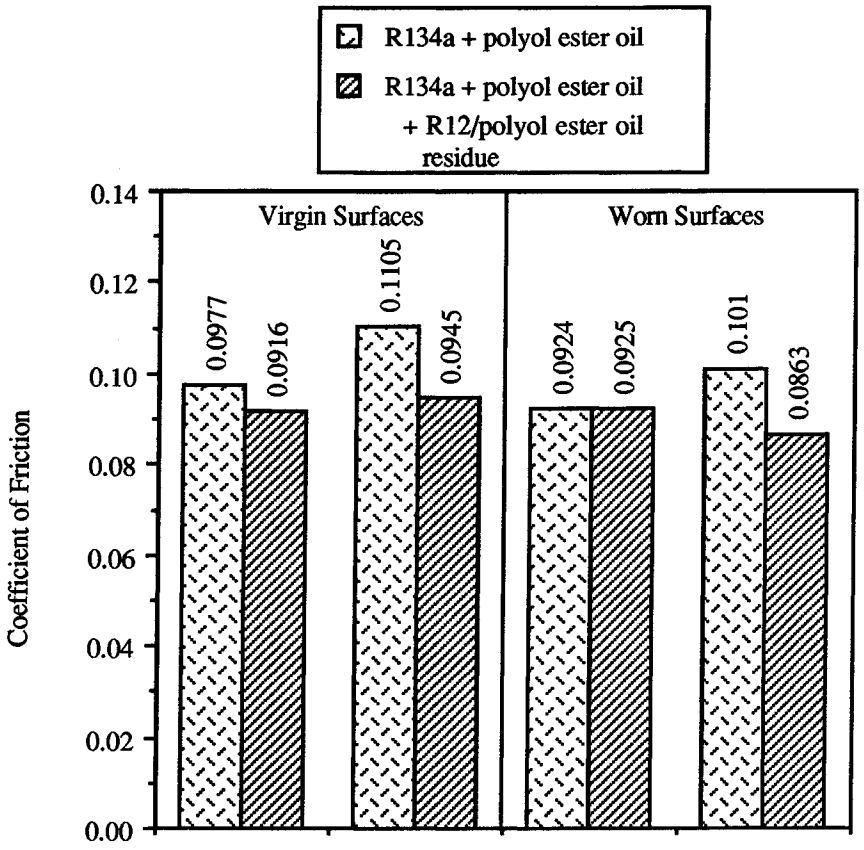

Figure 2.3 - Coefficient of Friction for Counterformal Contact
Duration of Each Test = 1 hour

The results from the tests generally confirmed our expectations for the tribological behavior of different oil-refrigerant mixtures. The presence of small amounts of R12 seemed to slightly improve the tribological characteristics of the mixture no matter what type of surface or oil was studied. Also, the formulated oils seemed to perform better, which is also consistent with our previous observations. The difference in tribological properties between the pure R134a-oil mixture and the one containing residual amounts of R12-oil was very small. Therefore, the effect of the residual amounts of R12-oil mixture on the overall performance of the R134a-based mixture can be considered negligible from the stand point of friction and wear.

The possibility that some other factors such as plate hardness or roughness might affect the friction and wear results was also considered. Figure 2.4 shows a regression analysis of the correlation between wear and surface roughness. It was concluded that this factor, as well as hardness, did not significantly affect the results.

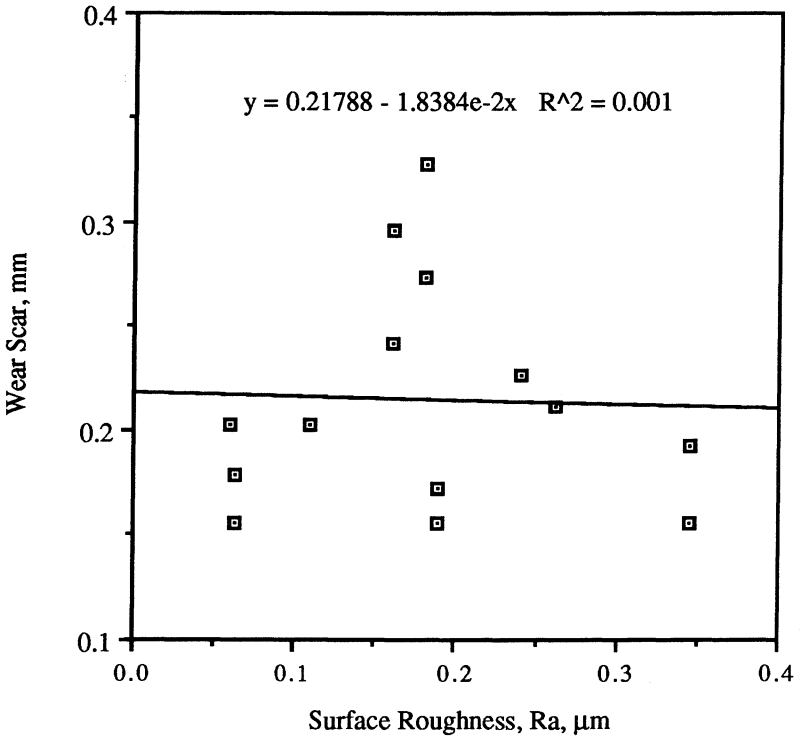

Fig. 2.4 - Correlation Between Wear on Pin and Plate Roughness for Counterformal Contact

2.4.2 Area Contact

During these tests, some unexpected scatter of friction and wear data was observed. Tests that were conducted under the same conditions sometimes gave different results. The scatter of data could be due to two different regimes of lubrication, i.e. boundary or mixed. The basic characteristic for the first type was the comparatively high friction coefficient and substantial wear. The second was characterized by a much lower coefficient of friction and wear. Typical records of the high friction regime are given in Figure 2.5. The low friction regime is illustrated in Figure 2.6. It is also possible that a switch from one regime of lubrication to the other occurs during the test, as in the test record shown in Figure 2.7.

Various reasons for this kind of behavior were studied. The surface hardness and roughness of all plates were measured. However, for the tests conducted, as with the rolling piston tests, no relationship was found between these parameters and friction and wear. A regression analysis for the influence of the surface hardness on wear is shown in Figure 2.8.

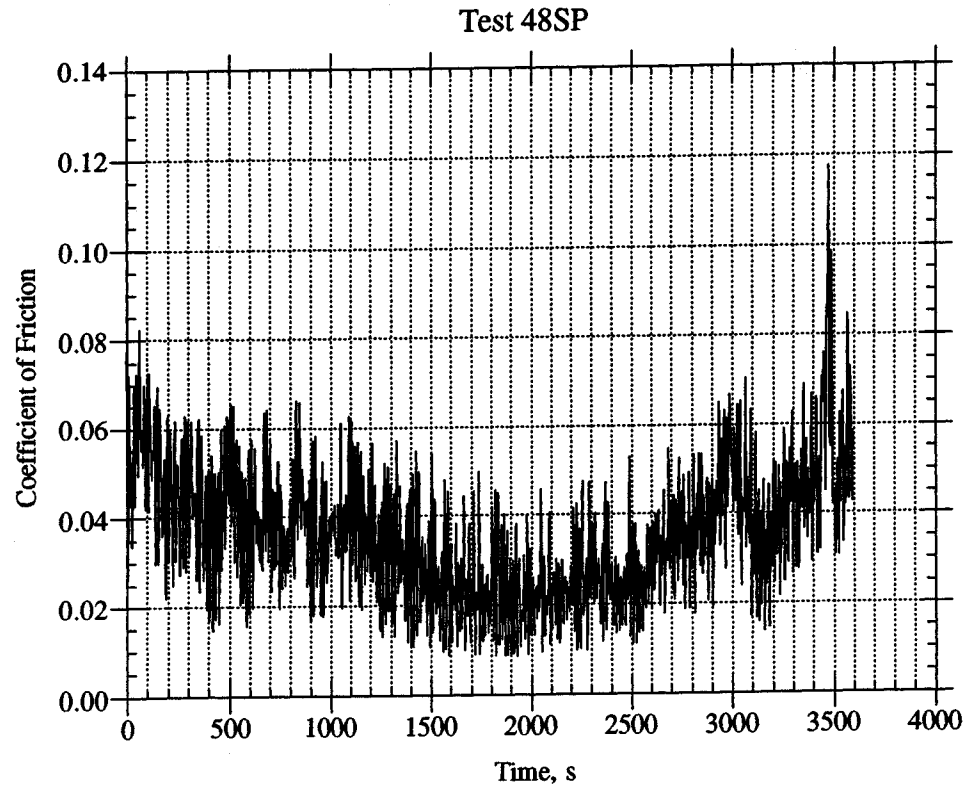

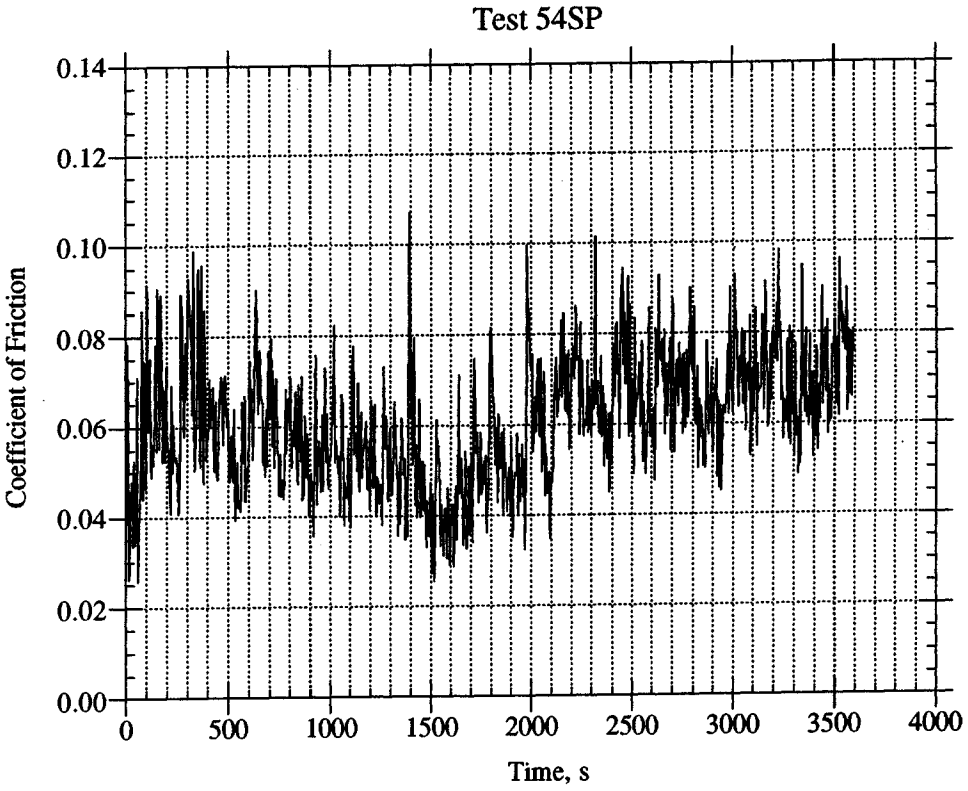

Fig 2.5 - Typical Examples of the High Friction Regime for the Area Contact

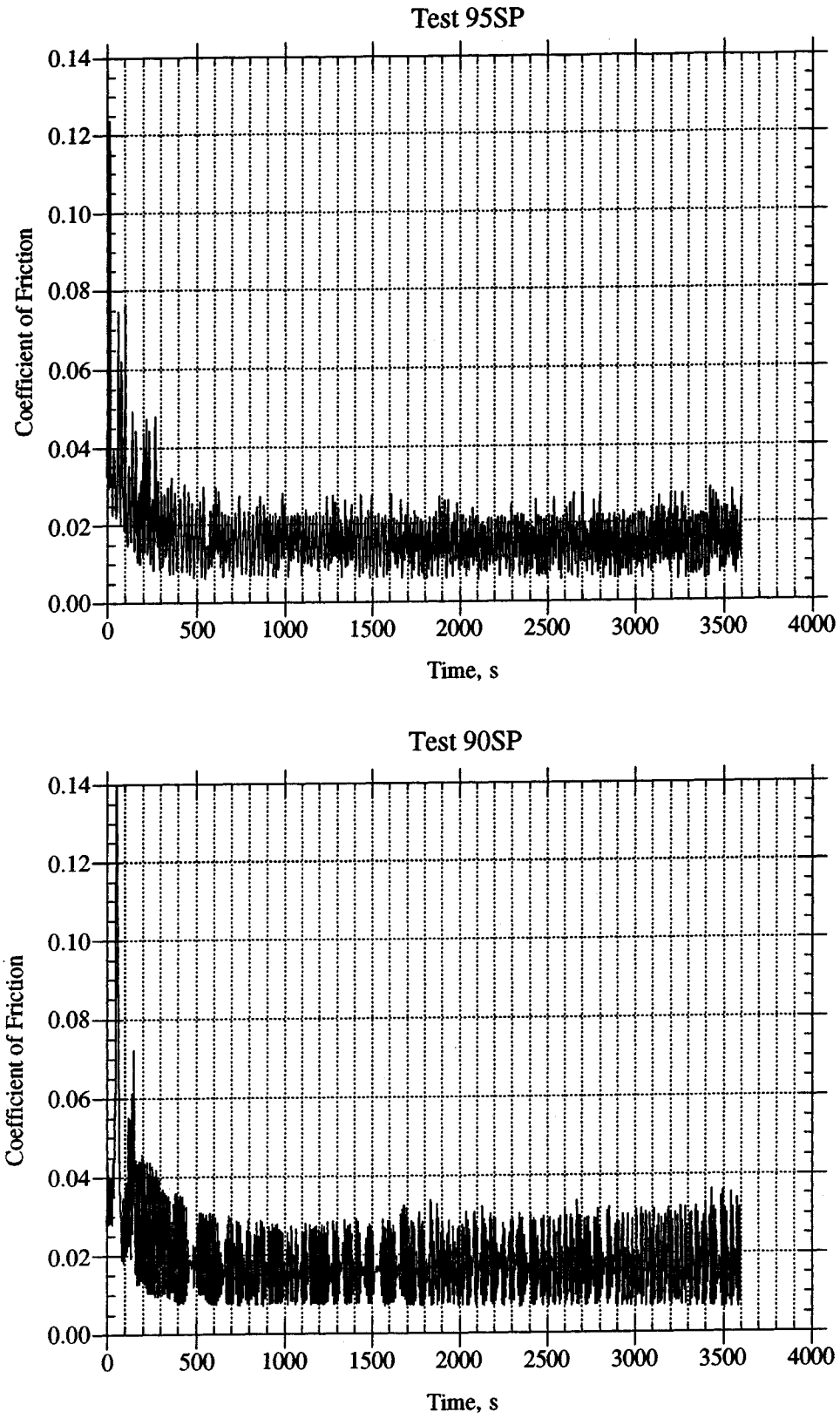

Fig. 2.6 - Typical Examples of the low Friction Regime for the Area Contact

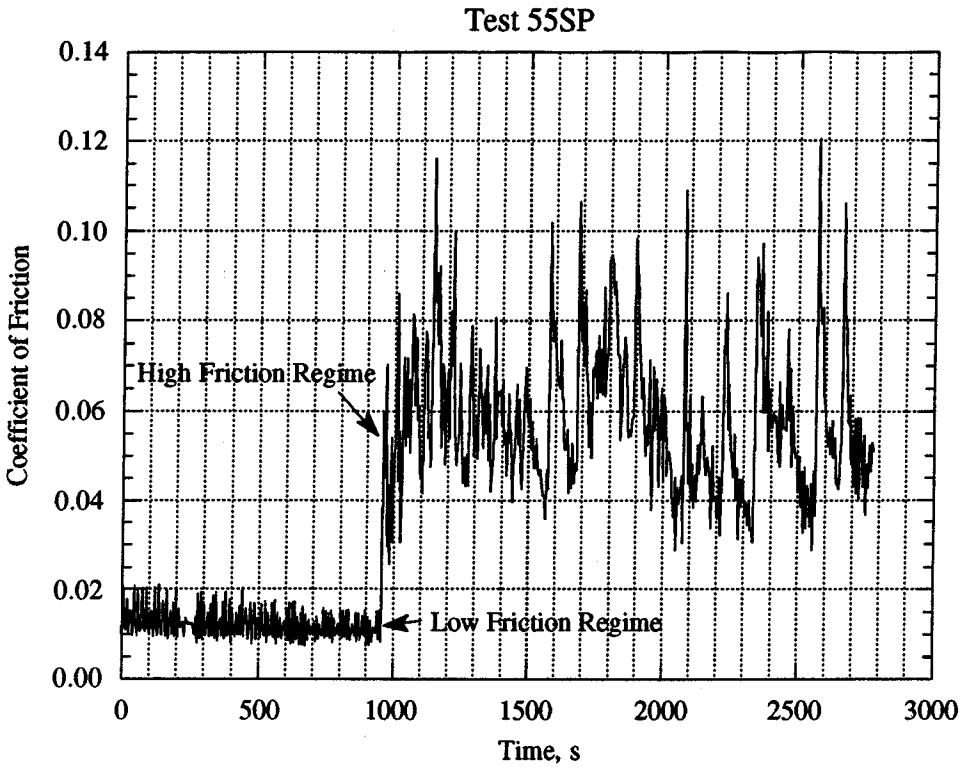

Fig. 2.7 - Typical Example of a Switch from a Low Friction to a High Friction Regime for the Area Contact

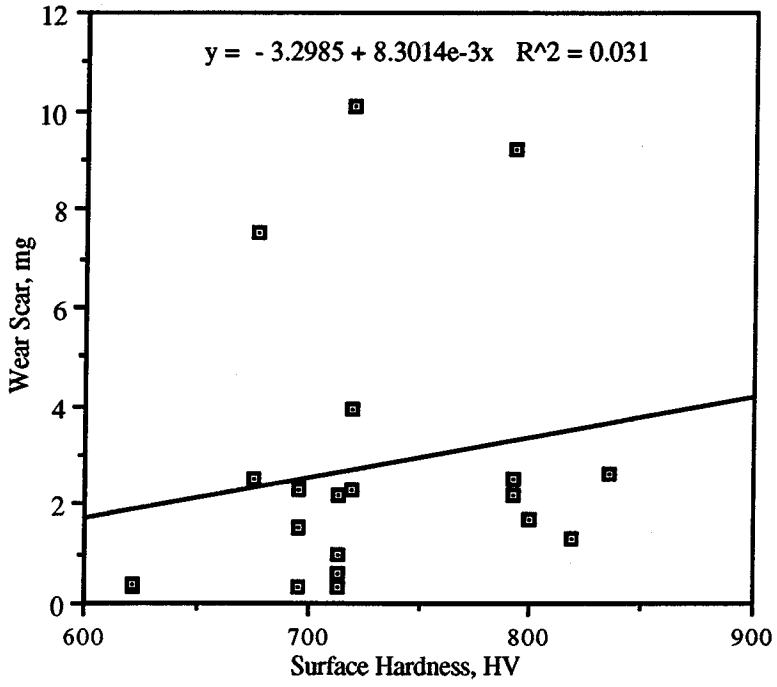

Fig. 2.8 - Correlation Between Wear and Plate Hardness for Area Contact

Some tests were also run on the same plate, and sometimes these tests showed different regimes of friction and wear. This excludes the possibility that this factor is the major reason for this kind of behavior.

Next, the axial load records were studied. The goal was to check whether some geometrical irregularities of the specimens and the testing machine itself could produce enough fluctuations in the load to cause changes in the lubrication regime. A typical load record is shown in Figure 2.9.

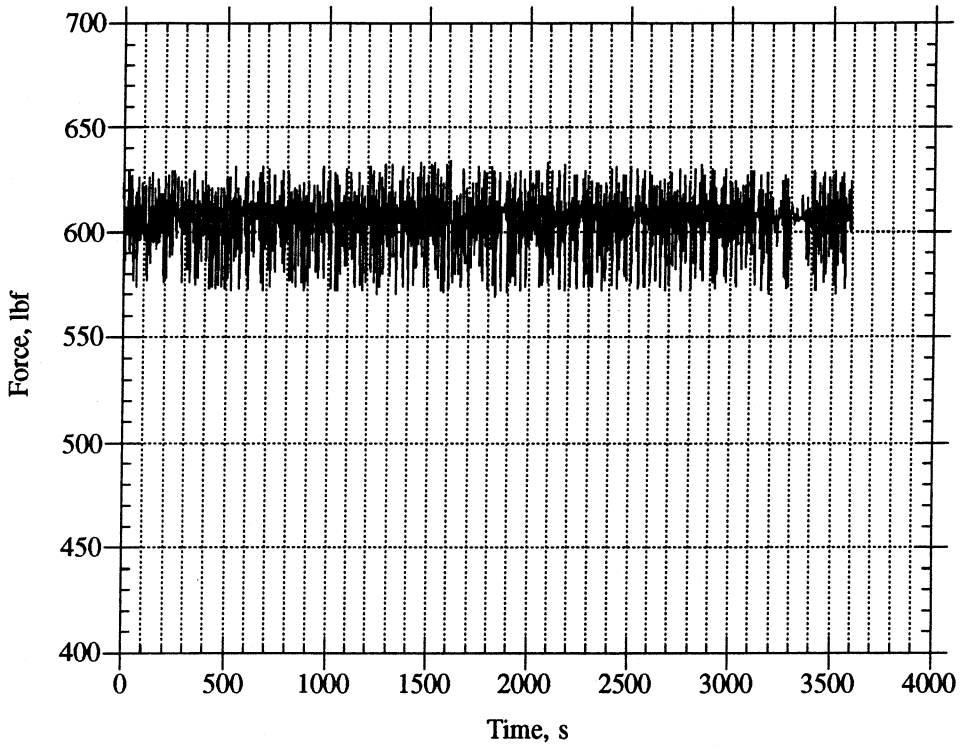

Fig. 2.9 - Axial Force Record for Test 97SP

Typically, the oscillations were less than 12% in magnitude compared to the mean force value. The mean force value and the oscillations stayed fairly constant throughout the test. The maximum and minimum values of the load always occurred at certain position of the spindle which suggests that they were caused by the spindle rotation and some flatness deviations of the specimens. A comparison of the load dynamics and coefficient of friction records showed that the fluctuations of the force were not related to the regime of lubrication.

The possibility that the hydrodynamic liftoff of the lower specimen (the bronze shoe), might be the major factor for a particular regime of lubrication to occur, was also checked. Specimens with both convex, concave, and flat geometries were tested. The surface profile of

these specimens were obtained using the DEKTAK profilometer before and after the test. Typical examples of these profiles are shown in Figures 2.10 and 2.11. In both figures, the first surface profile is the one taken before the test, while the other two show the same specimen profile after the test. One of the profile measurements after the test was taken in a direction of sliding, while the other was taken perpendicular to this direction. According to hydrodynamics theory, the convex specimens can more easily develop fluid films between the surfaces, resulting in better lubrication condition. However, for the loads and speeds used in these tests, hydrodynamic lubrication did not exist and the initial surface geometry did not play a major role in the lubrication process.

Since none of the factors listed above seem to be the major reason for the lubrication regime, it was concluded that probably a complex combination of all these factors contribute to the changing from one regime to the other during the tests. A possible reason for the presence of the both regimes of lubrication is that the test conditions lie in some transitional zone in which a small change in any of the test parameters, may lead to a change in the regime of lubrication.

Based on the above conclusion, the data obtained from the tests were processed separately for the two different regimes of lubrication. The criterion used for this classification was the mean value of the friction coefficient and the appearance of the coefficient of friction record. In Table 2.6, data for the tests run with the base version of the PAG oil are presented. Most of the tests ran under boundary lubrication conditions. The reported wear is in milligrams, and was measured as a weight loss on the bronze shoe. Plate hardness is reported as well. Table 2.7 is analogous to Table 2.6 with the only difference that the data are from the tests conducted with formulated version of the PAG oil. The plots on Figures 2.12 and 2.13 are based on the data from Tables 2.6 and 2.7.

The comparison of the wear values for the tests run with only R134a-PAG oil mixtures with those conducted in the presence of R12-mineral oil residue are, in general, consistent with each other and with the results from the counterformal contact tests. The presence of R12-oil residues slightly improves the tribological properties of the refrigerant-oil mixture, but this improvement may be considered negligible from a practical point of view.

As previously stated, an XPS analysis was done on three separate specimens, and the results show that some films are present on their surfaces. The thickness of these films are of the order 30 angstroms. The chemical composition of these films are given in Table 2.8.

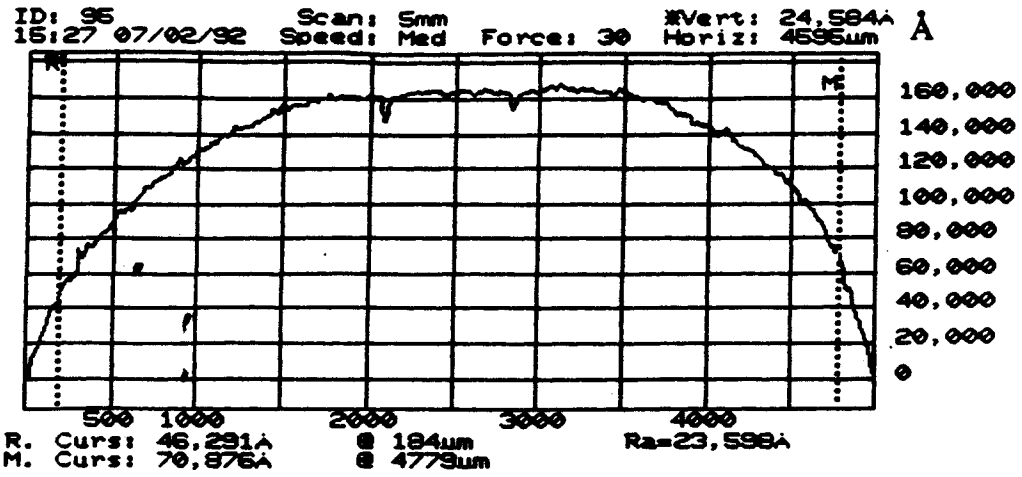

(a)

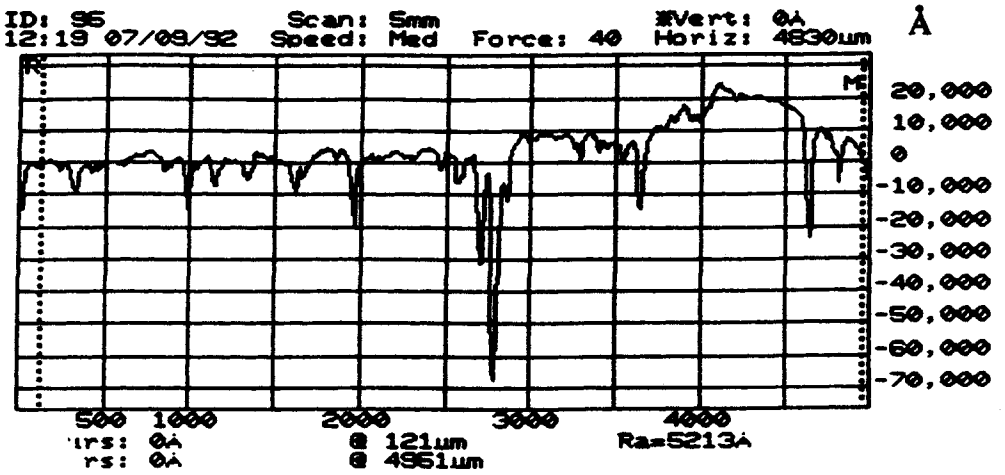

(b)

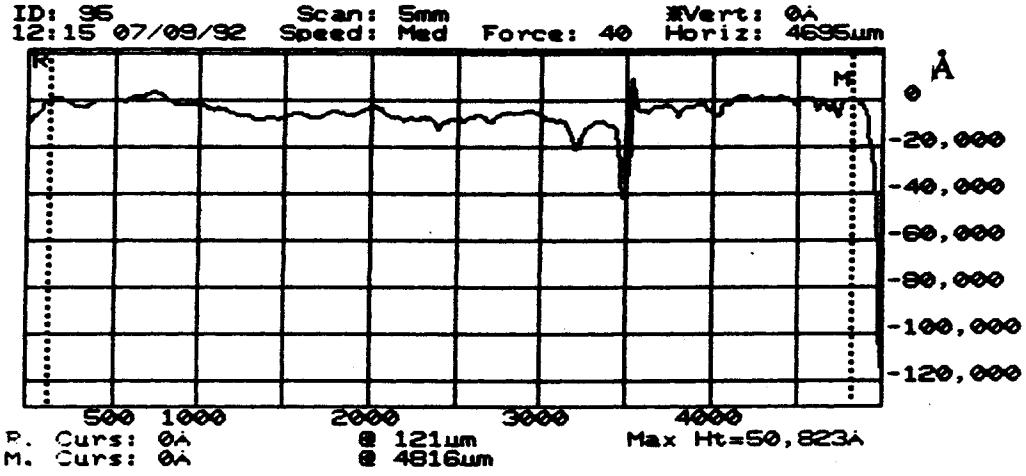

(c)

Fig. 2.10 - Surface Profiles of the Bronze Shoe Specimen:
(a) Surface Profile Before the Test - Convex Shape, (b) Surface Profile After the Test, Measured Along the Direction of Motion, and (c) Surface Profile After the Test, Measured Perpendicular to the Direction of Motion.

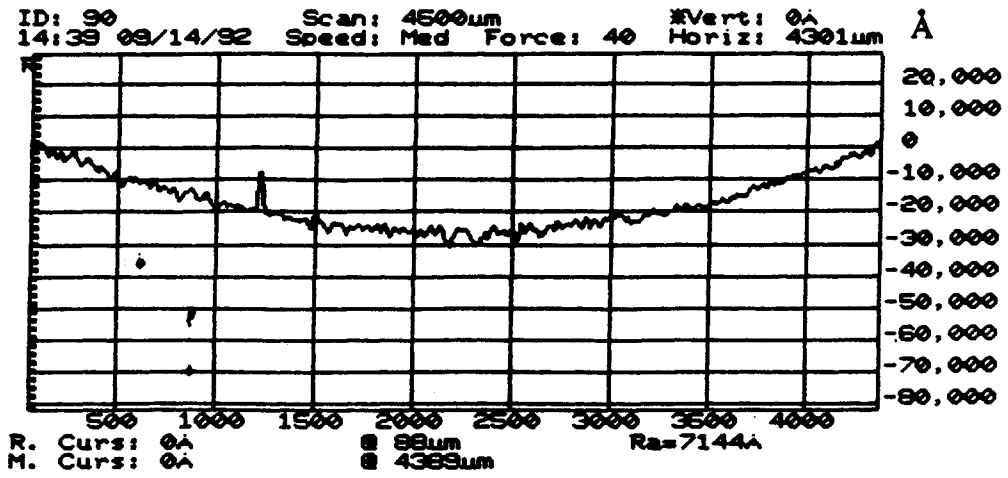

(a)

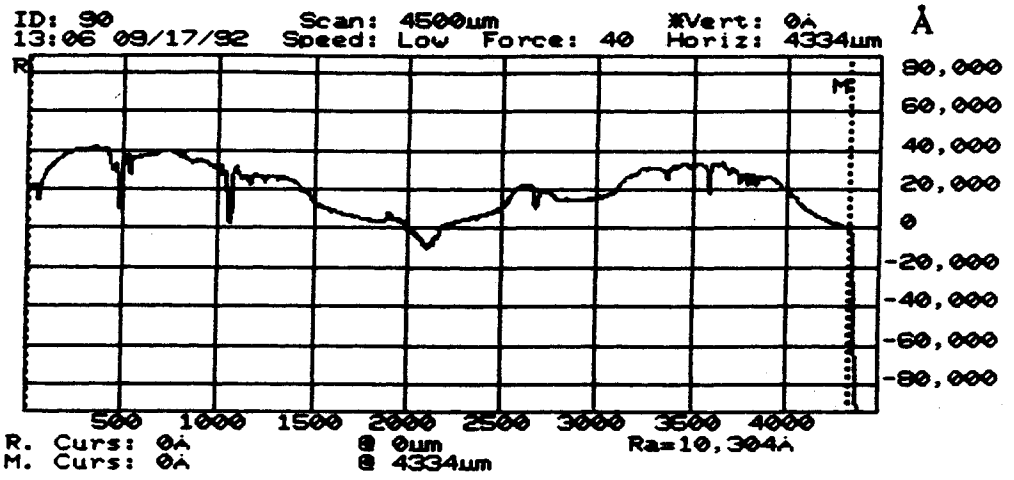

(b)

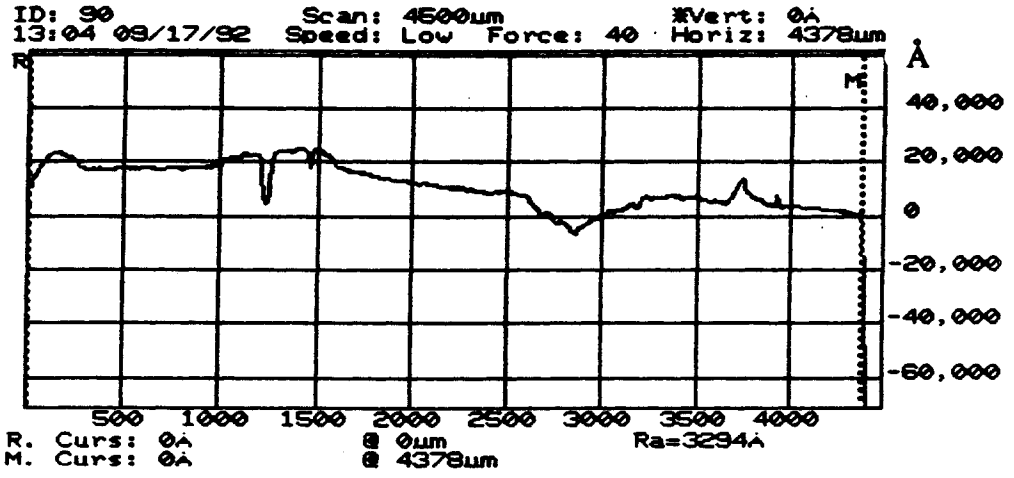

(c)

Fig. 2.11 - Surface Profiles of the Bronze Shoe Specimen:
(a) Surface Profile Before the Test - Concave Shape, (b) Surface Profile After the Test, Measured Along the Direction of Motion, and (c) Surface Profile After the Test, Measured Perpendicular to the Direction of Motion.

Table 2.6a - Friction and Wear Data for Area Contact: High Friction Regime

Duration of Each Test = 1 hour

Test #	Refrigerant	Oil	Frict. Coef.	Shoe Wear mg	Plate Hardness HV	Contact Pressure psi
97SP*	R134a+R12	PAG base + mineral	0.055	1.30	482	18000
88SP*	R134a+R12	PAG base + mineral	0.037	2.50	466	18000
87SP*	R134a+R12	PAG base + mineral	0.032	2.30	423	18000
49SP*	R134a+R12	PAG base + mineral	0.036	7.50	398	30000
48SP*	R134a+R12	PAG base + mineral	0.037	9.20	466	30000
			0.039	3.22		
89SP	R134a	PAG base	0.047	2.20	466	18000
86SP	R134a	PAG base	0.036	3.90	423	18000
47SP	R134a	PAG base	0.033	10.10	423	30000
			0.039	3.38		

Note: shaded values are weighted averages with respect to contact pressure

Table 2.6b - Friction and Wear Data for Area Contact: High Friction Regime

Duration of Each Test = 1 hour

Test #	Refrigerant	Oil	Frict. Coef.	Shoe Wear mg	Plate Hardness HV	Contact Pressure psi
53SP*	R134a+R12	PAG base + mineral	0.013	2.20	419	18000
52SP	R134a	PAG base	0.015	2.30	409	18000

* Only residual amounts of mineral oil present

Table 2.7a - Friction and Wear Data for Area Contact: High Friction Regime

Duration of Each Test = 1 hour

Test #	Refrigerant	Oil	Frict. Coef.	Shoe Wear mg	Plate Hardness HV	Contact Pressure psi
92SP*	R134a+R12	PAG form + mineral	0.042	1.00	419	18000
56SP*	R134a+R12	PAG form + mineral	0.037	2.3 1.67	471	18000
29SP*	R134a+R12	PAG form + mineral	0.070	3.6 2.61	492	18000
			0.050	1.76		
94SP	R134a	PAG form	0.051	1.50	409	18000
55SP	R134a	PAG form	0.042	3.21 2.37	409	18000
54SP	R134a	PAG form	0.061	3.40 2.52	397	18000
			0.051	2.13		

Table 2.7b - Friction and Wear Data for Area Contact: Low Friction Regime

Duration of Each Test = 1 hour

Test #	Refrigerant		Frict. Coef.	Shoe Wear mg	Plate Hardness HV	Contact Pressure psi
95SP*	R134a+R12	PAG form + mineral	0.017	0.30	409	18000
91SP*	R134a+R12	PAG form + mineral	0.027	0.40	366	18000
57SP*	R134a+R12	PAG form + mineral	0.010	0.30	419	18000
			0.018	0.33		
93SP	R134a	PAG form	0.022	0.60	419	18000
90SP	R134a	PAG form	0.019	0.30	366	18000
			0.020	0.45		

* Only residual amount of mineral oil present

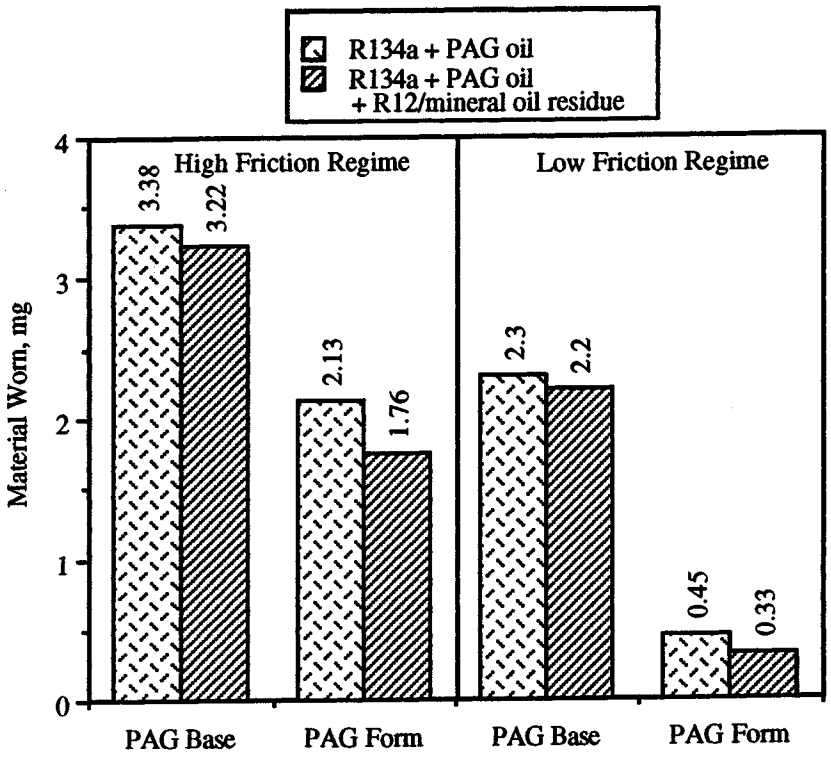

Fig. 2.12 - Wear Results for Area Contact
Duration of Each Test = 1 Hour

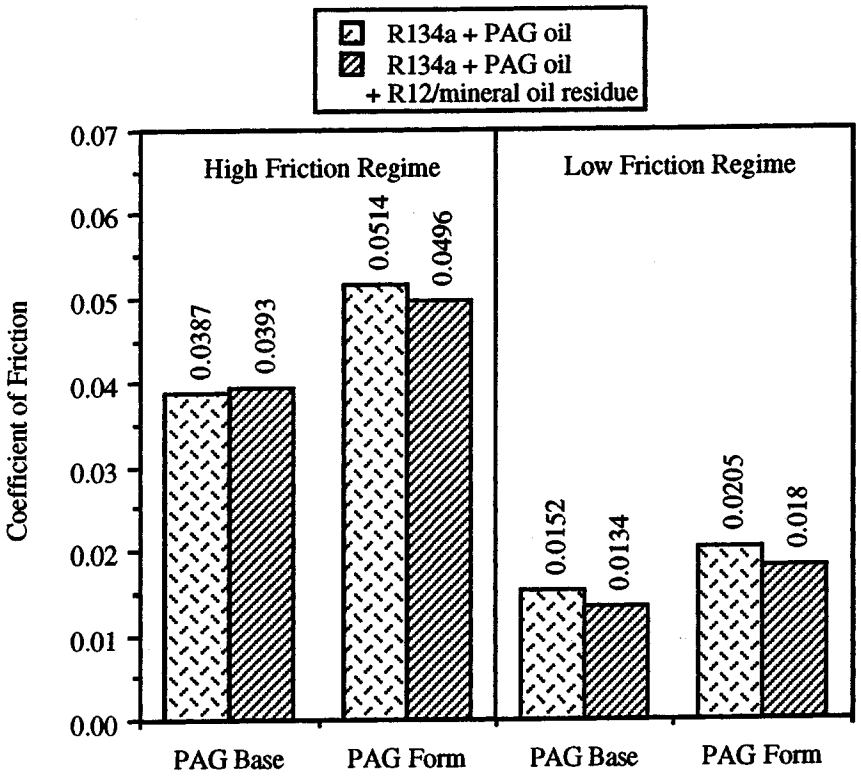

Fig. 2.13 - Coefficient of Friction for Area Contact
Duration of Each Test = 1 Hour

Table 2.8 - XPS Analysis Results for Area Contact

Element	% concentration		
	Specimen 1	Specimen 2	Specimen 3
Test #1 :	R12-mineral oil	R12-mineral oil	R12-mineral oil
Test #2 :	no 2nd test	R134a-PAG oil	R134a-PAG oil + residue
Oxygen, O1s	33.81	38.85	31.60
Copper, Cu2p3	13.31	11.74	11.84
Chlorine, Cl2p	0.74	0.64	0.90
Carbon, C1s	52.01	48.51	55.61
Fluorine, Fls	0.12	0.27	0.05

Since the accuracy of the percent concentration is 1%, the results indicate that the amount of chlorine and fluorine on all these specimens is approximately the same. Because chlorine is not present in R134a but is still present on specimens 2 and 3 after the tests, it can be concluded that possible chlorine surface films are formed during the R12-mineral oil test and are not worn off during the one hour R134a-PAG oil test with or without the presence of the R12-mineral oil residue. Since fluorine exists in R134a, it is not possible to say with certainty that the fluorine on the surface of specimens 2 and 3 also originated from the R12 test. The similarity in the composition of the surface films for the tests run with and without R12-mineral oil residue is one possible explanation why the friction and wear results shown in Figures 2.12 and 2.13 are similar for both tests run with and without R12-mineral oil residue.

Wide scan XPS spectra of the bronze shoe surface are given in Fig. 2.14. The specter taken after a test in R12-mineral oil mixture is essentially the same as those taken after the consecutive tests conducted in R134a-PAG oil only, and R134a-PAG oil + R12-mineral oil residue. This proves that the chemical composition of the surface that was formed during the first test remained unchanged in the following tests.

2.5 Summary of the Results

• For the tests conducted, the presence of R12 and a residual amount of alkylbenzene or mineral oil, do not have a negative effect on the lubricative properties of the R134a-oil mixture.

• For both the counterformal and area contacts under study, the presence of small residual amounts of R12-oil mixture tends to improve the tribological conditions of the contacts. These improvements, however, may be considered negligible.

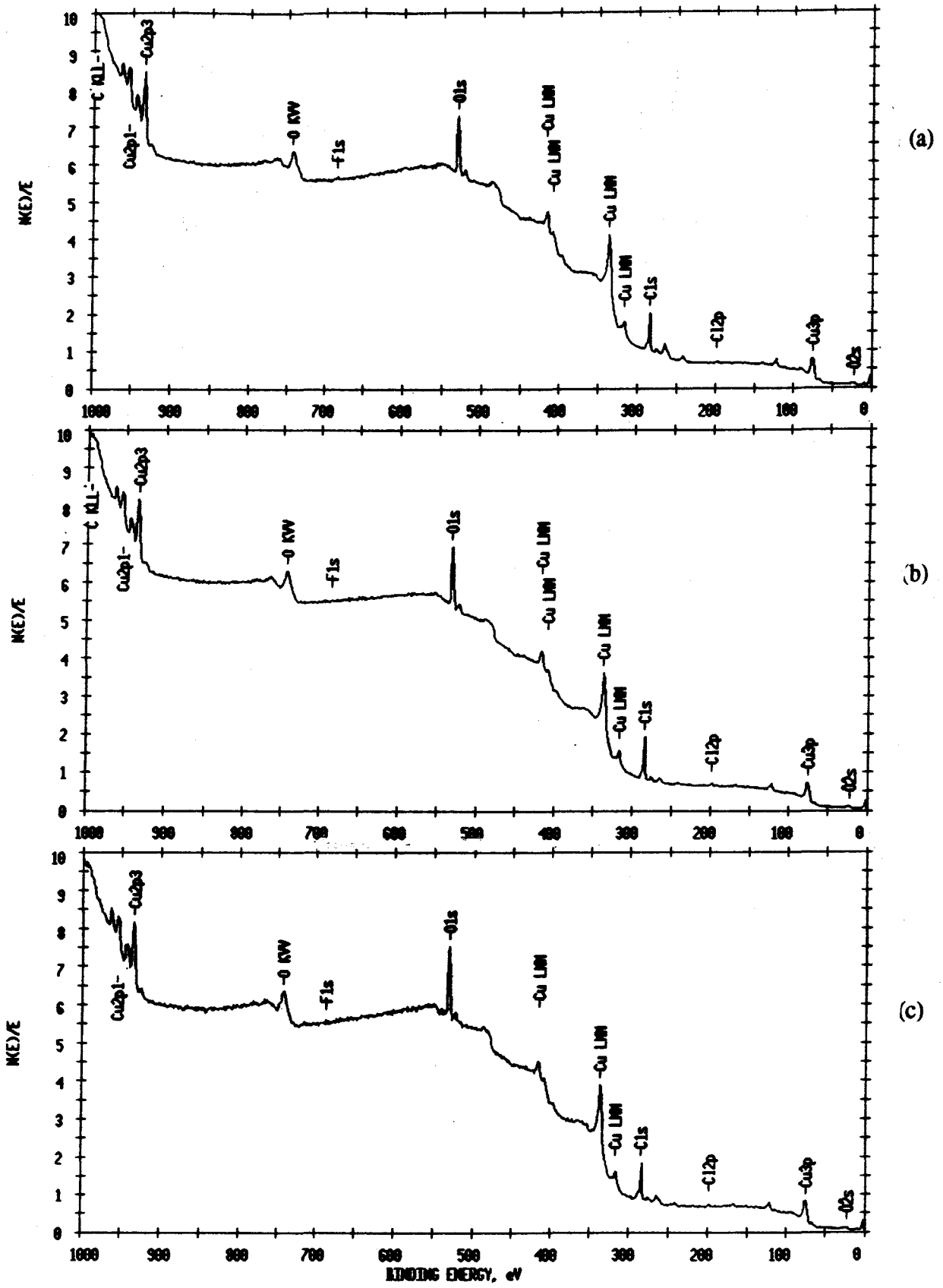

Fig. 2.14 - Wide Scan XPS Spectra of the Bronze Shoe Surface:
(a) Initial Specter - After a Test in R12/Mineral Oil Mixture, (b) After a Second Test in R134a/PAG Oil + R12/Mineral Oil Residue, and (c) After a Second Test in R134a/PAG Oil Only.

• Based on a 14-hour long test, the acid number of the PAG's did not show any measurable increase. Test duration, however might be too short to produce any oil degradation.

• For the tests conducted in this research, it may be concluded that the presence of R12-oil residue does not significantly affect the tribological properties of R134a-oil mixture.

2.6 References

1. **Davis B., Sheiretov T. and Cusano, C.**, Tribological Evaluation of Contacts Lubricated by Oil-Refrigerant Mixtures, ACRC-TR-16, March, 1992.

2. **Davis B. and Cusano C.**, The Tribological Evaluation of Compressor Contacts Lubricated by Oil-Refrigerant Mixtures, ACRC-TR-19, May, 1992.

CHAPTER 3

Evaluation of the Tribological Properties of Polyimide and Poly(amide-imide) Polymers

3.1 Introduction

A whole family of chlorinated hydrocarbons such as dichlorodifluoromethane (R12) and chlorodifluoromethane (R22), used as refrigerants in numerous applications will be replaced in the near future by ozone-safe chemical compounds, as required by the Montreal Protocol. The replacement refrigerants do not contain chlorine in their chemical structure. In addition to the thermodynamical problems associated with the new compounds, some tribological problems arise as well. In a previous study [1], it was shown that chlorine containing refrigerants react chemically with metal surfaces thus forming protective surface films. The prime candidate replacement refrigerant, tetrafluoroethane (R134a), fails to form such protective films. Therefore, future lubrication of critical components operating in refrigerant environments will be mainly provided by either liquid lubricants or self-lubrication materials.

The automotive air conditioning swash plate compressor is a typical example where friction and wear problems, associated with the replacement of R12 by R134a, may occur. The critical tribo-contact, which is between the shoe and the plate, is lubricated under normal conditions by an oil-refrigerant mixture. In some cases, however, marginal or boundary lubrication conditions exist, especially at start-ups. If the refrigerant has no lubrication properties, which is the case with R134a, the compressor may fail due to excessive friction and wear. One possible solution to this problem is to use self-lubrication materials for one of the contact mating surfaces. Polymers are probably the largest class of self-lubricating materials. Hence, tribological properties of polyimide and poly(amide-imide) polymers, which are some of the best self-lubrication materials, were evaluated.

3.1.1 Typical Operating Conditions for the Critical Contact in a Swash Plate Compressor

Some typical steady-state values of the contact pressure, sliding velocity, and plate temperature of the shoe-plate contact of a presently used swash plate compressor are given in Table 3.1. The contact pressure and the sliding velocity are average values over one shaft rotation. The temperature rise is due to the frictional heating of the contact. Its magnitude depends on the particular compressor design and its heat dissipation characteristics. It also depends on the thermal and tribological properties of the contacting materials. The replacement of the currently used materials with polymers will change the contact

temperature. This change, however, is difficult to estimate. Therefore, a temperature value of 250°F was assumed for all the tests, as a first approximation to the temperatures that may be generated in real machines.

Table 3.1 - Typical Operating Conditions of a Swash Plate Compressor

Contact Pressure	Sliding Velocity	PV Value	Plate Temperature @ 4000 rpm
1000 psi	40 fps	2,400,000 psi•fpm	250 °F

3.1.2 Selection of Self-Lubricating Materials for the Contact Under Study

The self-lubricating materials chosen for this study were several grades of Vespel, a Du Pont manufactured thermosetting resin, and Torlon, a poly(amide-imide) injection moldable plastic manufactured by Amoco. The latter was expected to provide slightly higher wear rates when compared to the most costly polyimide resins but it does have the advantage of being injection moldable. The major considerations for choosing these materials were their exceptional ability to operate under high temperatures (up to 500°F), as well as their outstanding wear resistant characteristics. These, however, are not the only polymers that possess such outstanding tribological properties. Several new high performance thermoplastics have been developed recently which have high temperature stability, high strength, and also high resistance against wear. Among these thermoplastics are polyetherketone (PEEK) and thermotropic liquid crystal polymers (LCP). All these materials have been tested under identical conditions [2], and polyimides proved to be superior to the other polymers. In another study conducted by the National Center of Tribology (UK), the wear rates of six groups of polymeric materials were compared [3]. The polyimide and poly(amide-imide) polymers showed somewhat higher wear rates than some fiber filled thermosets and thin layer of metal-backed polytetrafluorethylene (PTFE). The latter, however, cannot operate at high temperatures. The polyimides constitute a relatively broad class of materials with different properties. The addition of fillers to the base polymer can also significantly change its friction and wear properties [4, 5]. The polymer grades tested in this study are among the most widely used, and the tests are meant to provide a more general estimation of the performance of these materials under the conditions of interest. It is also believed that the wear rates and the general trends of their behavior obtained under the conditions studied will be similar to those of other materials from the same class. Polyimides and other polymers for high temperature applications have been extensively studied for their tribological characteristics. One aspect of these studies has been to determine the limiting contact pressures and speeds under which these

polymers can successfully operate. A plot of some limiting pressures and sliding velocities under dry sliding conditions is given in Fig. 3.1.

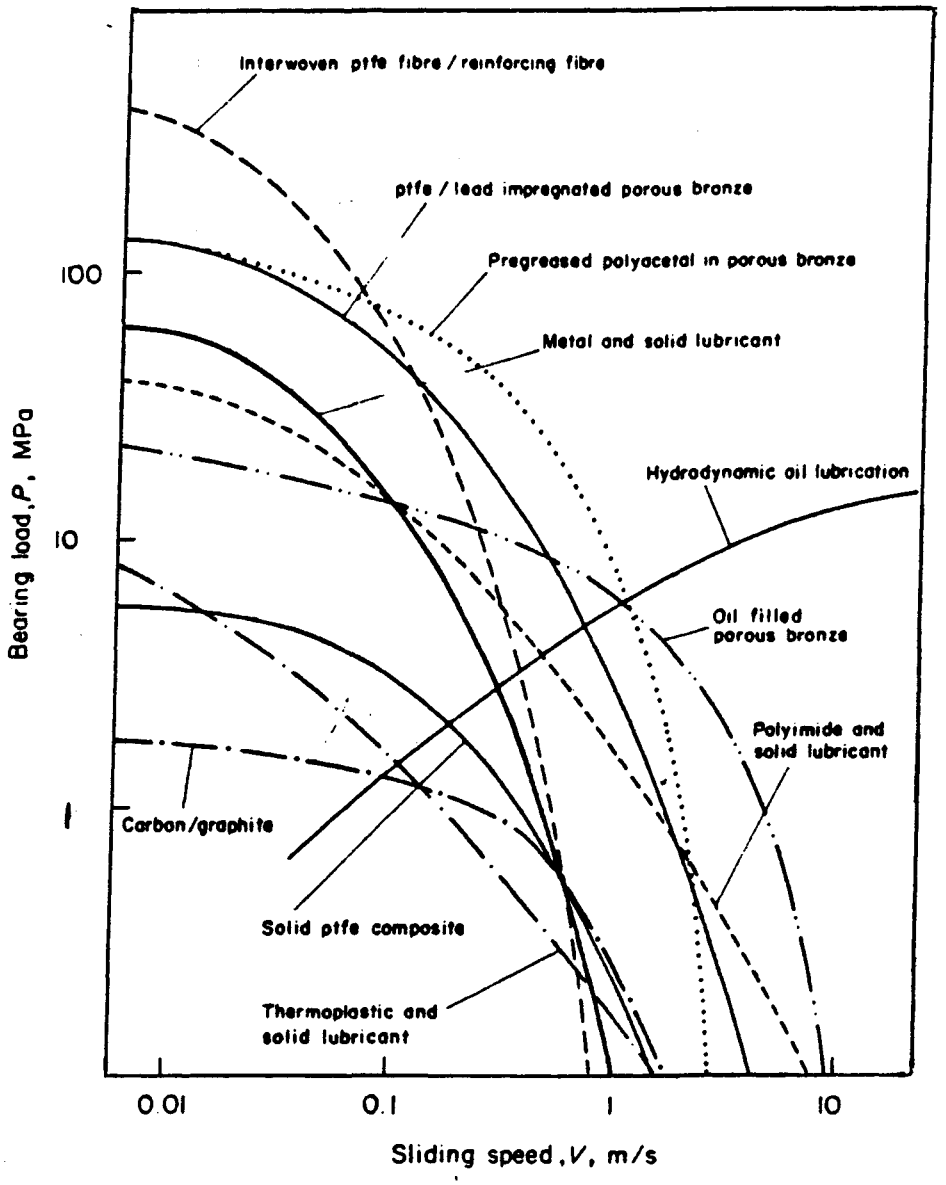

Fig. 3.1 - Limiting Loads and Speeds on Some Self-Lubricating Materials [6]

For many years the PV factor (P = pressure, V = velocity) has been used to design tribo-contacts under boundary or dry lubricated condition. This factor is generally given in units of psi•fpm. Some limiting PV's for the polymers of interest have been obtained by Friedrich [2], Tewari [7], and Sliney [8]. The PV limit itself depends on the conditions of the test and will vary with the environmental temperature, counterface material properties and surface roughness, type of environment, temperature dissipating characteristics of the test facility, and the ratio of the pressure and the velocity in the PV value. However, from

the data accumulated to date, it is evident that these materials should not be expected to operate in dry sliding conditions at PV values above 150,000 psi•fpm if moderate wear rates are desired. The major limiting factor is the high temperature generated in the interface. Under lubricated conditions, the PV values under which these materials can operate, can be on the order of a million psi•fpm [9]. Since the shoe-plate contact of the air conditioning swash plate compressor is expected to operate with sufficient lubrication for most of its life, it is quite possible that some polymer grades may perform satisfactory under this condition. If better tribological properties are desired, some composite materials based on a thermosetting polyimide resin matrix, are capable of continuous operating under dry conditions, at contact pressures of up to 4,000 psi, PV values of 600,000 psi•fpm and at temperatures of over 570 °F [10].

3.1.3 Study Goals

In this study, the polymers of interest were tested under a broad range of pressures, sliding velocities, contact temperatures, environments and counterface surface roughness, in order to provide more general information about their tribological characteristics.

The goals of this study are as follows:

• Evaluate the effect of different environments on the tribological characteristics of the materials under study. These are primarily refrigerant environments (R22, R134a), both gaseous and liquid. For comparison purposes, some tests in air and argon are conducted as well.

• Evaluate the combined effect of temperature and refrigerant environment on the friction and wear properties of the contact pairs studied.

• Study the effect of the counterface surface roughness.

• Obtain values for the friction coefficient and the wear rates of the materials under study for different PV values under both dry and lubricated sliding conditions.

3.2 Experimental Procedure

All experiments were conducted in a specially designed high pressure tribometer. A complete description of the test facility and its capabilities is presented elsewhere [1].

3.2.1 Simulation of Critical Contact

3.2.1.1 Geometry of Specimens

The critical contact in the automotive swash plate compressor is that between the shoe and the plate. The shoe pivots on a steel ball and makes an area contact with the plate. The polymers were tested both as plate and shoe materials. In the first case, they were rubbed against a bronze shoe, while in the second case, the mating surface was a ductile cast iron plate. The geometry of the specimens is given in Figure 3.2, and the area of contact is given in Figure 3.3. The geometric data for the various types of shoe specimens are given in Table 3.2. The size of the contact diameter of the specimens was measured with an optical microscope. The load on the specimen was then adjusted, depending on the size of each specimen, to obtain the desired value for the contact pressure. The values given in Table 3.2 are average values for the whole set of specimens. The variations in the area were in the range of a few percent. Geometrically similar shoe specimens with different contact diameters were necessary in order to provide a wider range of contact pressures which could be tested.

Table 3.2 - Material and Geometry of Shoe Specimens

Shoe Material	Contact Diameter, D_S (in.)	Contact Area, A ($in.^2$)
Torlon	0.201	0.0317
Vespel	0.183	0.0263
Bronze (small)	0.197	0.0305
Bronze (large)	0.425	0.1420

3.2.1.2 Specimen Holders

In order to effectively be able to test the equivalent geometries of the critical contacts in the compressor , specimen holders were designed and made. For the case in which a polymer plate was tested, a 0.442 in. bronze shoe was used. The polymer plates tested are 2 in. or 2.120 in. diameter disks held in place by specimen holders. The specimen holder for the 2 in. plates is shown in Figure 3.4. Four small screws are equally spaced around the circumference of the holder to keep the polymer disk in place. The specimen holder for the 2.12 in. disks has similar design. The specimen holder for the bronze shoe is shown in Figure 3.5.

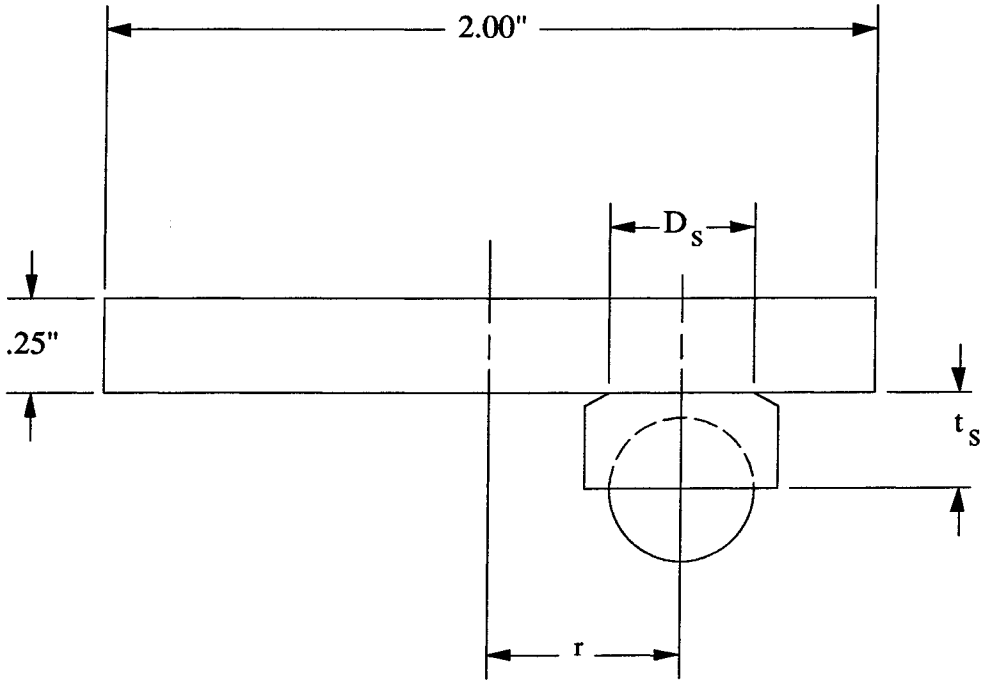

Fig. 3.2 - Geometry of Specimen

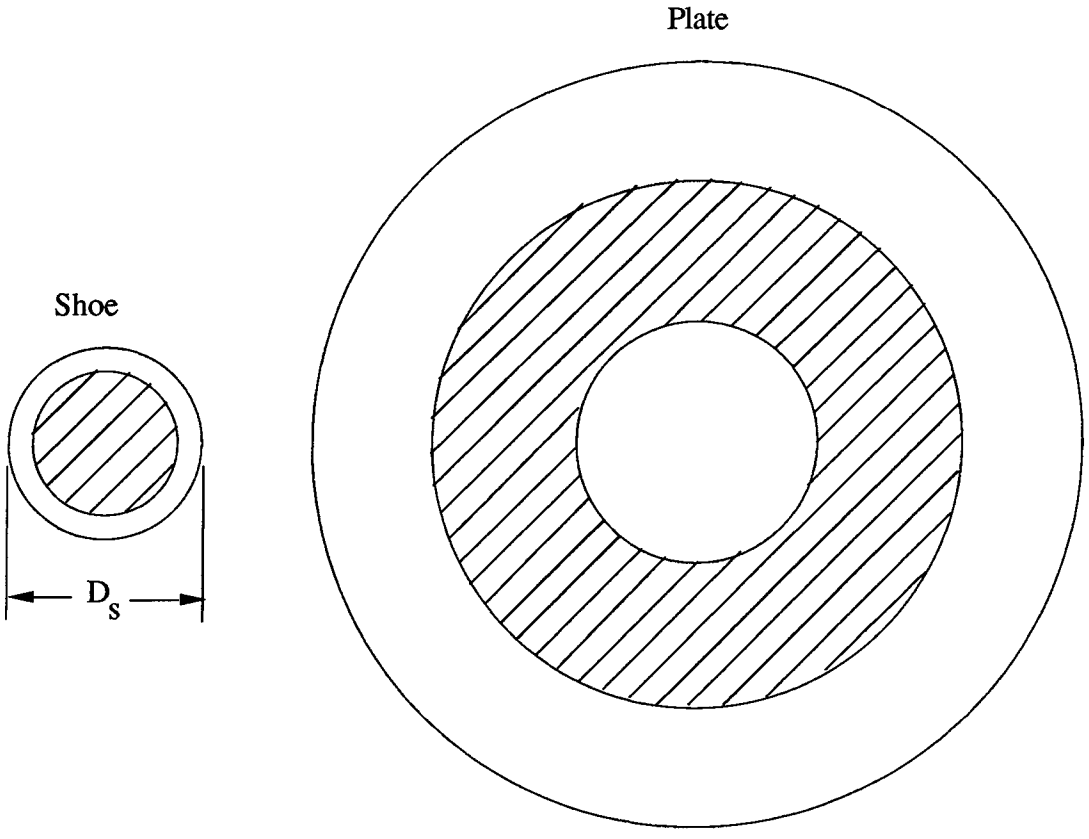

Fig. 3.3 - Area of Contact

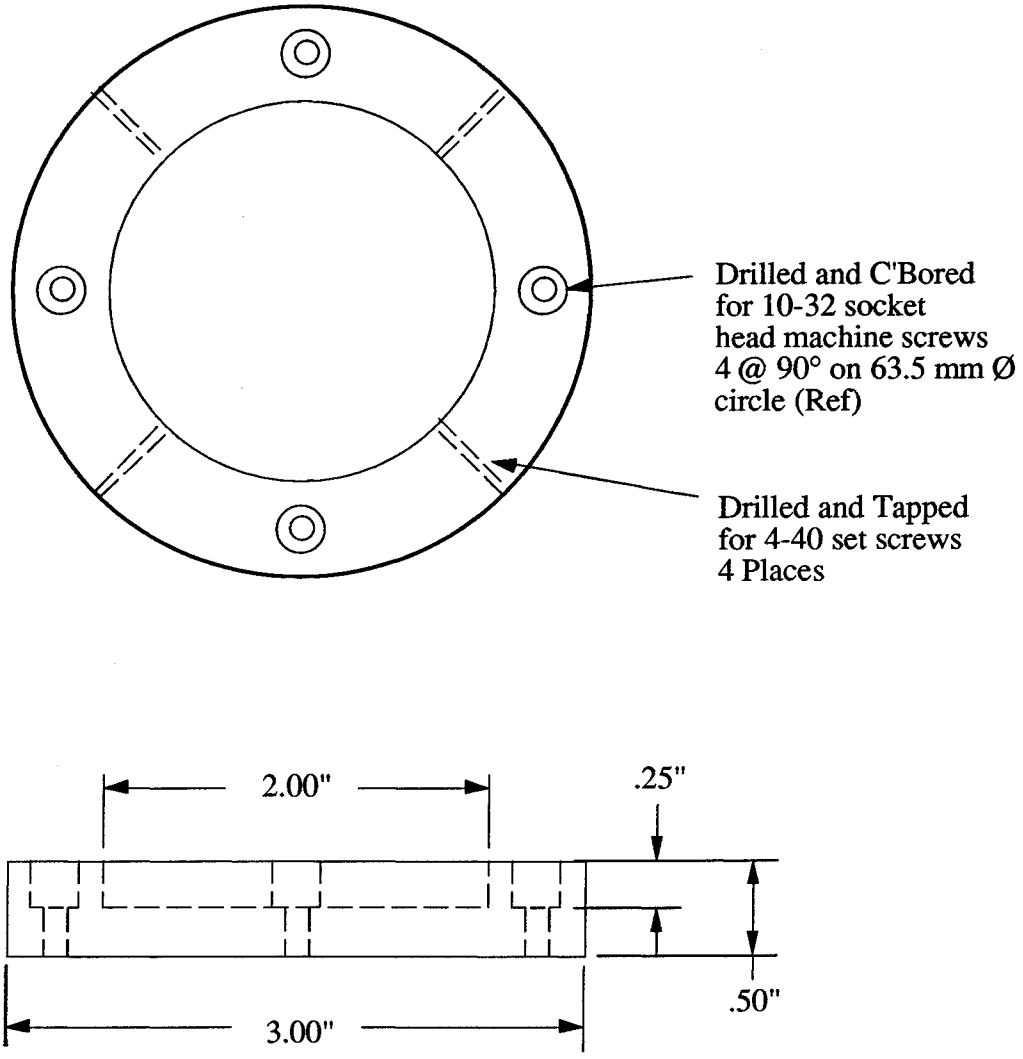

Figure 3.4 - Polymer Plate Holder

The radius from the center of the specimen holder to the location of the ball which holds the shoe is 0.5 in.

An 80-55-06 ductile cast iron plate was used as the mating surface when testing polymer shoes. The cast iron plates are 3.0" in diameter, and four evenly spaced holes are drilled into the plate so that it can be attached directly to the spindle. Two specimen holders for the polymer shoes were tried. The first was similar to the one used with the bronze shoes (ball-socket joint). This design was not a good option for the polymer shoes since the large frictional force produced a couple with respect to the pivot point, resulting in an uneven pressure distribution over the area of the specimen.

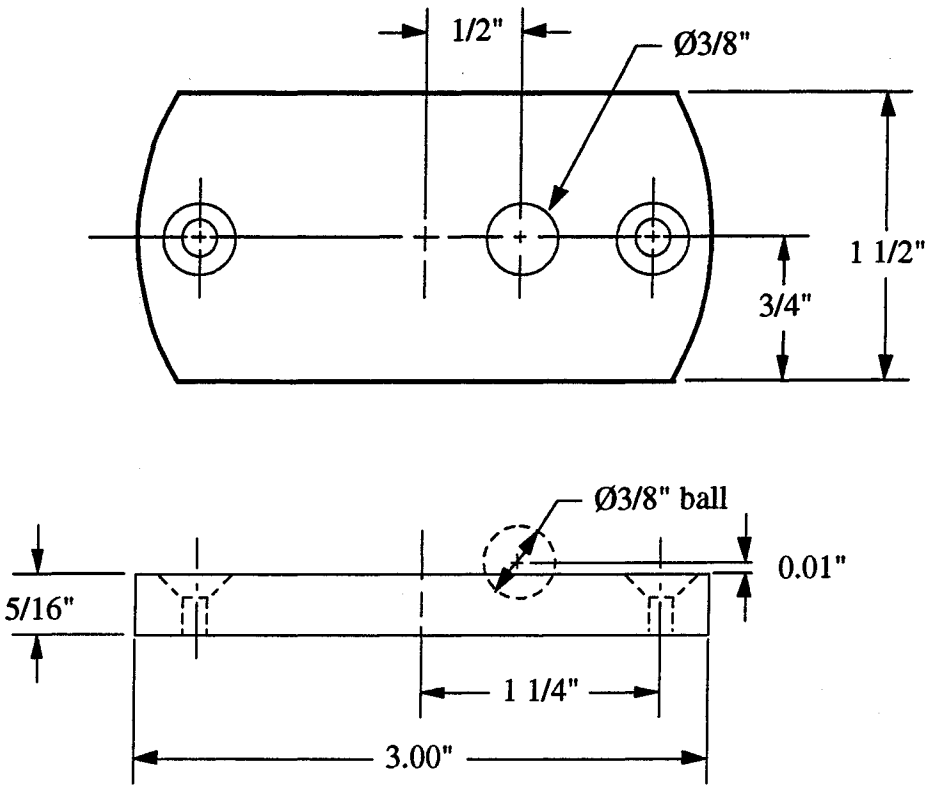

Fig. 3.5 - Bronze Shoe Holder

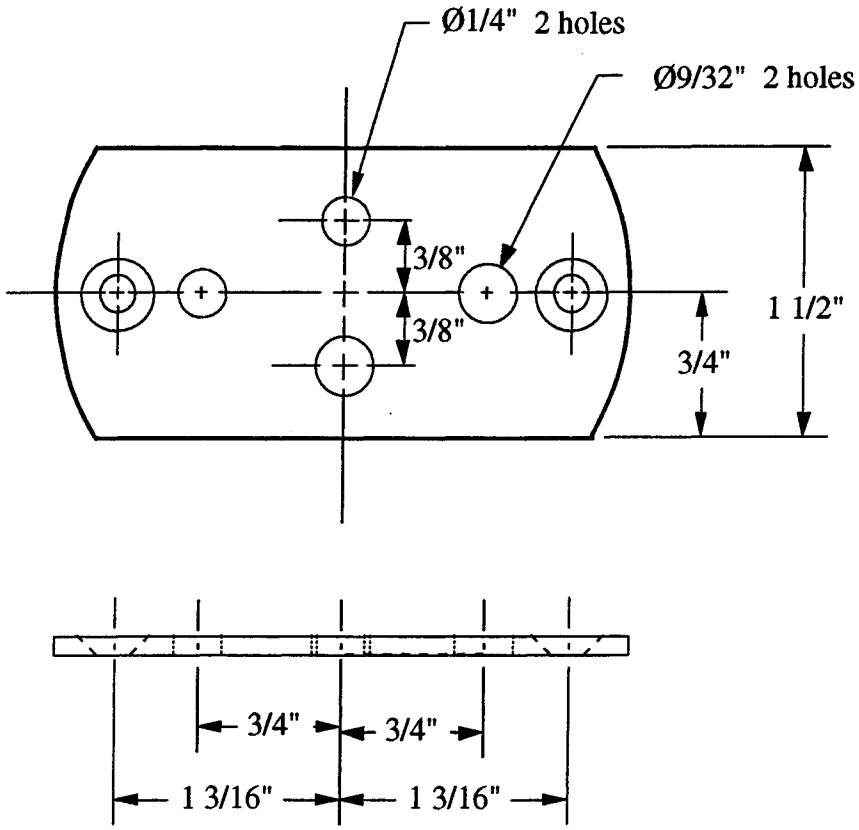

Fig. 3.6 - Polymer Shoe Holder

The uneven pressure distribution led to uneven wear on the surface of the specimen. In addition, the contact area tended to change throughout the test, making the validity of the preset contact pressure questionable. In order to eliminate the tilting problem, a specimen holder which did not allow the shoe to pivot was used. The polymer shoes are 3/16" in diameter, and their specimen holder is shown in Figure 3.6. Two holes were placed on the holder, one at 3/8" from the center and the other at 3/4" from the center so that two tests could be conducted on the same plate. The tests conducted with the second specimen holder gave a more uniform pressure distribution and wear on the surface of the polymer shoe and allowed more accurate estimates of the contact pressure and PV value.

3.2.1.3 Materials of Specimens

Three grades of Vespel polyimide and one grade of Torlon poly(amide-imide) were tested. The designation, description and characteristics of different grades are given in Table 3.3.

The major considerations for choosing these polymers were their exceptional ability to operate at high temperatures (up to 500 °F), as well as their outstanding wear resistance characteristics. A brief summary of the most important mechanical and tribological properties of the Torlon and Vespel grades tested is given in Table 3.4.

All the shoe specimens of a given polymer grade were machined from the same rod stock in order to ensure the same mechanical properties. Standard Vespel stock parts were used as the SP-21D polyimide plates. The Torlon plates were cut from the same compression molded round stock. Torlon specimens were sent to Amoco Performance Products, Inc. for postcuring in order to remove any adverse effects that might have been caused by the machining process. All specimens were postcured at the same time and under the same conditions. Vespel specimens did not need any postcuring because a thermosetting polyimide resin is used for their manufacture.

ASTM #536 80-55-06 ductile cast iron was used for the metal plates. The bronze shoes were made of silicon leaded bronze with 61.5-63.0% Cu, 1.5-3.5% Mn, 0.5-1.5% Si, 0.4-0.8% Pb, 0.5% max. Al, 0.4% max. Fe, 0.5% max. impurities, and Zn the remainder.

3.2.1.4 Surface Characteristics of Specimens

The Vespel plates were used as supplied. The average roughness of the surface was 1.3 μm Ra. The surface roughness was measured with a Sloan-Dektak stylus profiler. All polymer shoes and the Torlon plates were machined on a lathe to an average surface roughness of 1.7 μm Ra.

Table 3.3 - Description and Characteristics of Polymer Materials

Design Designation	Description	Characteristics	Test Specimens
Vespel SP-21D	15% by weight graphite filler	Graphite added to provide low friction and wear	Plates
Vespel SP-211	15% by weight graphite filler and 10% by weight Teflon fluorocarbon resin fillers	Has lowest coefficient of friction over a wide range of operating conditions. Also has lowest wear rate up to 300°F	Shoes
Vespel SP-3	15% by weight molybdenum disulfide	MoS_2 added to provide lubrication in vacuum or dry environments	Shoes
Torlon 4301	12% by weight graphite powder and 3% fluorocarbon	Designed for bearing use. Good wear resistance, low coefficient of friction, and high compressive strength	Plates and Shoes

Table 3.4 - Selected Properties of Polymers Used in Friction and Wear Tests

Properties	Torlon 4301	Vespel SP-3	Vespel SP-21D	Vespel SP-211
Tensile Strength @73°F, 10^3psi	23.7	8.2	9.5	7.5
Tensile Strength @245°F, 10^3psi	17.0	-	7.7	5.4
Tensile Strength @450°F, 10^3psi	10.6	-	5.8	3.8
Compressive Strength, 10^3psi	24.1	18.5	16.3	5.4
Shear Strength @73°F, 10^3psi	16.1	-	11.2	-
Degradation Temperature @264psi, °F	534	-	680	-
Coeff. of Lin. Therm. Exp., 10e-6in/in-°F	14	29	27	30
Thermal Cond., BTU-in./hr-ft^2-°F	3.7	3.2	6.0	5.3
Hardness, Rockwell"E"	72	40 to 55	25 to 45	1 to 20

The polymer surface roughness did not seem to have any significant effect on the friction and wear results. The initial surface was quickly changed to some steady-state roughness, usually much lower than the initial roughness, after just a few minutes of sliding.

More care was taken for the preparation of the mating metal surfaces. Bronze shoes were machined and then ground to an average surface roughness of 0.20 μm Ra. The cast iron plates were induction hardened to Rockwell C 38 minimum and ground to an average surface roughness of 0.15 μm Ra. The range of the surface roughness readings was from 0.06 μm to 0.22 μm Ra with its distribution shown in Fig. 3.7. In order to study the effect of the surface roughness on the friction and wear results, some surfaces were prepared manually by using different grits sand paper.

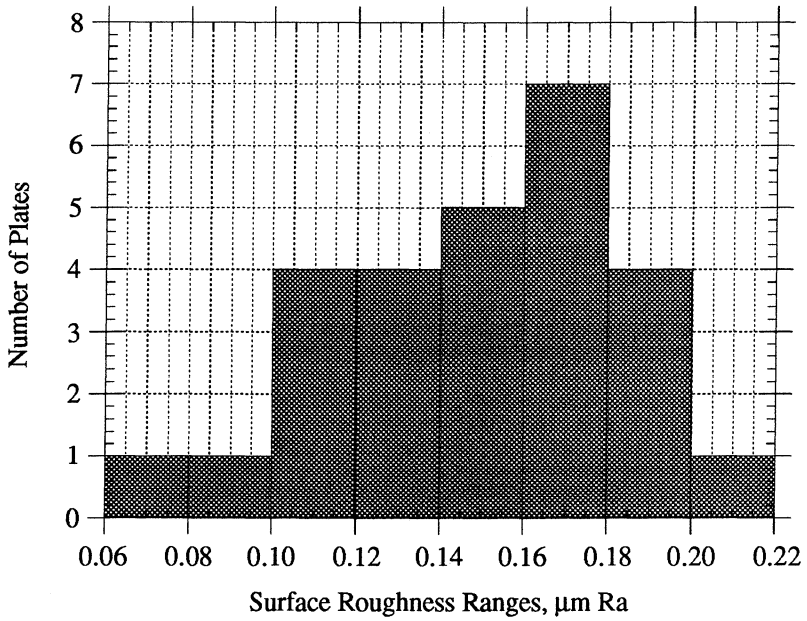

Fig. 3.7 - Distribution of Cast Iron Plate Surface Roughnesses

3.2.2 Test Conditions and Test Duration

The contact pressure used in the tests ranged from 100 psi up to the compressive strengths of the materials used. In some cases, specimens were broken during the loading. These tests and the corresponding contact pressures are not presented in this study. The contact pressure was varied both in order to obtain different PV values, and to define the range of pressures at which the polymers studied can successfully operate. The sliding velocity was varied over a broad range for the same purpose. The environmental

temperature was kept the same for most of the tests and was only changed in order to obtain some data at room temperature to compare with other studies, or when running a test in liquid refrigerants environment. The environmental pressure was kept constant for all the tests, except when testing in liquid refrigerants. The tests conducted in air and argon are for comparative purposes only.

The duration of the tests was chosen so that wear can be easily measured. Also, the duration of the tests was substantially longer than the initial run-in period which could extend from a few minutes at the higher PV values (above 100,000 psi•fpm) to almost half an hour at the lowest PV's. Test data from other studies [2, 4, 11] suggest that the wear rate remains constant after steady-state conditions are reached. Therefore, the duration of the tests would not significantly influence the friction coefficient and the wear rates obtained. The test conditions and duration are summarized in Table 3.5

Table 3.5 - Test Conditions

Test Conditions	Range of Change
Contact Pressure	100 - 4,000 psi for dry sliding conditions 500 - 13,000 psi for lubricated conditions
Sliding Velocity	25 - 664 fpm
Environmental Temperature	20 - 250°F • 20°F - R134a Liquid Refrigerant • 73°F - R134a at Room Temperature • 250°F - Nominal Test Conditions
Surface Roughness of the Cast Iron Plate	0.06 - 0.40 μm Ra
Environmental Pressure	25 psig for all gas tests 225 psig for liquid refrigerant tests
Test Duration	1 - 10 hr
Environment	Air Argon Tetrafluoroethane (R134a), gas Tetrafluoroethane (R134a), liquid Chlorodifluoromethane (R22), gas Polyalkylene glycol base oil (PAG-Base) + R134a

3.2.3. Friction and Wear Measurements

The frictional force and the load on the specimen were monitored constantly throughout the test by a computer controlled data acquisition system. The latter is discussed in more detail in Chapter 5 of this study. It was not possible to record the wear rate during the test. The test facility monitors the linear displacement as the specimen is worn out, but with the typical wear rates under the conditions studied, this linear displacement would be on the order of a thousandth of an inch after ten hours of testing. The instrumentation on the tribometer is not sensitive enough to obtain such an accurate measurement. The wear of the specimens was obtained by weight loss measurements. The weight of the specimen was measured with an analytical balance before and after the test. The balance has an accuracy of one hundredth of a milligram.

The wear measurements were complicated by water desorption from the polymer. Sliney [12] has studied the water desorption rates for polyimide composite material at 390°F. According to this study, about 50% of the total loss due to water desorption occurred during the first hour of the test. Then, over 90% of the loss was recorded after about five hours of testing. The process, however, became much slower thereafter. The opposite process, water absorption, is similar with respect to the time intervals involved. Data for the total amount of moisture absorbed are given in polymer manufacturers manuals [9, 13]. These data were verified under conditions typical for this study. Virgin specimens were tested both in air and R134a refrigerant environment at 250°F. These tests did not reveal any significant difference between the air and refrigerant environments, which was an indication that the polymers did not degrade in the refrigerant environment. Since there was no evidence of chemical degradation the whole amount of weight loss was attributed to water desorption. Data from the literature and the results obtained in this study are given in Table 3.6. The difference in the data is due to the different relative humidity under which the data were obtained.

Table 3.6 - Percent by Weight Water Absorption for Various Polymers

Polymer Grade	Torlon 4301	Vespel SP-21D	Vespel SP-211	Vespel SP-3
References [1,9]	0.280 %	0.190 %	0.210 %	0.230 %
This Study	0.464 %	0.606 %	0.206 %	0.174 %

Since tests with various durations were conducted, the water desorption rate as a function of time had to be measured. The water desorption rate of virgin plates and plates that had been tested for two hours at 245°F were measured. These are presented in Fig. 3.8. The values of interest are the one-hour weight loss and the ten-hours weight loss,

since most of the tests were either one or ten hours long. In one hour, the water desorbed from the specimens was about 0.18% by weight for all polymer grades. The water desorbed in ten hours, which is close to the saturated conditions, is given in Table 3.6.

The weight loss due to wear was obtained by subtracting the weight loss due to water desorption from the total weight loss measured.

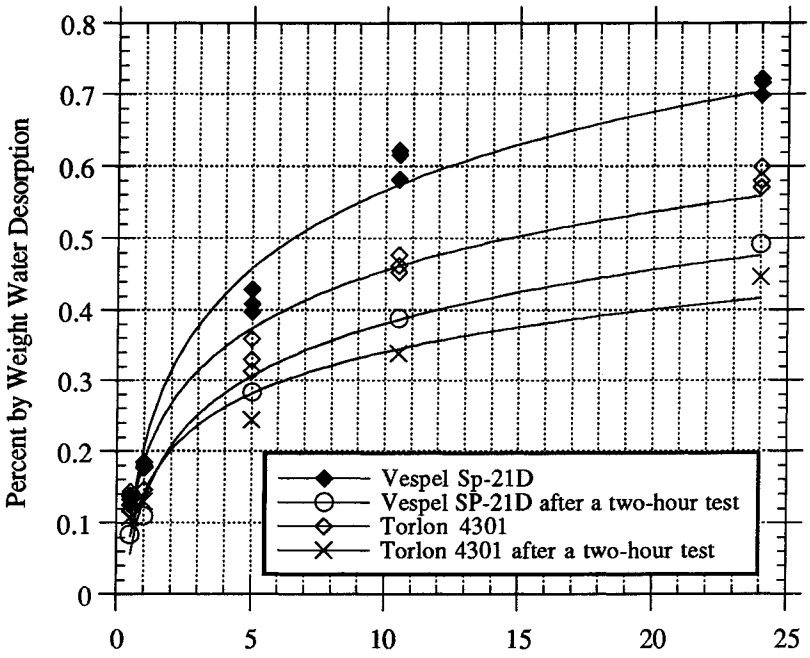

Fig. 3.8 - Water Desorption Rates

3.3. Estimates of the Interface Temperature

3.3.1 Theoretical Background

As already mentioned, the major limiting factor for the application of polymers in dry sliding conditions is the interfacial temperature rise. For thermoplastic polymers, it may lead to material softening and loss of strength or even melting. For thermosetting materials, it leads again to a loss in mechanical properties and to thermal degradation.

The maximum temperature of a single asperity can be obtained by superimposing the flash temperature at the tip of the asperity and the average interface temperature [14]: $T = \theta + T_a$. The mean surface temperature $T_a = T_0 + C\mu Wv$, where T_0 is the temperature of the environment, μ is the coefficient of friction, W is the load on the contact, v *is* the sliding velocity, and C is a constant characterizing the thermal transfer properties of the materials and the geometry of the contact. The temperature T_a can be measured with a thermocouple or some other method. The flash temperature θ, however, is extremely difficult to obtain. Many attempts have been made to measure the actual temperature at the

interface with limited success so far [11]. There are theoretical methods for estimating the flash temperature [15]. According to Jaeger's general analysis for two semi-infinite bodies in relative motion, the flash temperature is given by two different formulae for the stationary and the moving bodies (Fig. 3.9).

For the stationary body, the flash temperature is:

$$\theta = 0.2375\frac{r\mu pvA}{kl} \tag{3.1}$$

where:

μ is the friction coefficient

p is the contact pressure, Pa

v is the sliding velocity, m/s

l is the half length of the side of the square area of contact, m

k is the thermal conductivity of the material, W/m°K

r is the percentage of the heat generated that is conducted into the stationary body

A is the apparent area of contact, m^2

For the moving body, the flash temperature is given by:

$$\theta = 0.267\frac{(1-r)\mu pvA}{kl}\left(\frac{vl}{\alpha}\right)^{-\frac{1}{2}} \tag{3.2}$$

where:

$\alpha = k/\rho c$ is the thermal diffusivity, m^2/s

ρ is the density of the moving body, kg/m^3

c is the specific heat of the moving body, J/kg°K

Depending on the sliding velocities, two extreme cases can be distinguished. At low speeds, sufficient time is available for a thermal equilibrium to be reached. In this case, the value of r can be found by equating the flash temperatures of the two bodies while assuming the formula for the stationary body for both of them. Then substituting for r and doing some simplifications, the expression for the flash temperature becomes:

$$\theta = 0.2375\frac{\mu pvA}{l\left(k_1 + k_2\right)} \tag{3.3}$$

Here k_1 and k_2 are the thermal conductivities of the two materials in contact. In the case of high speeds, the expression for the flash temperature becomes:

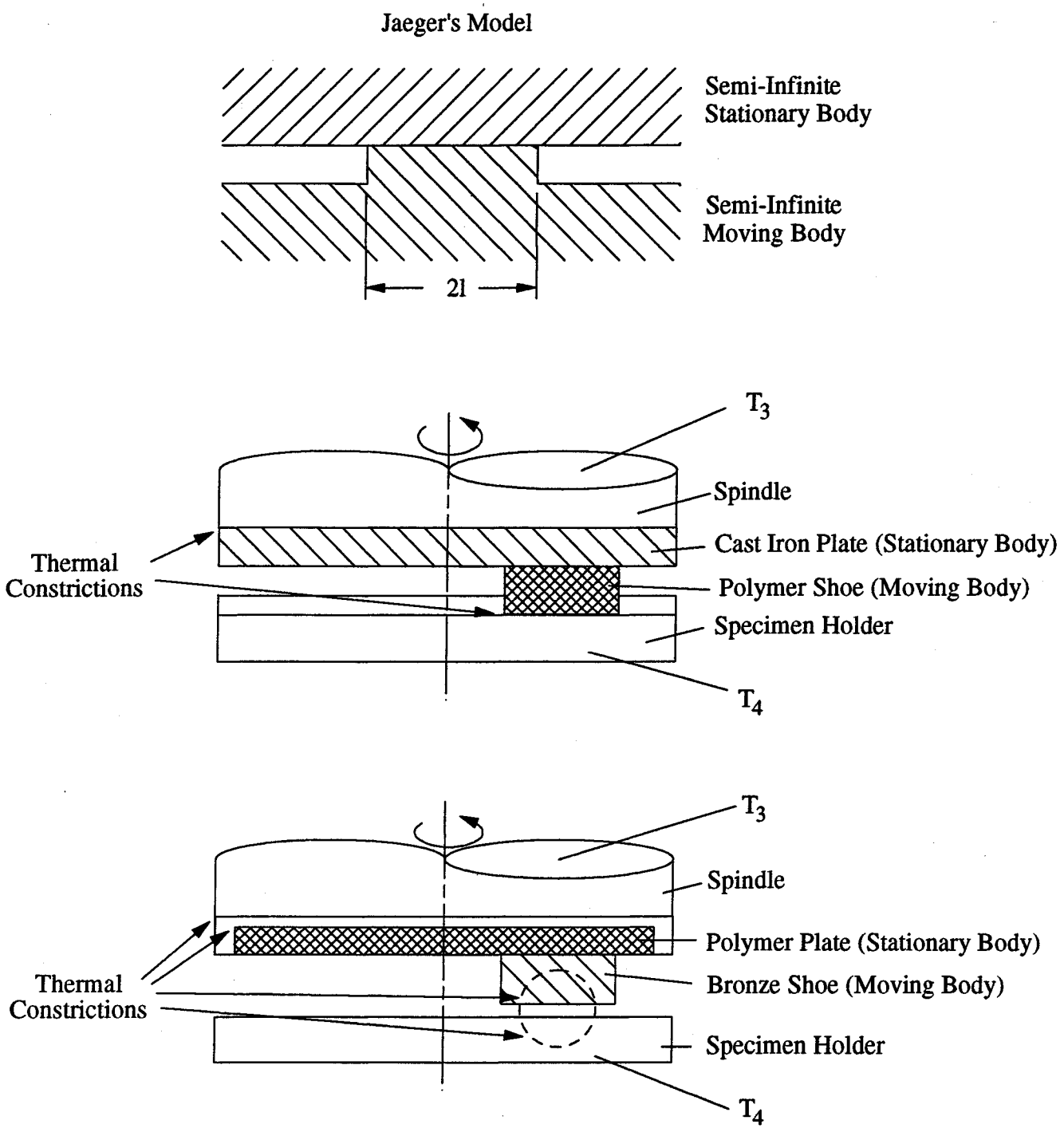

Fig.3.9 - Applied Jaeger's Model to the Contacts Studied

$$\theta = \frac{0.267\frac{\mu pvA}{l}\left(\frac{vl}{\alpha_2}\right)^{-\frac{1}{2}}}{k_2 + 1.124k_1\left(\frac{vl}{\alpha_2}\right)^{-\frac{1}{2}}} \tag{3.4}$$

The distinction between the two limiting cases is based on the value of parameter L_i, known as the Peclet number and defined as:

$$L_i = \frac{lv\rho c}{2k} \tag{3.5}$$

If $L_i < 0.5$ formula (3.3) is used. If $L_i > 10$, then formula (3.4) gives the best results. The main uncertainty in applying these equations to friction and wear problems, as Lancaster [14] points out, is the length l. This length depends on many parameters such as the surface roughness of both specimens, the mode of deformation, i.e. whether elastic or plastic deformation prevails, and the elastic modulus of both mating materials at the given conditions. Even if all these parameters are known, the estimation of l will not be an easy task. In the case of polymers sliding against metal surfaces, this problem is complicated by the fact that some polymer film is transferred onto the metal surface, and as a consequence, the contact is essentially between the polymer and the film. Hence, both surfaces can undergo large elastic deformations. In addition, polymers are visco-elastic and their modulus of elasticity depends on factors such as temperature and sliding velocity. Another complication arises from the fact that the mating surfaces are constantly changing throughout the sliding process. All the above complications make an accurate estimation of the flash temperature almost impossible.

It seems, however, that it is possible to define at least the upper and lower bounds of the flash temperature. The lower bound of the flash temperature can be obtained if an assumption is made that the real area of contact is equal to the apparent area. In this case the heat generated will be distributed over the whole apparent area. Hence Jaeger's formulae can be applied with

$$l = \frac{1}{2}\sqrt{A} \tag{3.6}$$

The formulae for calculating the upper bound of the flash temperature are giveh by Lancaster [21,22]. In this study, it is postulated that the whole load on the specimen is carried by a single contact which is plastically deformed. Hence the flow pressure

(approximately equal to the indentation hardness) of the polymer enters into the formulae and the half side length of the contact is given by:

$$l = \frac{1}{2}\sqrt{A}\sqrt{\frac{p}{p_m}} \tag{3.7}$$

where p_m is the flow pressure. It can be seen from the above equation that the only difference between these two approaches lies in the assumptions for the size of the contact area. When $p \rightarrow p_m$, the two methods will give the same answers since the real area of contact will approach the apparent area.

There is, however, one more complication to equation (3.7). The flow pressure is temperature dependent. Lancaster has suggested that the value of p_m be modified on the basis of the flash temperature found in equation (3.3) or (3.4). The modification is given by an exponential law:

$$p_m = p_o e^{-\lambda(T_0+\theta)} \tag{3.8}$$

where $\lambda = 0.005$ for most polymeric materials and p_0 is the flow pressure found at room temperature. This approach suggests that a number of iterations have to be made in order to obtain the final value of the flash temperature.

Real surfaces will make contact on numerous asperities, i.e. many heat sources will be present on the surface simultaneously. The heat generated by each asperity will be different from the others and will depend on the current load distribution among the points into contact. Whether the real flash temperature will be closer to the upper or the lower bound will depend on the ratio between the real and the apparent area of contact.

3.3.2 Thermal Properties of Contacting Materials

The thermal properties of Vespel and Torlon were obtained from manufacturers publications. Data for the cast iron plates and the bronze shoes were taken from the ASM Handbook [16, 17]. Thermal and other relevant material properties of the specimen under study are summarized in Table 3.7

3.3.3 Estimates of the Interface Temperature

There are two cases of interest: a polymer shoe sliding on a cast iron plate, and a bronze shoe sliding on a polymer plate. In both cases the shoe was assumed to be the moving body while the plate the stationary body. This, however, is exactly opposite to the

movement of the specimens in the tribometer where the plate rotates with the spindle and the shoe is held stationary with respect to the test chamber. For the flash temperature calculations, however, it is the relative motion that really matters (Fig. 3.9).

Table 3.7 - Selected Thermal Properties of the Materials Tested

Material	Density ρ kg/m^3	Thermal Conductivity k W/m°K	Specific Heat c J/kg°K	Thermal Diffusivity α m^2/s	Flow Pressure p_m MPa
Torlon 4301	1460	0.54	1248	2.96×10^{-7}	170
Vespel SP-21D	1510	0.87	1130	5.10×10^{-7}	133.1
Vespel SP-211	1550	0.76	1130	4.34×10^{-7}	102
Vespel SP-3	1600	0.47	1130	2.60×10^{-7}	127.6
SiPb Bronze	8400	39	375	1.24×10^{-5}	---
88-55-06 Ductile Cast Iron	7100	36	461	1.01×10^{-5}	---

3.3.3.1 Polymer Shoe Sliding on a Cast Iron Plate

An example of an estimate of the interface surface temperature is given in this section. The results for the various tests conducted under different conditions are summarized in tables and given under the Results and Discussion section of this chapter.

Schematics of the thermal arrangement for both the polymer shoe on cast iron disk, and bronze shoe on polymer disk are given in Fig. 3.9. According to these schematics, the only temperatures that were directly measured were T_3 and T_4. They correspond to the environmental temperatures T_0 for the two bodies in contact. For the case under consideration T_3 was about 15°F higher than T_4. This was due to the fact that the thermal conductivity of the polymer shoe was much lower than that of the cast iron plate, and most of the heat generated at the contact was conducted through the plate. There certainly was some temperature difference between the surface of the plate and T_3 due to the thermal constriction between the plate and the spindle and the thermal resistance of the spindle itself. It is, however, believed that this temperature difference was small compared to both T_3 and the estimated flash temperature due to the high thermal conductivities of the plate and the spindle. Therefore, without sacrificing much in accuracy, it can be assumed that the mean temperature of the plate was approximately equal to T_3. Thus the total interface temperature becomes:

$$T = T_3 + \theta \tag{3.10}$$

An example of the flash temperature (θ) estimation is given below. The calculations are based on the following test conditions:

• contact pressure	p = 500 psi (3.445 MPa)
• sliding velocity	v = 100 fpm (0.508 m/s)
• PV value	pv = 50,000 psi•fpm (1.75 MPa•m/s)
• coefficient of friction	μ = 0.413
• ave. contact temperature	T_3= 245°F (118.3°C)
• apparent contact area	A = 0.0263 in^2 (16.98 mm^2)

and from Table 3.7, the material properties of the bodies in contact are:

• polymer thermal conductivity	k_2 = 0.87 W/m°K
• plate thermal conductivity	k_1 = 36 W/m°K
• polymer thermal diffusivity	$\alpha_2 = 5.10 \times 10^{-7}$ m^2/s
• polymer flow pressure	p_m = 102 MPa

First, the lower bound will be estimated. The half side length of the contact area is given by:

$$l = \frac{1}{2}\sqrt{A} = \frac{1}{2}\sqrt{16.98} = 2.06 \text{ mm}$$

Then, the flash temperature is given by:

$$\theta = \frac{0.267\frac{\mu pvA}{l}\left(\frac{vl}{\alpha_2}\right)^{-\frac{1}{2}}}{k_2 + 1.124k_1\left(\frac{vl}{\alpha_2}\right)^{-\frac{1}{2}}} =$$

$$= \frac{(0.267)\frac{(0.413)(3.445\times10^6)(0.508)(16.98\times10^{-6})}{2.06\times10^{-3}}\left[\frac{(0.508)(2.06\times10^{-3})}{4.34\times10^{-7}}\right]^{-\frac{1}{2}}}{(0.76)+(1.124)(36)\left[\frac{(0.508)(2.06\times10^{-3})}{4.34\times10^{-7}}\right]^{-\frac{1}{2}}} = 20.44\ ^\circ\text{C}$$

Next, the upper bound of the flash temperature will be estimated. According to Lancaster's method, the half side length of contact area is given by:

$$l = \frac{1}{2}\sqrt{\frac{pA}{p_m}} = \frac{1}{2}\sqrt{\frac{(3.445\times10^6)(16.98\times10^{-6})}{(102\times10^6)}} = 0.38 \text{ mm}$$

Then, from formula (3.5), the Peclet number becomes:

$$L_i = \frac{vl\rho c}{2k} = \frac{(0.508)(0.38\times10^{-3})(1550)(1130)}{(2)(0.76)} = 222$$

Since $L_i > 10$, formula (3.4) holds, and the flash temperature can be estimated a

$$\theta = \frac{0.267\dfrac{\mu pvA}{l}\left(\dfrac{vl}{\alpha_2}\right)^{-\frac{1}{2}}}{k_2 + 1.124k_1\left(\dfrac{vl}{\alpha_2}\right)^{-\frac{1}{2}}} =$$

$$= \frac{(0.267)\dfrac{(0.413)(3.445\times10^6)(0.508)(16.98\times10^{-6})}{0.38\times10^{-3}}\left[\dfrac{(0.508)(0.38\times10^{-3})}{4.34\times10^{-7}}\right]^{-\frac{1}{2}}}{(0.76)+(1.124)(36)\left[\dfrac{(0.508)(0.38\times10^{-3})}{4.34\times10^{-7}}\right]^{-\frac{1}{2}}} = 152.6\ ^\circ\text{C}$$

This value has to be modified to account for the variable flow pressure. From equation (3.8)

$$p_m = p_0 e^{-\lambda(T_0+\theta)} = (102\times10^6)e^{-0.005(118.3+152.6)} = 26.3\times10^6 \text{ Pa}$$

With this new flow pressure, a new value for l is calculated, then a new value for θ and so forth. After several iterations the final value for the flash temperature is calculated as θ = 85 °C.

The temperature values estimated by the two methods give a temperature difference of about 60°C. The real flash temperature will be somewhere in between these two.

3.3.3.2 Bronze Shoe Sliding on a Polymer Plate

The calculations for the flash temperature in this case follow the same procedure as for the polymer shoe on the cast iron plate. The bronze shoe is the moving while the

polymer plate is the stationary body. The environmental temperature T_0 is equal to T_4 because the thermal conductivity of the polymer plate is much lower than that of the bronze shoe and most of the heat will be conducted through the shoe. For these tests, T_4 was higher than T_3 by only 3-5 °F.

There is one important simplification of formula (3.4) that can be made in this case. The bronze thermal conductivity is much greater than the thermal conductivity of the polymer. Therefore, neglecting the much smaller term, the expression for the flash temperature becomes:

$$\theta = 0.267\left(\rho_2 c_2 k_2\right)^{-1/2} \mu p A v^{1/2} l^{-3/2} \tag{3.9}$$

The lower bound formula for the flash temperature, making use of equation (3.6), becomes:

$$\theta = 0.755\left(\rho_2 c_2 k_2\right)^{-1/2} \mu p A^{1/4} v^{1/2} \tag{3.10}$$

Substituting for l from equation (3.7), the upper expression gives:

$$\theta = 0.755\left(\rho_2 c_2 k_2\right)^{-1/2} \mu p^{1/4} A^{1/4} v^{1/2} p_m^{3/4} \tag{3.11}$$

From this expression, it is evident that the sliding velocity will have a stronger effect than the contact pressure on the magnitude of the flash temperature. An example of the flash temperature estimation is given below. The conditions for the test were:

- contact pressure — p = 500 psi (3.445 MPa)
- sliding velocity — v = 100 fpm (0.508 m/s)
- PV value — pv = 50,000 psi•fpm (1.75 MPa•m/s)
- ave. coefficient of friction — μ = 0.318
- ave. contact temperature — T_4 = 245°F (118.3°C)
- apparent contact area — A = 0.142 in^2 (91.6 mm^2)

Also, the material properties from Table 3.7 are:

- bronze shoe thermal conductivity — k_2 = 39 W/m°C
- bronze shoe density — ρ_2 = 8,400 kg/m^3

- bronze shoe specific heat $c_2 = 375$ J/kg°C
- polymer flow pressure $p_m = 170$ MPa

The flash temperatures calculated from formulae (3.10) and (3.11), respectively are: $\theta = 5.2$°C and $\theta = 51$°C (after iterations). Again there is substantial difference between the two temperature estimates. Lancaster's method seems to better account for the physical phenomena that occur in the interface when the sliding velocity or contact pressure is changed. It accounts for the change of the real area of contact with the pressure. It has been proven [14] that this method gives good predictions when applied to some thermoplastic materials to predict the PV value at which melting on the surface will occur.

3.4 Results and Discussion

3.4.1 General Remarks

The mechanism of friction and wear in a polymer-metal interface is still not very well understood. In most tests, some polymer is transferred onto the metal surface and, after this has occurred, the contact is partially between the polymer and the transferred film. It is also generally accepted that the polymer transfer onto the metal surface is extremely important for the tribological effectiveness of the interface [18, 19, 20]. The type, appearance, and mechanical properties of the transferred film depend on various factors such as chemical composition of the bulk polymer, contact pressure and sliding velocity, interface temperature, and type of environment. Analyses of friction and wear results have revealed that, for a single contact spot, the lubrication of polymers can be represented as a sequence of events such as contact-adhesive interaction, shear of the surface layer, repeated plastic deformation, separation of a particle from the polymer, transfer onto the counterface, repeated deformation of the transferred layer, dispersion, and removal from the friction zone [20, 21].

3.4.2 Friction Coefficient and Wear Rates at Various PV Values

3.4.2.1 Dry Contacts

Most of the tests in this set were conducted at an environmental temperature and pressure of 250°F and 25 psig, respectively and in a R134a refrigerant environment. Polymers were used both as plates and shoes. The range of the contact pressures applied was from 100 to 2000 psi, and the sliding velocity ranged from 40 to 800 fpm. The test duration was either one or ten hours. The friction and wear data for different materials tested are summarized in Tables 3.8 through 3.11.

Table 3.8 - Friction and Wear Data for Torlon 4301 Shoes Slid Against Cast Iron Plates. Dry Sliding Conditions. R134a Environment. Temperature = 245°F

Pressure psi	Velocity fpm	PV psi•fpm	Friction Coefficient	Shoe Wear in./1000hr	Specific Wear $10^{-10}\frac{in.^3 \bullet min.}{ft \bullet lbf \bullet hr}$
500	50	25000	0.30	0.20	80
500	75	37000	0.20	0.14	38
500	100	50000	0.27	0.24	47
500	150	75000	0.40	0.29	39
500	200	100000	0.48	0.36	36
500	300	150000	0.25	0.35	24
500	400	200000	0.52	0.41	20
500	600	300000	0.47	0.89	30
500	800	400000	0.22	0.70	18
1000	800	800000	0.22	1.10	14

Table 3.9 - Friction and Wear Data for Vespel SP-3 Shoes Slid Against Cast Iron Plates. Dry Sliding Conditions. R134a Environment. Temperature = 245°F

Pressure psi	Velocity fpm	PV psi•fpm	Friction Coefficient	Shoe Wear in./1000hr	Specific Wear $10^{-10}\frac{in.^3 \bullet min.}{ft \bullet lbf \bullet hr}$
500	50	25000	0.34	0.15	59
500	100	50000	0.41	0.38	77
500	150	75000	0.43	0.57	75
500	200	100000	0.26	0.66	66
500	300	150000	0.27	0.59	40
500	400	200000	0.33	1.27	65
500	600	300000	0.25	1.30	42
500	800	400000	0.22	0.86	22

The wear rate, in inches per 1000 hours, as a function of the PV value, is given in Fig. 3.10. From this plot, it is evident that in all cases the wear rate increased with the PV. The rate is higher at the low PV's and, depending on the material, tends to level off at values between 400,000 and 800,000 psi•fpm. The lowest wear rates were obtained with Vespel SP-211 and the highest with Vespel SP-3. Torlon, in the form of shoes and plates, showed intermediate wear results. From the plot, it can also be seen that the wear rates of Torlon plates were slightly higher than those for the Torlon shoes. This difference can be attributed to the different flash temperature rise and to the different counterface material, bronze in the first case and cast iron in the second. On the same plot, data for the oil lubricated contacts are presented as well. These are very similar for all the materials studied, and, as a rule, are one order of magnitude lower than the wear rates obtained under dry sliding conditions.

Table 3.10 - Friction and Wear Data for Vespel SP-211 Shoes Slid Against Cast Iron Plates. Dry Sliding Conditions. R134a Environment. Temperature = 245 °F

Pressure psi	Velocity fpm	PV psi•fpm	Friction Coefficient	Shoe Wear in./1000hr	Specific Wear $10^{-10}\frac{in.^3 \bullet min.}{ft \bullet lbf \bullet hr}$
250	664	166,000	0.34	0.15	9.5
500	664	332,000	0.33	0.50	16
750	664	498,000	0.28	0.55	12
1000	664	664,000	0.25	0.72	12
2000	664	1,328,000	0.21	0.64	5.2

Table 3.11 - Friction and Wear Data for Torlon 4301 Plates Slid Against Bronze Shoes. Dry Sliding Conditions. R134a Environment. Temperature = 245 °F

Contact Pressure psi	Sliding Velocity fpm	PV psi•fpm	Friction Coefficient	Plate Wear in./1000hr	Specific Wear $10^{-10}\frac{in.^3 \bullet min.}{ft \bullet lbf \bullet hr}$
500	50	25,000	0.40	0.18	78
500	100	50,000	0.32	0.27	58
500	150	75,000	0.29	0.39	83
1000	400	400,000	0.13	0.71	14

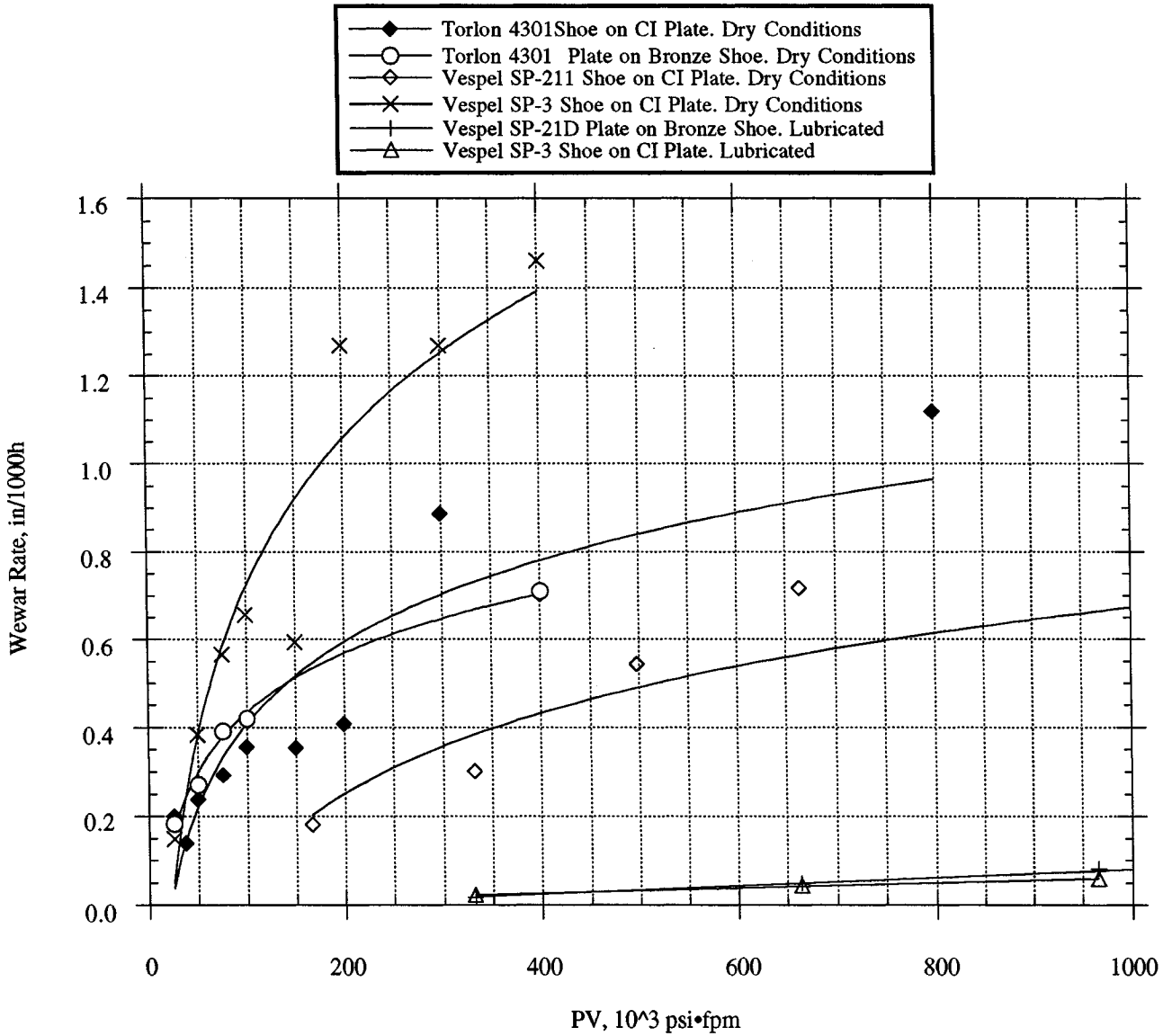

Fig. 3.10 - Effect of PV on the Wear Rate for Various Material Pairs and Sliding Conditions

The effect of the PV on the specific wear rate is given in Fig. 3.11. The specific wear rate decreases with increasing PV value. This effect is more pronounced with the Torlon specimens. Also, the rate of change of the specific wear rate is highest at the lowest PV's and tends to level off for the highest PV's.

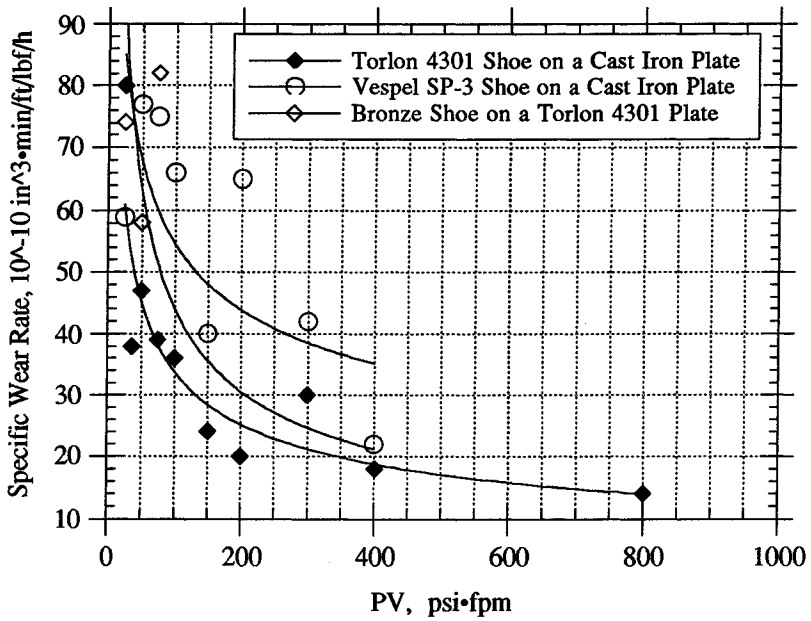

Fig. 3.11 - Effect of the PV on the Specific Wear Rate for Various Material Pairs.

Under dry sliding conditions, a considerable scatter of friction and wear data was observed. This erratic behavior, especially for the friction coefficient, seems to be typical for these materials. Jones [23] has reported ranges of the friction from 0.15 to 0.60 at 500°F. This range is similar to that observed in this study. Plots for the ranges and distribution of the friction coefficient for the various materials studied are given in Figures 3.12 and 3.13. The mean value and the range of the friction coefficient for the materials studied are given in Table 3.12.

Table 3.12 - Mean Value and Range of the Friction Coefficient

Contact Pair Materials	Mean Friction Coeff.	Minimum Friction Coeff.	Maximum Friction Coeff.
Torlon on Cast Iron	0.33	0.20	0.52
Torlon on Bronze	0.30	0.19	0.40
Vespel SP-211 on Cast Iron	0.30	0.21	0.40
Vespel SP-3 on Cast Iron	0.29	0.20	0.43

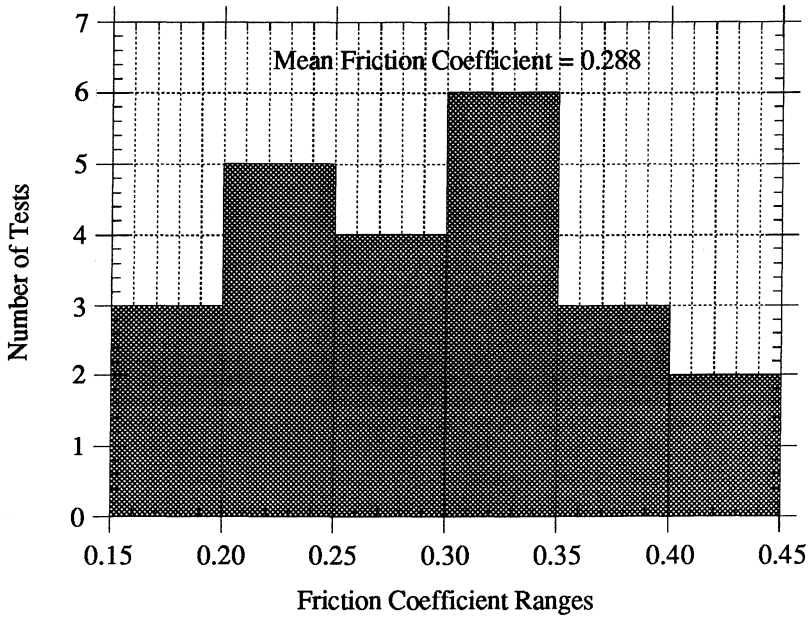

Fig. 3.12 - Range and Distribution of the Friction Coefficient for Vespel SP-3 Shoes Sliding on Cast Iron Under Dry Conditions

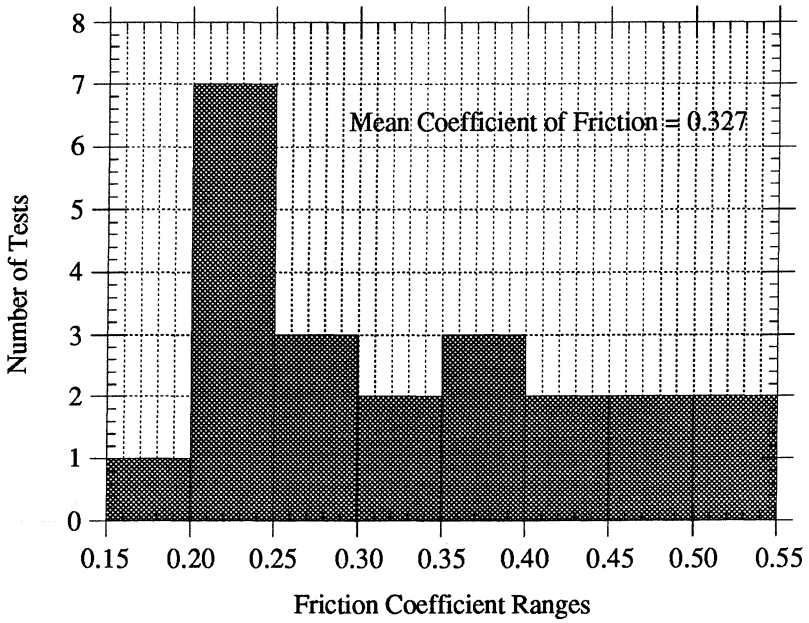

Fig. 3.13 - Range and Distribution of the Mean Coefficient of Friction for Torlon 4301 Shoes Sliding on Cast Iron Plates Under Dry Conditions

The values for the friction coefficient given in the above tables and plots are the mean values obtained by averaging all the data points that were obtained during a test. In most cases, the friction coefficient varied significantly throughout the test as well. It is very difficult to define any general rule for the change of the friction coefficient throughout the test. At moderate PV's (about 50,000 psi•fpm), it generally started at some low value at the beginning of the test when initial polymer transfer probably takes place. In the first few minutes, the friction coefficient increased to a much higher value, then dropped a little, and finally reached some steady-state condition. It should be emphasized that the steady-state condition was characterized by considerable variation as well. A typical record of the range of the friction coefficient throughout a test is given in Fig. 3.14. Since the run-in process was relatively short, an expanded plot of the first 100 minutes of testing is presented in Fig. 3.15. In this test, a Vespel SP-211 shoe was tested on a cast iron plate.

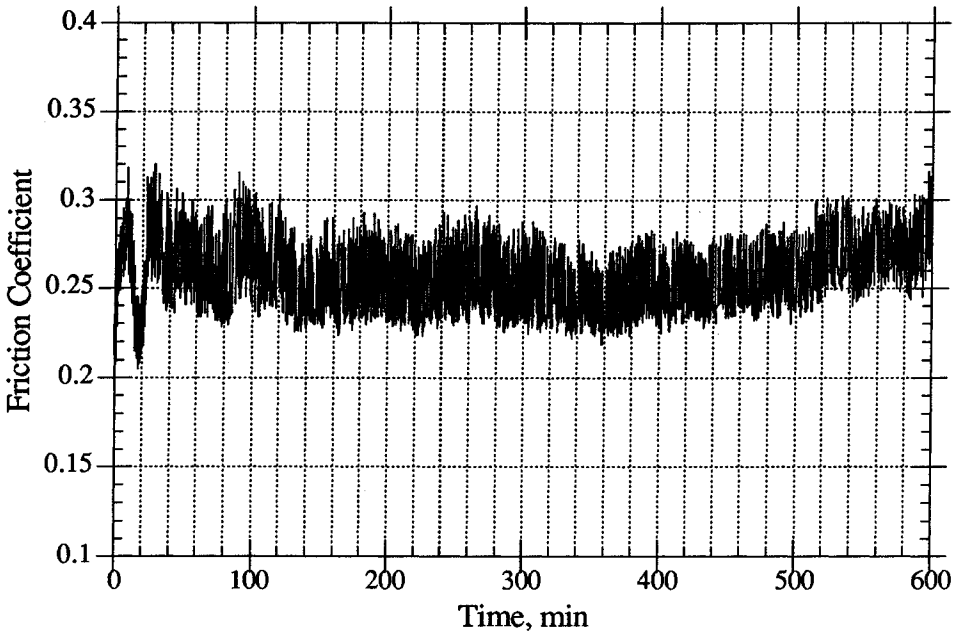

Fig. 3.14 - A Typical Record of the Friction Coefficient in Dry Sliding Conditions

Some of the friction records showed cyclic change in the friction coefficient from a lower to higher value. This phenomenon was more pronounced when tests were conducted at a lower (70°F) temperature. This "saw-teeth" appearance of the record is thought to be due to a cyclic process of polymer transfer onto and from the mating metal surface. A plot showing this kind of behavior is given in Fig. 3.16.

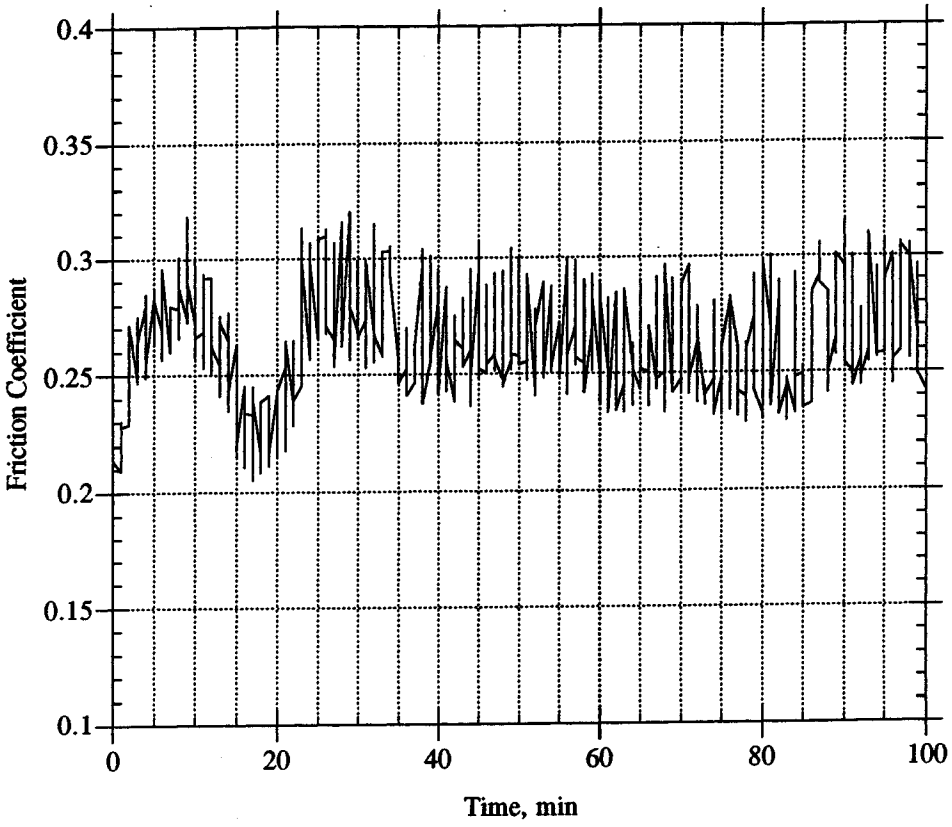

Fig. 3.15 - Initial Variation of the Friction Coefficient in Dry Sliding Conditions

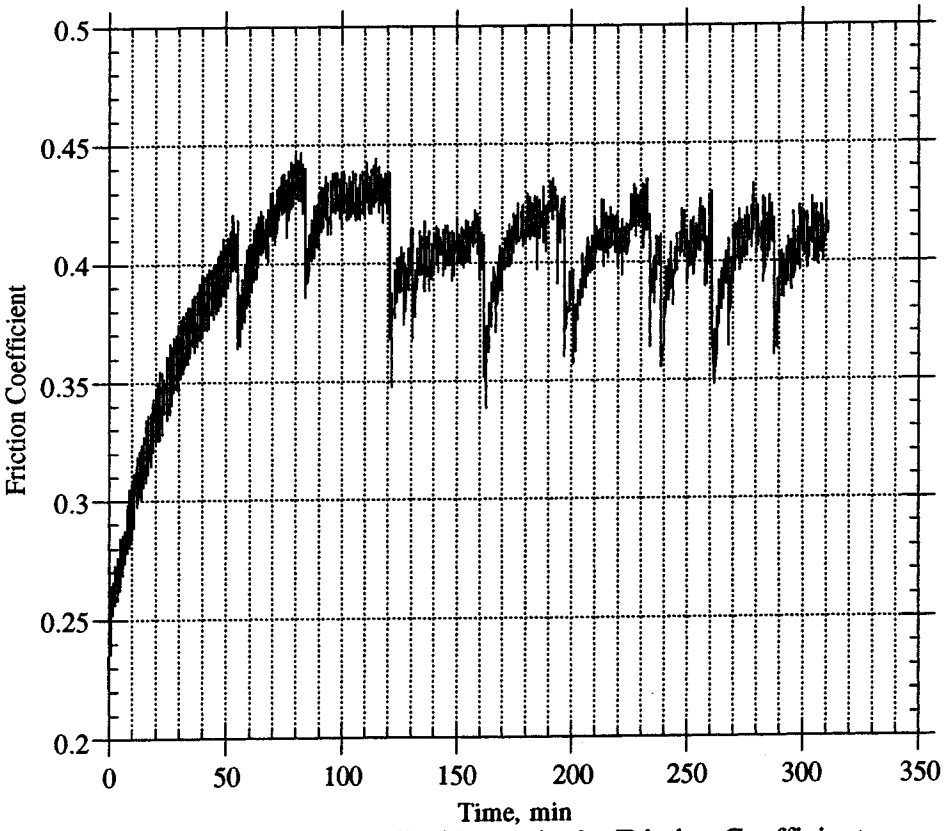

Fig. 3.16 - Cyclic Change in the Friction Coefficient

3.4.2.2 Oil Lubricated Contacts

The relatively good performance of polyimide and poly(amide-imide)s in dry sliding conditions has to be viewed as an insurance in periodic extreme boundary lubrication conditions which a component may experience rather than a normal condition of operation. For the contacts under study, the tribological properties under lubricated conditions may be the decisive factor for the applicability of these polymers as real component materials.

The conditions for this set of tests were as follows:

- Contact pressure: in the range of 500 to 12,900 psi
- Sliding velocity: either 40 or 664 fpm
- Environmental temperature: 165°F
- Environment: R134a, gas
- Environmental pressure: 25 psig
- Lubricant: polyalkylene glycol (designated as PAG base in Table 2.3). Contacts were fully submerged into the lubricant.

Test results for the lubricated contacts are presented in Tables 3.13 and 3.14, and in Fig. 3.10. The wear rates, in inches per 1000 hours, under lubricated conditions are approximately a factor of ten lower than those in dry conditions with the same PV value. Since the wear rates are much lower for this kind of test, the lines representing these data are very close to the abscissa in Fig. 3.10. A separate plot for the lubricated tests is given in Fig. 3.17.

The data presented in Fig. 3.17 show almost a linear increase in the wear rate with the PV. In fact, almost all these tests were conducted at the same sliding velocity and only the contact pressure was varied. From Tables 3.13 and 3.14, it can be concluded that the specific wear rate is not affected by the increase in the pressure. This, however, is true only below a certain pressure limit. The tests conducted at high contact pressures (9,600 and 12,900psi) showed much higher specific wear. This is probably due to the fact that other wear mechanisms are involved which are not present at the lower pressures. Such wear mechanism could be surface fatigue and delamination.

3.4.3 Effect of the Environment

Tests in this set were conducted in four gaseous environments: R134a, R22, air, and argon. In addition, tests in liquid R134a were performed. The environments of interest were R134a and R22, while air and argon were used for comparative purposes only. The other conditions for the tests are given in Table 3.1. Polymer grades with graphite, PTFE, and MoS_2 fillers were tested.

Table 3.13 - Friction and Wear Data for Vespel SP-3 Shoes Slid Against Cast Iron Plates. PAG Base Oil - R134a Environment. Temperature = 165°F. Test Duration = 1 Hour.

Pressure psi	Velocity fpm	PV psi•fpm	Friction Coefficient	Shoe Wear in./1000hr	Specific wear $10^{-10}\frac{in.^3 \bullet min.}{ft \bullet lbf \bullet hr}$
500	664	332,000	0.083	0.021	0.68
1000	664	664,000	0.073	0.043	0.68
1500	664	996,000	0.074	0.058	0.63

Table 3.14 - Friction and Wear Data for Vespel SP-21D Plates Slid Against Bronze Shoes. PAG Base Oil - R134a Environment. Temperature = 165°F. Test Duration = 1 Hour.

Pressure psi	Velocity fpm	PV psi•fpm	Friction Coefficient	Shoe Wear in./1000hr	Specific wear $10^{-10}\frac{in.^3 \bullet min.}{ft \bullet lbf \bullet hr}$
9,600	40	384,000	0.033	0.043	1.2
12,900	40	516,000	0.029	0.127	3.2
500	664	332,000	0.084	0.018	0.53
1000	664	664,000	0.059	0.048	0.74
1500	664	996,000	0.054	0.079	0.84
2000	664	1,328,000	0.053	0.108	0.84

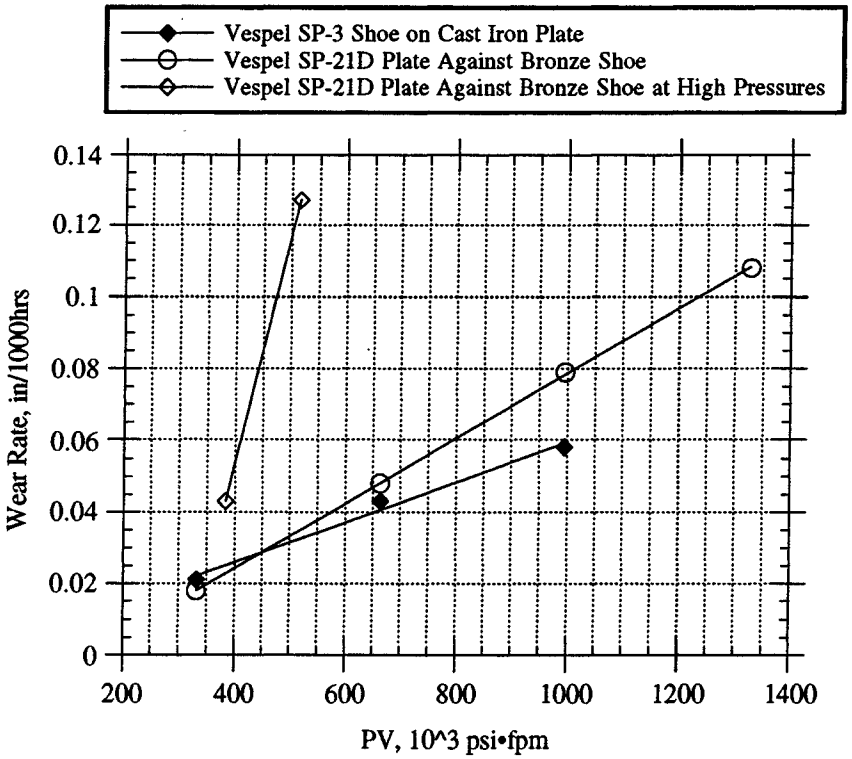

Fig 3.17 - Wear Rate as a Function of the PV for Lubricated Conditions

There are reports in the literature that the environment may affect the tribological characteristics of polyimide and poly(amide-imide) polymers. Fusaro [18] has studied the effect of air moisture on the wear rates of different grades of polyimides and polyimide composites. The presence of moisture in the atmosphere tends to increase the wear rates, especially at temperatures higher than the transition temperature. The effect of a nonoxidizing atmosphere has been studied as well. Lancaster [14] reports that wear tests conducted in a nitrogen environment have produced wear rates one hundred times lower than those in air for some polymer grades. Fusaro [22] has also studied the effect of an argon atmosphere on the friction and wear of thin polyimide films used as a binder material for graphite fluoride and molybdenum disulfide solid lubricants. The polyimide films tested in argon showed both lower friction coefficient and wear rates. This difference in the wear rate ranged from two to ten times depending on the environmental temperature for the test.

It seems that the environment may affect the material properties in three ways: first it may change the behavior of the base polymer material, second it may change the properties of the counterface material, and third it may change the properties of the fillers that have been used in the particular polymer grade.

The effect of different refrigerants on Torlon and Vespel base polymers has not yet been determined. These polymers are resistant to the most common commercially used solvents and other chemical compounds. They are virtually unaffected by alphatic and aromatic hydrocarbons, chlorinated and fluorinated hydrocarbons, and most acids at moderate temperatures. [9, 13]. The refrigerants used belong to the family of chlorinated and fluorinated hydrocarbons. There are data for the chemical resistance of Torlon and Vespel to carbon tetrachloride, ethylene chloride, and 2-chloroethanol. In all these environments the polymers retain 100% of their tensile strength and did not seem to be adversely affected in any other way. The chlorinated refrigerant (R22) is chemically similar to the above compounds, and therefore should not be expected to cause any polymer degradation. Refrigerant R134a is chemically more inert than the chlorinated hydrocarbons and more thermally stable, therefore, it probably should not affect the properties of the base polymers as well.

The tribological properties of a particular polymer grade may still be affected by the presence of a refrigerant, even if the base polymer is not. This effect may be due to the behavior of the filler materials. Graphite is a typical example for the latter. Its ability to form a low shear stress layer on the surface of the mating material is strongly affected by the presence of moisture. The friction coefficient of a polymer with PTFE filler decreases in dry air, but it is not affected by water [27]. On the other hand , MoS_2 has good lubrication properties in vacuum and dry atmospheres.

Refrigerants may have some effect on the counterface materials as well. Refrigerant R22, for example, is very likely to react with the metal surfaces similar to R12, which forms soft chloride protective surface films [1].

Coefficient of friction and wear rate results from the tests conducted in various environments are summarized in Table 3.15 and Fig. 3.18. These results show some difference in the behavior of the polymer grades depending on the filler material used.

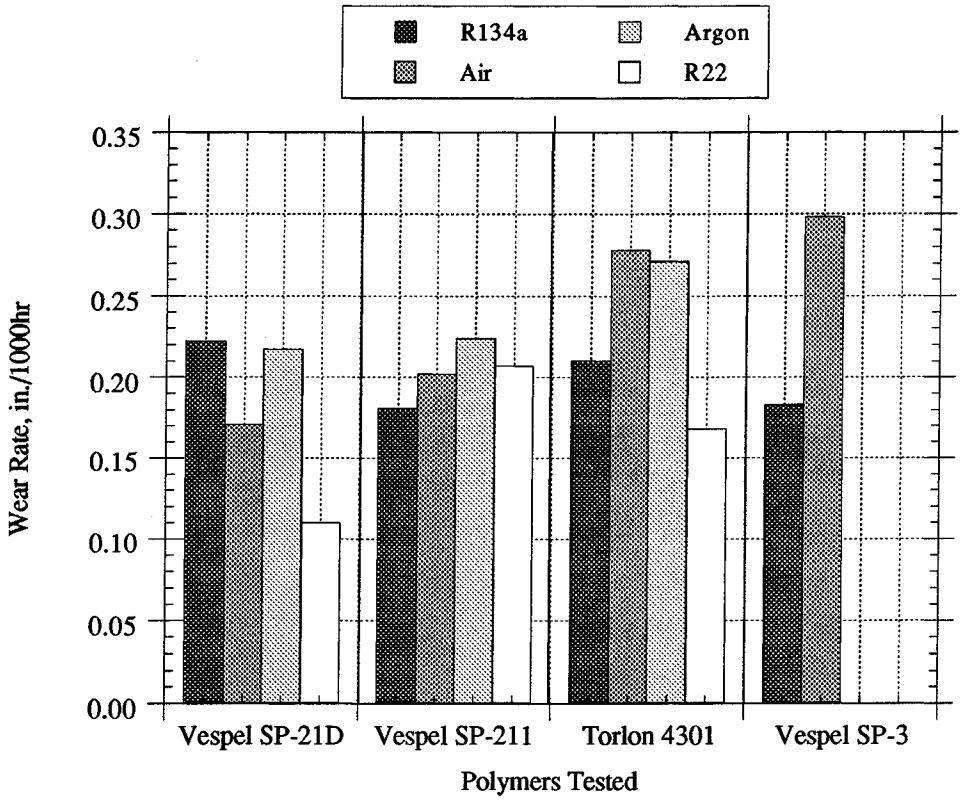

Fig. 3.18 - Effect of the Environment on Polymers Wear Rate

The graphite filled polymers under study were the Vespel SP-21D, Vespel SP-211, and Torlon 4301 grades. According to the results obtained, all these polymer grades may be considered insensitive to the test environment. The wear rates in R134a, air, and argon were very similar. It could be expected that the air environment would produce the highest wear rate. With these materials, however, the wear rate and especially the friction coefficient were lower when tested in air. A possible explanation for this behavior may be that the moisture in the air improves the lubricating characteristics of graphite filler.

Table 3.15 - Effect of the Environment on Friction Coefficient and Wear Rate for Various Polymers

Contact Pair Materials and Test Conditions	Wear Rate, 10^{-10} in^3•min/ft/lbf/h					Coefficient of Friction				
	R134a	Air	Argon	R22	Liquid R134a†	R134a	Air	Argon	R22	Liquid R134a†
Vespel SP-21D Plate on Bronze Shoe P=1000 psi, V=800 fpm, T=245°F, Duration 2hr	0.22	0.17	0.28	0.11	---	0.081	0.048	0.061	0.068	---
Vespel SP-211D Shoe on CI Plate P= 500 psi, V=100 fpm, T=245°F, Duration 10hr	0.27	0.20	0.23	0.20	0.05	0.39	0.29	0.34	0.33	0.19
Torlon 4301 Shoe on CI Plate P= 500 psi, V=100 fpm, T=245°F, Duration 10hr	0.21	0.28	0.27	0.17	---	0.35	0.29	0.51	0.34	---
Torlon 4301 Plate on Bronze Shoe P=1000 psi, V=400 fpm, T=245°F, Duration 1hr	0.79	0.74	0.69	0.63	---	0.13	0.12	0.15	0.14	---
Torlon 4301 Shoe on CI Plate P=500 psi, V=450 fpm, T=245°F, Duration 1hr	0.14	0.16	0.19	---	---	0.34	0.25	0.35	---	---
Vespel SP-3 Shoe on CI Plate P=500 psi, V=100 fpm, T=245°F, Duration 10hr	0.18	0.30	---	---	0.08	0.35	0.40	---	---	0.16

† The tests in liquid R134a were conducted with the same contact pressure and sliding velocity but at different environmental temperatute = 20°F

Since moisture was not present in the argon and R134a gases, the graphite filler did not perform very well in these environments. This behavior was more pronounced with the Vespel SP-21D grade where graphite is the only filler material, and less pronounced with the Torlon 4301 and the Vespel SP-211 which have 10% PTFE as a filler as well.

In R22 environment, the polymers tested provided lower wear rates if not lower friction coefficient. The explanation for this behavior may be a chemical reaction with the counterface metal surface which eventually produces soft, easily sheared films.

It was expected that Vespel SP-3 would show different behavior from the other grades due to the different filler used (MoS_2). It is well known that molybdenum disulfide is not particularly suitable for use in an oxidizing environment. The results for tests run in air and R134a (which can be considered inert), showed a substantially higher wear rate and slightly higher friction coefficient for tests conducted in air. These results are in line with those obtained by Fusaro [22] for MoS_2, polyimide binder thin films.

The major goal for the tests conducted in liquid refrigerant was to find out whether polymer degradation would occur. For some of the tests, the polymers were kept in this environment for 48 hours before the test, and the results were then compared to specimens that were stored in dry air. It was hypothesized that if degradation due to the liquid refrigerant occurred, it would also change the tribological behavior of the polymer. The weight of the specimens, which could also be an indicator of material degradation, was also measured before and after the specimens were submerged in the refrigerant. All these tests did not reveal any material degradation and the friction and wear results obtained were similar to those in a gaseous R134a environment. Since the temperatures were very low (27 °F), the wear results were closer to those obtained from tests at ambient temperature.

3.4.4 Effect of the Counterface

Counterface effects can be divided into two major categories. The first is the effect of the surface roughness of the counterface on the friction and wear of the polymer. The second is the effect of the physical and chemical properties of the mating material.

3.4.4.1 Effect of the Counterface Surface Roughness

The effect of the counterface surface roughness on the tribological performance of various polymers has been extensively studied [7, 11, 20, 21, 24, 25]. It is generally accepted that the increase in the surface roughness also leads to an increase in the wear rates. The correlation between surface roughness parameters and the coefficient of friction is very weak and no general rule can be derived [11]. Polyimides are no exception from this general trend. They, however, seem to be less sensitive to the surface roughness of the

mating material than other polymers [21]. From the data available in the literature [5, 21, 24, 25], it is evident that the slope of the wear rate is steeper at the lower counterface surface roughness values, typically in the range of 0.1 - 0.6 μm Ra [21]. The Ra is not the only surface roughness parameter that influences the wear rate. The average slope of the asperities, the number of the asperity peaks, and the mean radius of curvature of the asperity peaks also have effects on the wear rate. A detailed report on the effects of surface topography on the wear of polyimide polymers is given by Play [5]. Despite the great deal of analytical ingenuity and experimental attention to detail, as Lancaster in a discussion to the same study points out, the results do not really lead to any firm conclusions in identifying which particular parametric combinations of the initial topography are of primary importance in determining steady-state wear. The reason is that the initial counterface topography is modified by the sliding process, and this modified topography ultimately controls the steady-state wear rate. For low initial value of the surface roughness, the polymers tend to polish the surface [21]. There is some indication [21, 25] that, for each polymer and operating conditions, there is some optimal initial value of the counterface surface roughness for which the minimal wear rates are obtained. This effect can be explained by the change in the predominant wear mechanism from adhesive at the lower surface roughnesses to abrasive at the higher roughnesses.

The effect of surface roughness on the friction coefficient is not as significant as on wear. This is due to the fact that most of the friction is generated between the polymer and the transferred film. Therefore, the surface roughness only slightly influences the frictional characteristics, and its effect is primarily due to high asperity peaks that protrude above the polymer film transferred, and lead to an increase in the plowing component of the friction force.

In order to study the effect of the initial counterface surface roughness on polymer friction and wear, cast iron plates with two different surface roughnesses were prepared by using different grit size sand paper. For the rougher surface, a 120 grit sand paper was used. This produced a surface roughness of 0.41 μm Ra. The other surface was produced with a 600 grit paper and subsequent polishing with 0.03 μm Al_2O_3 particles. The surface roughness obtained was 0.062 μm Ra. Traces of both the rougher and the smoother surfaces are given in Fig. 3.19.

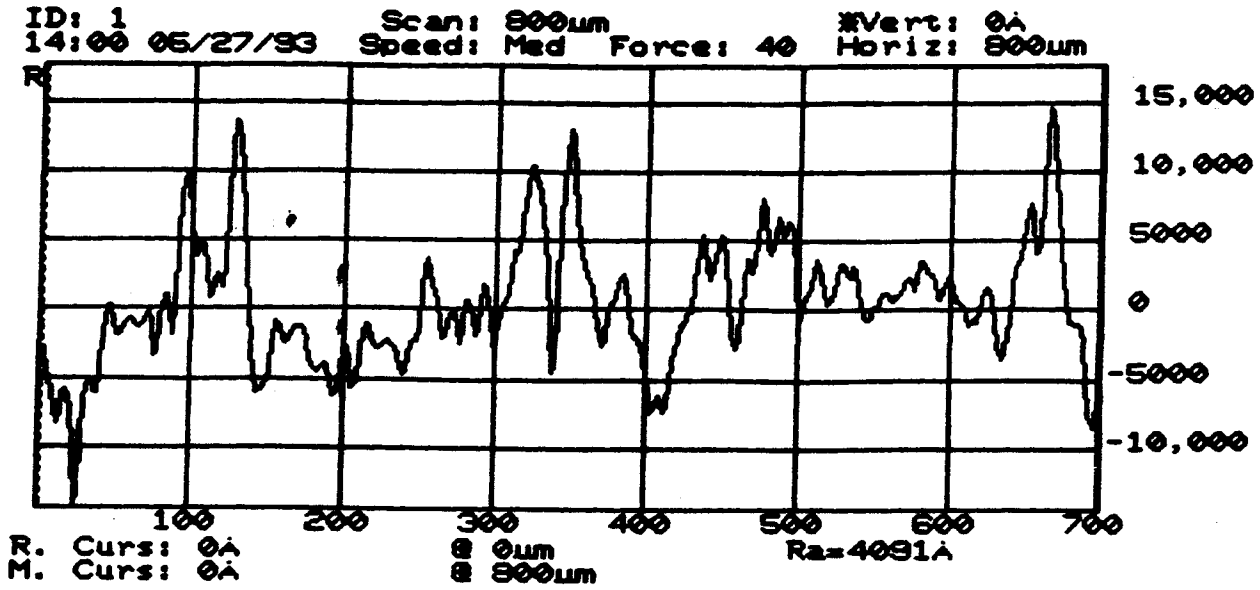

(a)

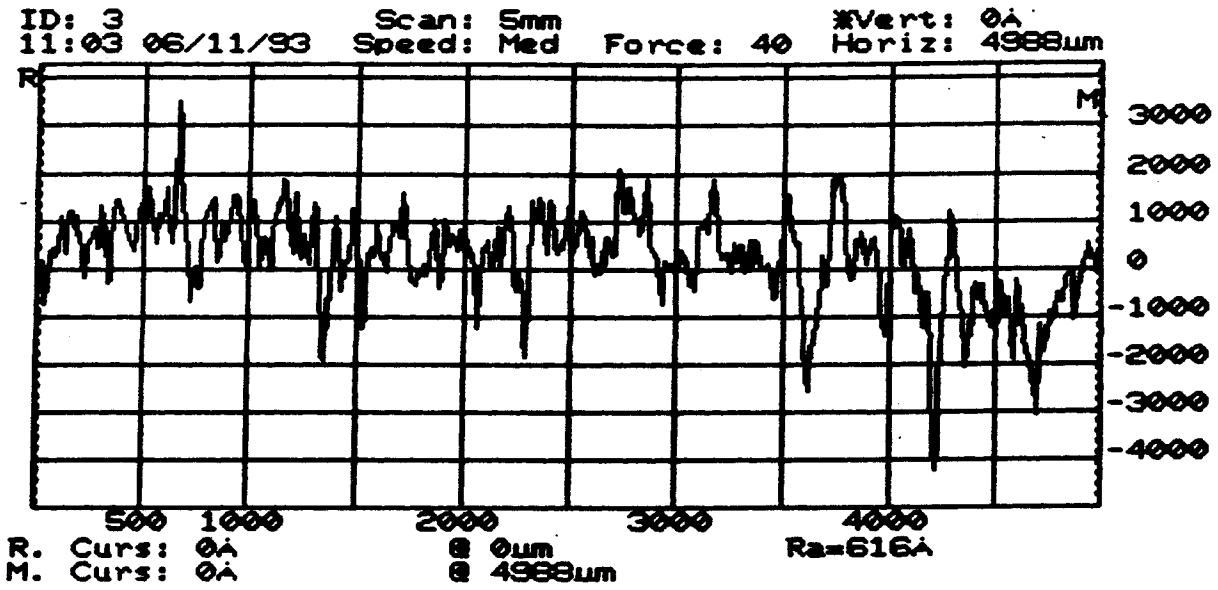

(b)

Fig. 3.19 - Surface Profiles of the Cast Iron Plates Used to Determine the Effect of the Surface roughness on the polymer Shoe Wear Rate

(a) Surface roughness 4,091 Å (0.41 μm) Ra

(b) Surface Roughness 616 Å (0.062 μm) Ra

Torlon 4301 and Vespel SP-211 shoes were tested on both surfaces. The other conditions of the tests were: temperature of 245°F, contact pressure of 500 psi, and sliding velocity of 100 fpm. The results from these tests are given in Table 3.16 and Fig 3.20. For both materials, an increase in the wear rate of more than two times was observed for the rougher surface. The friction coefficient for the rougher surface was slightly lower but generally of the same order. The rougher surface produced a wider fluctuation of the friction coefficient throughout the test.

Table 3.16 - Effects of the Counterface Surface Roughness on Polymer Friction and Wear

Material	Torlon 4301		Vespel SP-211	
Plate Roughness, μm Ra	0.062	0.41	0.062	0.41
Wear Rate, in/1000 h	0.15	0.49	0.16	0.40
Average Friction Coefficient	0.34	0.28	0.38	0.29

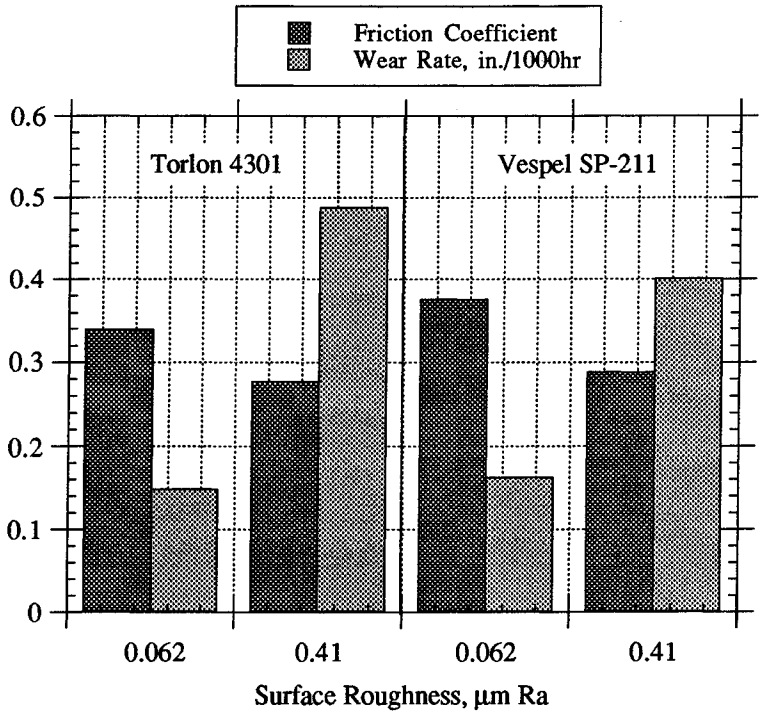

Fig. 3.20 - Effect of Counterface Surface Roughness on Polymer Friction and Wear

A study of the counterface surfaces with an optical microscope after the test revealed thicker, lump-like polymer transfer on the rougher surface, and thinner and more uniform films on the smoother surface.

3.4.4.2 Effect of the Counterface Material Properties

The effect of the counterface material properties is primarily due to their different ability to form adhesive bonds with the polymers. Other properties of the counterface, such as the hardness of the material, have little or no effect on the polymer wear rate [24]. The effect of the counterface material properties is more significant with the lower surface roughnesses when the adhesive component of the friction prevails. Fusaro [11] has studied the effect of different counterface materials in dry sliding against polyimide composites. For the materials tested, up to almost five order-of-magnitude differences in the wear rate were reported. Giltrow [24] has observed that the polymer transfer film on copper and aluminum alloys is less dense and coherent, and the composite wear rates are higher. A difference in the wear rate for different counterface materials is given in the Torlon Engineering Polymers Design Manual [9] as well. For example, the wear rate obtained with brass is 1.5 to 2.1 times that obtained with C1018 steel.

In this study, two counterface materials were used: ductile cast iron and SiPb bronze. Since different polymer grades of Vespel were used for the plates and the shoes, only the data obtained with the Torlon can be compared. Torlon disks produced slightly higher wear rates (see Fig. 3.10) when sliding against bronze shoes than on cast iron plates. This difference, however, was small and could be considered insignificant.

3.4.5 Effect of the Interface Temperature

Temperature, as previously stated, is the major limiting factor for the application of polymers at high PV values. Virtually all the mechanical properties of polymers decrease with temperature. For example, for the particular polymer grades studied, the tensile strength at 245°F is 20% lower than at 73°F (see Table 3.4). The tribological characteristics of the materials can be expected to be influenced by the drop in the mechanical strength.

Temperature affects the relaxation characteristics of the polymers as well. Fusaro [26] has found that polyimides exhibit a temperature at which a transition from high friction coefficient and relatively low wear rates to much lower friction coefficient and higher wear rates occurs. In dry air, the transition occurs at about 40±10°C. If moisture is present, however, the transition temperature may shift to a higher value. In the present study, a series of tests were conducted at 73°F and 245°F.The purpose of these tests was to verify that the 245°F temperature, at which most of the tests in this study were conducted, was above the transition temperature.

The results from these tests are given in Table 3.17. The wear rates for both Torlon and Vespel at 73°F are one order of magnitude lower than those obtained at 245°F. Also, on the average, the friction coefficient tends to be higher. The data given in the table are average values of three tests. All the tests were conducted at a contact pressure of 500 psi

and a sliding velocity of 100 fpm. A comparison between the values given in Table 3.17 and data obtained by Anderson [3] is given in Fig. 3.21.

The polymer grades used by Anderson were polyimide with 15% by weight graphite which is similar to Vespel SP-21D, and polyimide with 15% by weight graphite plus 10% by weight PTFE which is similar to the Vespel SP-211 grade. The specific wear rates obtained in this study are somewhat lower than those presented by Anderson. This may be due first to the fact that the tests in our study were conducted at a much higher PV value, and as previously mentioned, the specific wear rates tend to decrease with the PV. Second, the tests were conducted in different environments, air in the case of Anderson's test and R134a in these tests. Third, the counterface material was different, steel for the Anderson's data and cast iron for this study. Still the results are consistent and show the same trends.

As previously stated,the flash temperature is a fairly complicated function of many parameters, and all these parameters should be the same in order to get the same temperature rise. Upper and lower bound estimates for the flash temperature were made for all the tests conducted in this study. These estimates, though not very accurate, can provide some information on whether the test conditions for the polymer were close to its thermal degradation temperature. At higher PV's, the difference between the upper and the lower flash temperature bounds increases, and this makes the predictions for the real temperature at the interface even more uncertain. Data for the maximum, minimum and average flash temperature for some of the tests in this study are given in Tables 3.18 and 3.19.

A correlation between the estimated average interface temperature and the wear rate, in inches per 1000 hours, is presented in Fig. 3.22. From the figure, it can be seen that, for the Torlon, the estimated average interface temperature for some of the tests was above the degradation temperature, while for Vespel, all specimens operated within their specified temperature range. The main reason for the higher interfacial temperature of Torlon is its higher elastic modulus, resulting in a smaller real contact area over which the temperature was distributed. The estimated flash and interface temperatures may be used to define the limiting sliding velocity for a particular contact.

Table 3.17 - Average Friction Coefficient and Wear Rate at Different Temperatures

Temperature	73°F	245°F
Ave. Specific Wear Rate, $10^{-10}\frac{in.^3 \bullet min.}{ft \bullet lbf \bullet hr}$		
• Torlon 4301	17	45
• Vespel SP-211	13	41
Ave. Friction Coefficient		
• Torlon 4301	0.40	0.33
• Vespel SP-211	0.40	0.29

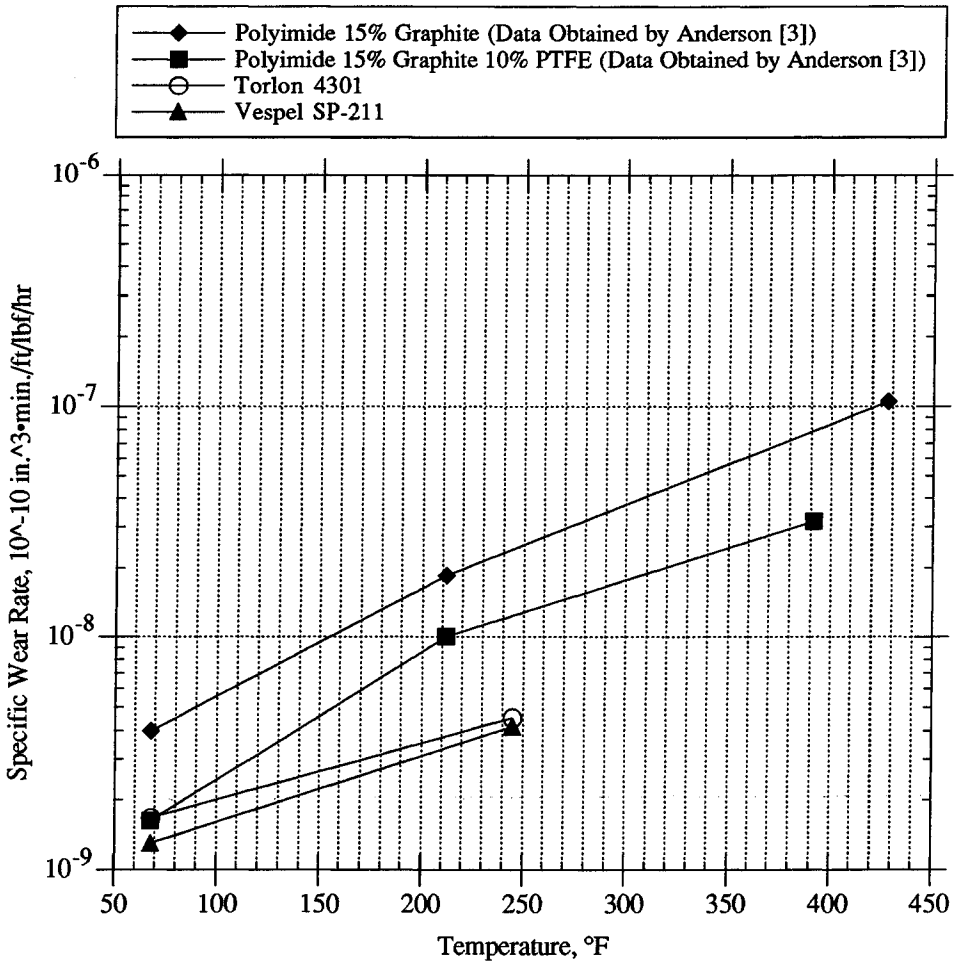

Fig. 3.21 - Effect of the Environmental Temperature on the Polymer Specific Wear Rate

Table 3.18 - Estimates of the Interface Temperature for Torlon Shoes Slid Against Cast Iron Plates. Dry Sliding Conditions. R134a Environment. Environmental Temperature = 245°F

Pressure psi	Velocity fpm	Friction Coefficient	Min. Flash Temperature °F	Max. Flash Temperature °F	Ave. Flash Temperature °F	Interface Temperature °F	Shoe Wear in./1000hr
500	50	0.30	50	133	91	304	0.20
500	75	0.20	48	127	88	300	0.14
500	100	0.27	61	185	122	334	0.24
500	150	0.40	88	298	194	406	0.29
500	200	0.48	115	383	250	462	0.36
500	300	0.25	91	316	203	415	0.35
500	400	0.52	180	534	358	510	0.41
500	600	0.47	207	586	397	610	0.89
500	800	0.22	131	446	288	500	0.70

Table 3.19 - Estimates of the Interface Temperature for Vespel SP-3 Shoes Slid Against Cast Iron Plates. Dry Sliding Conditions. R134a Environment. Evvironmental Temperature = 245°F

Pressure psi	Velocity fpm	Friction Coefficient	Min. Flash Temperature °F	Max. Flash Temperature °F	Ave. Flash Temperature °F	Interface Temperature °F	Shoe Wear in./1000hr
500	50	0.34	50	109	81	293	0.15
500	100	0.41	68	185	127	340	0.38
500	150	0.43	84	235	160	372	0.57
500	200	0.26	70	198	135	347	0.66
500	300	0.27	86	252	172	385	0.59
500	400	0.33	111	318	216	428	1.27
500	600	0.25	111	325	219	432	1.30
500	800	0.22	115	338	226	439	0.86

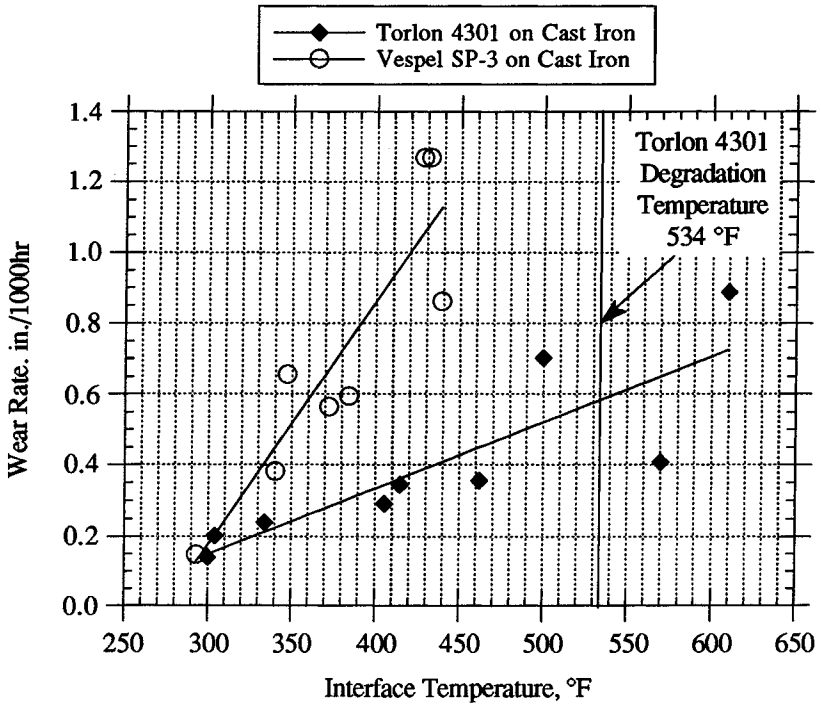

Fig. 3.22 - Effect of the Estimated Interface Temperature on the Wear Rate of Polymers

3.4.6 Effects of the Sliding Velocity and the Contact Pressure

The PV value has proven to be a convenient parameter for defining the limits of successful operation for polymers because it is proportional to the heat generated at the interface. It cannot be used as a sole parameter for the tribological characterization of the polymers under study. This is due to the fact that both the contact pressure and the sliding velocity have upper bounds. The contact pressure is limited by the mechanical strength of the material. The sliding velocity is limited by the flash temperature rise. These limits are complex functions of various parameters. The mechanical strength for example, changes with the temperature, i.e. with the sliding velocity. And the flash temperature, which limits the velocity, depends on the contact pressure as well. The friction coefficient is also a function of both the contact pressure and the sliding velocity.

There are no unique values for the contact pressure or the contact velocity that can be recommended as upper limits. The reason for this is that the interface temperature is also a strong function of the thermal properties of the mating material, the environmental conditions, and the temperature dissipation characteristics of the specimens. Some general observations on these limits, however, can still be made.

It is often assumed that polymers can successfully operate at contact pressures as high as one third of their compressive strength [19]. For the Torlon and Vespel polymers, these are contact pressures in the range of 6-8 thousand psi. Tests with contact pressures

close and above this limit were conducted both in lubricated and in dry conditions. While Vespel SP-21D successfully operated at about 2,000 psi, an increase to 9,600 psi led to one order of magnitude rise in the wear rate. Examination of the surfaces of the specimen under a microscope suggested that, at the higher load, a different wear mechanism had developed. While with pressures below 2,000 psi, the wear scar was smooth and uniform, the higher pressures caused some pits to appear on the surface. This change in the surface appearance, shown in Fig. 3.22, was probably due to delamination and surface fatigue phenomena that were not present at the lower pressures. The fatigue strength of polymers drops significantly with the temperature [9, 13]. An upper bound for the contact pressure at which delamination will not occur is not known because of the limited number of tests conducted. But from the tests conducted and from communications with the polymer manufactures, it can be concluded that contact pressures up to 2,000 psi do not cause surface fatigue for both Torlon and Vespel grades. The upper limit of the contact pressures recommended by the manufacturers when these materials are used as bearing materials, and long operating life is necessary, is in the range of 600 to 1,500 psi for a temperature of 245°F. Pressure does not significantly affect the specific wear rate (see Tables 3.10 - 3.14). This conclusion is confirmed by data obtained by Anderson [3], Clarke [21] and Fusaro [4]. Anderson has reported that for polyimides, the specific wear remains constant up to a value of about one third of the compressive strength.

The influence of sliding velocity on specific wear rate depends on the specimen geometry, the thermal properties, and the relaxation parameters of the polymer. Anderson [3], Friedrich [2], Clarke [21], and Fusaro [19] have studied the effect of sliding speed on the specific wear rate for various polymers, including the polyimides. The specific wear rate tends to decrease with sliding speed below about 2 m/s (400 fpm), and then increase for sliding velocities above 3-5 m/s. This same general trend was observed in the tests conducted in this study, and as mentioned earlier, the increase in wear rate at the higher velocities is probably due to the relaxation behavior of the polymers. The decrease in the specific wear rate with increasing PV value, presented in Fig. 3.11, is in fact due to the increase in the sliding velocity since the contact pressure for all the data points was constant. Further increase in the sliding velocity would probably lead to an increase in the specific wear due to the interface temperature rise which may exceed the degradation temperature.

The velocity limit can be defined as the velocity at which the interface temperature exceeds the degradation temperature of the polymer. For the tests conducted in this study, this limit was reached only with the Torlon 4301 shoes sliding on cast iron plates at 500 psi and velocities of 600 and 800 fpm (see Fig. 3.22). In all other tests, the velocity limit was not reached due to the limitations of the tribometer which can only go up to 800 fpm with

the specimen holder used. However, an estimate of the velocity limit, based on formulae (3.4) and (3.11), can be made. Plots of these limits, as a function of the contact pressure and at different temperatures, are given in Fig. 3.23. For a given contact pair, its average friction coefficient was assumed (Table 3.12). The plots are based on the average flash temperature calculated. The maximum pressure considered in the figure is 4000 psi, which can be assumed to be close to the pressure limit for these materials. The same relationships are presented in a log-log scale in Fig 3.23. From these plots, it is evident that Vespel can perform at much higher velocities than Torlon, and is preferred in applications where excessive frictional heating of the contact is expected.

The contact pressure and the sliding velocity affect the friction coefficient as well. For almost all polymeric materials,the friction coefficient tends to decrease as the contact pressure is increased. The reason for this is that polymers have very low modulae of elasticity and the deformation of the asperities on the surface remains elastic for a very wide range of pressures. Hence the increase in the real contact area is slower than the increase in the contact pressure. In order to study the effects of the contact pressure and the sliding velocity on the friction coefficient, tests at different combinations of pressure and velocity were conducted. The test duration for all tests was 15 minutes. The record of the friction coefficient was started after a 10 minutes run-in period during which the friction coefficient reached its steady-state value. All tests were conducted at 245°F in R134a refrigerant environment. Wear data for this test are not available due to their short duration. The results from these tests are given in Table 3.21 and Fig. 3.24. As expected, the friction coefficient, in general, dropped with increasing contact pressure. The relationship between the friction coefficient and the sliding velocity was not so obvious, and no general trends could be observed.

According to formulae (3.4) and (3.11), the velocity has a stronger effect on the flash temperature rise than the contact pressure. It could be expected, therefore, that tests conducted at the same PV but at different ratios of the contact pressure and the sliding velocity would produce different results, with the wear rate increasing with the sliding velocity. To verify this hypothesis, tests at a constant PV = 50,000 psi•fpm were conducted.

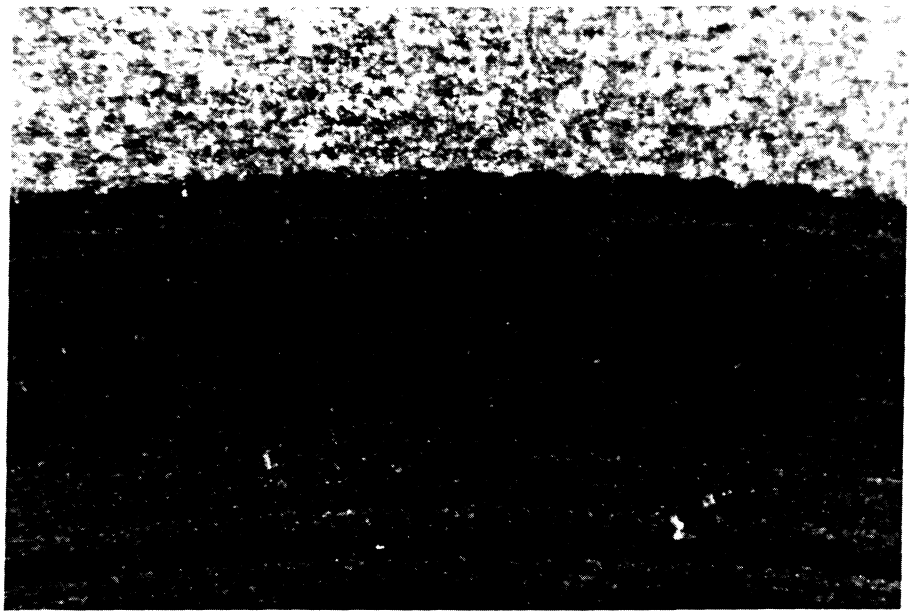

(a)

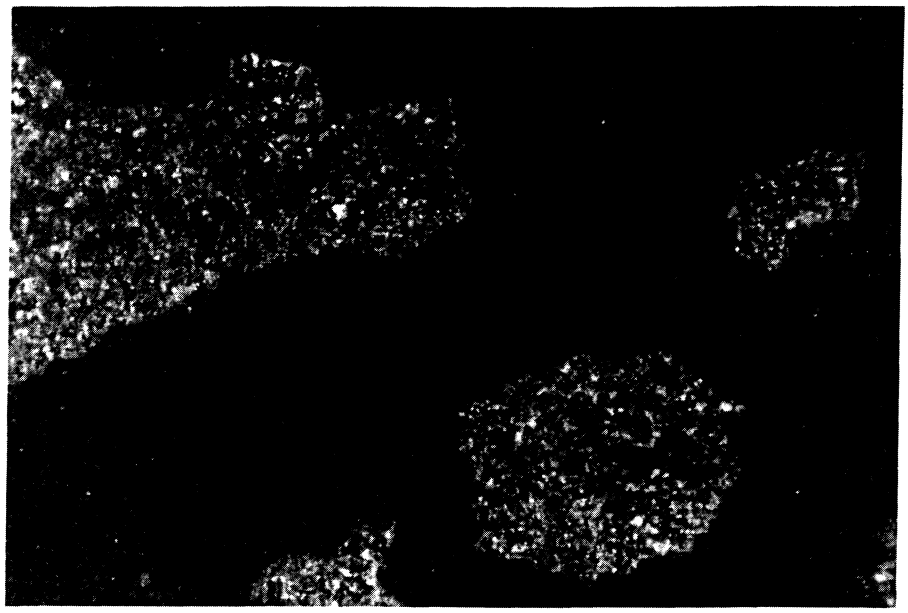

(b)

Fig. 3.22 - Worn Vespel SP-21D Polymer Plate Surfaces
(a) Contact Pressure = 1000 psi, and (b) Contact Pressure = 9,600 psi.
Test Conditions: Env. Temperature = 245°F, Sliding Velocity = 100 fpm, R134a Environment. Test Duration = 1 Hour

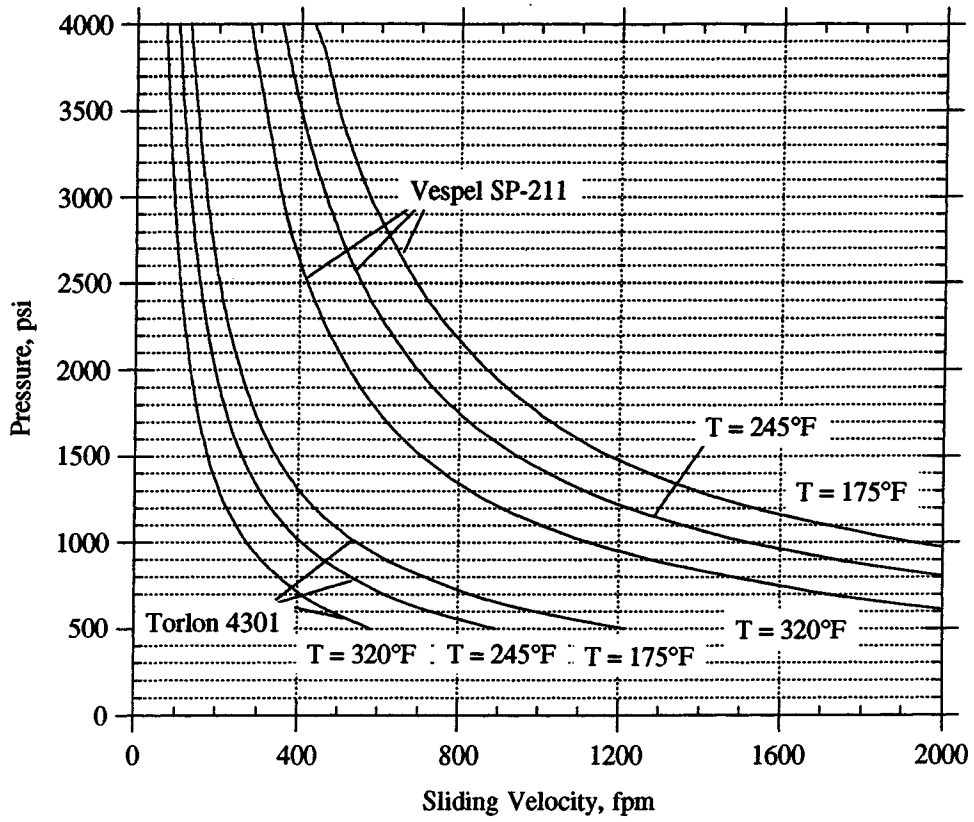

(a)

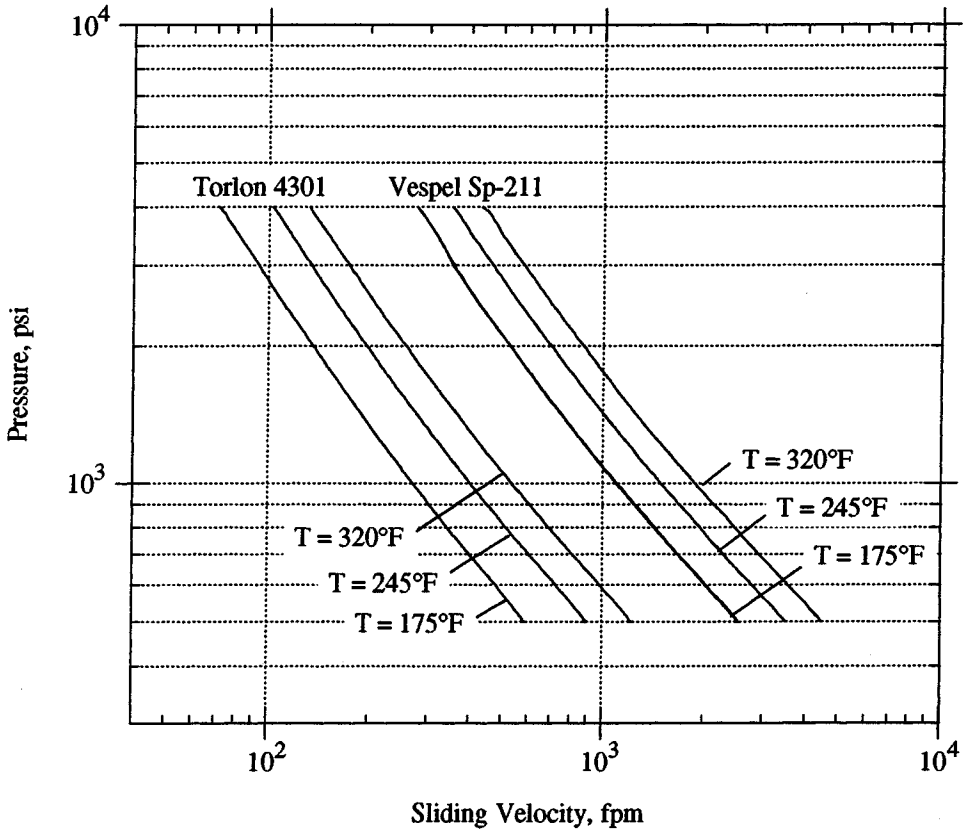

(b)

Fig. 3.23 - Estimated Pressure-Velocity Limits at Various Environmental Temperatures (a) Liner Scale, and (b) Log-Log Scale

Table 3.20 - Effect of the Contact Pressure and the Sliding Velocity on the Friction Coefficient

Pressure psi	Friction Coefficient @ v = 25 fpm	Friction Coefficient @ v = 125 fpm	Friction Coefficient @ v = 250 fpm
200	0.48	0.61	0.45
400	0.47	0.51	0.44
800	0.40	0.44	0.41
1200	0.37	0.39	0.37
1600	0.34	0.35	0.42

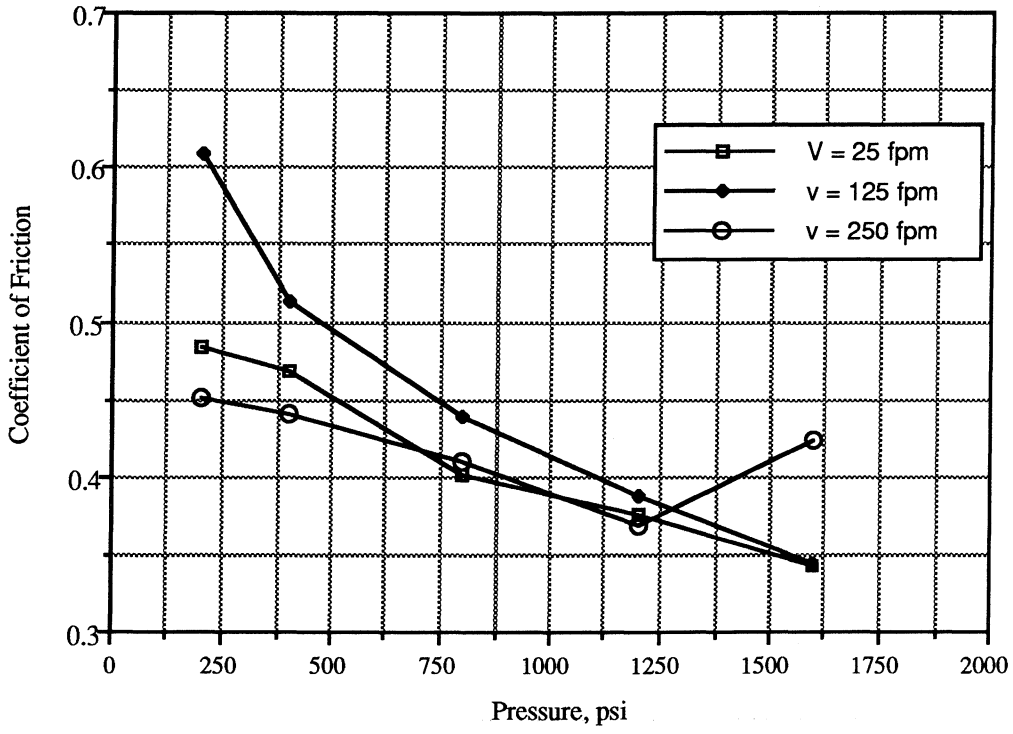

Fig. 3.24 - Effect of the Contact Pressure and the Sliding Velocity on the Coefficient of Friction

The pressure was varied from 100 to 500 psi and the sliding velocity from 100 to 500 fpm. In these tests, a bronze shoe was slid on a Torlon 4301 plate. The environmental temperature was 245°F and the environment was R134a refrigerant. As expected, an increase in the wear rate with the sliding velocity was observed. The data for these tests are summarized in Table 3.23 and Fig. 3.25. Similar tests at which the PV was kept constant while the pressure-to-velocity ratio was varied have been conducted by Clarke and Allen [21]. These tests also showed that wear tends to increase with increasing velocity.

Table 3.23 - Friction and Wear Data for Torlon 4301 Plates Slid Against Bronze Shoes. Dry Sliding Conditions. R134a Environment. Temperature = 245°F

Contact Pressure psi	Sliding Velocity fpm	PV psi•fpm	Friction Coefficient	Plate Wear in./1000hr	Specific Wear $10^{-10}\frac{in.^3 \bullet min.}{ft \bullet lbf \bullet hr}$
500	100	50000	0.32	0.27	58
400	125	50000	0.32	0.30	63
300	167	50000	0.26	0.39	82
200	250	50000	0.31	0.31	63
100	500	50000	0.27	0.48	49

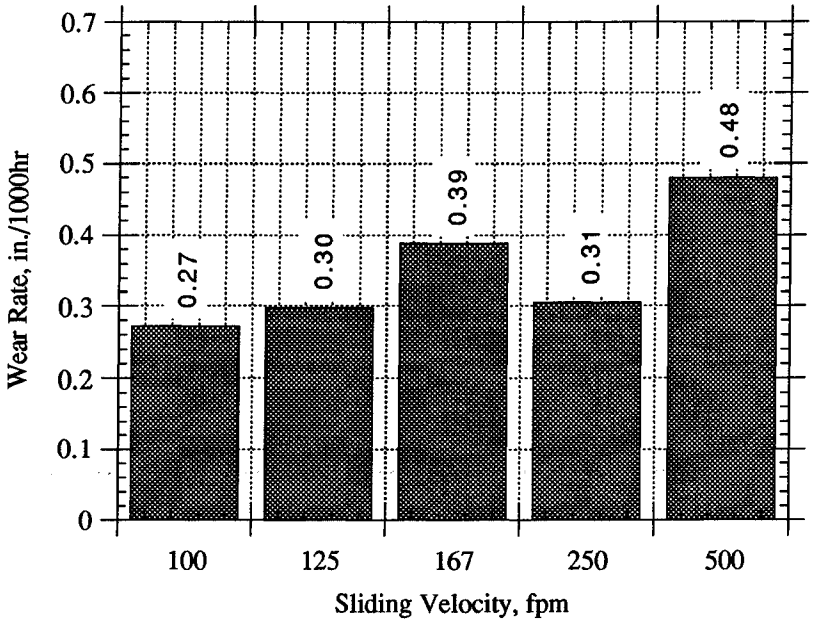

Fig. 3.25 - Effect of the Sliding Velocity at a Constant PV Value

3.4.7 Wear Surface Morphology and Transfer Films

Most polymers, when slid on metal surfaces, transfer films onto the counterface. The properties and appearance of these films, to a great extend, determine the tribological phenomena at the interface. Four different types of polyimide film transfer have been defined in the literature [4]. These are: thin platelets, thin continuous layer, thick flattened particles, and thick "ridge-like" layers. It has been proven that the thin and uniform films are the most beneficial from the stand point of friction and wear. The formation of the transferred film depends on many factors. The most decisive, according to the observations made in this study, are the environmental temperature and the number of overlaps. Other factors, such as the counterface surface roughness, material, and test environment, are not as significant.

The wear surface morphology and the transfer films were studied with an optical microscope, a scanning electron microscope (SEM), and a stylus surface profiler (DEKTAK).

3.4.7.1 Surface of Polymers Before and After the Test

As expected, initial surface roughness of polymers did not have any effect on the steady-state friction coefficient or wear rate. The surfaces of the polymer shoes became very smooth after just a few minutes of sliding and remained smooth for the test duration. Surface profiles and surface roughness values of a polymer shoe before the test and after a few minutes of sliding are shown in Fig. 3.26. The corresponding pictures showing the surfaces of the polymer shoe are shown in Fig. 3.27. Polymer plates that were tested under higher pressures produced rougher surfaces (see Fig. 3.22).

3.4.7.2 Surface of Cast Iron Plates Before and After the Test

The surface of the cast iron plates was examined before and after tests conducted in various environments, PV's, and a number of overlapping passes. Also, the surfaces of plates with various surface roughnesses were examined. Temperature seems to be the major factor for the formation of the transfer films. With temperatures below the transition (tests at 73°F) very little polymer is transferred to the surface. There is also some polishing effect, i.e. there are scratches on the surface. For tests conducted at 245°F, the polymer transfer is more dense and continuous or "ridge-like" films are formed. A comparison between the surface transfer films generated at different temperatures is given in Fig. 3.28.

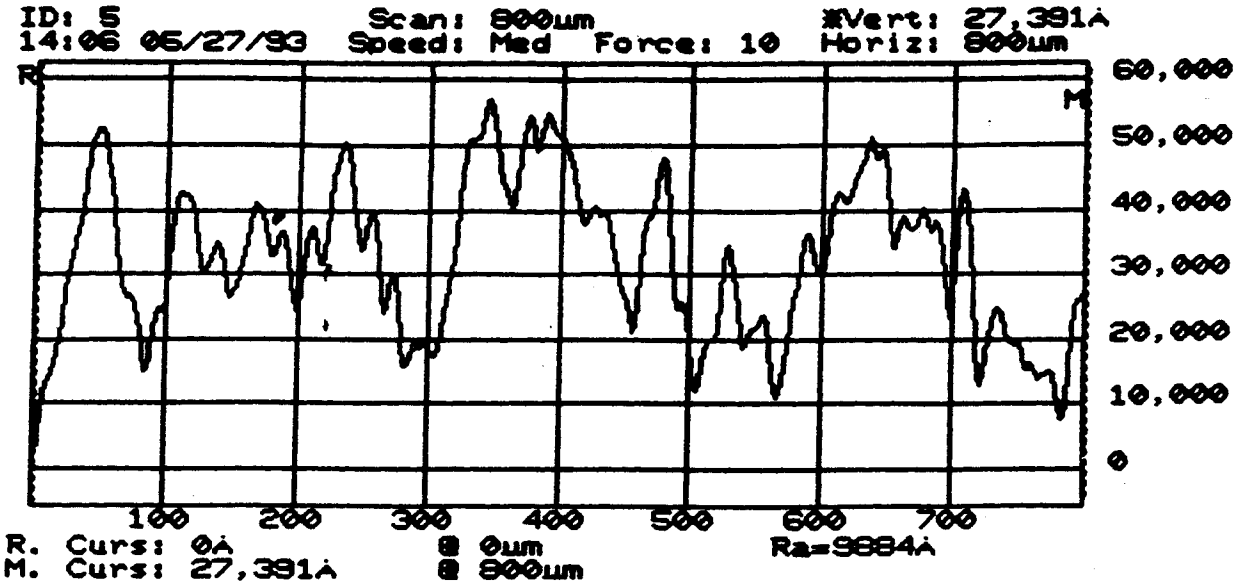

(a)

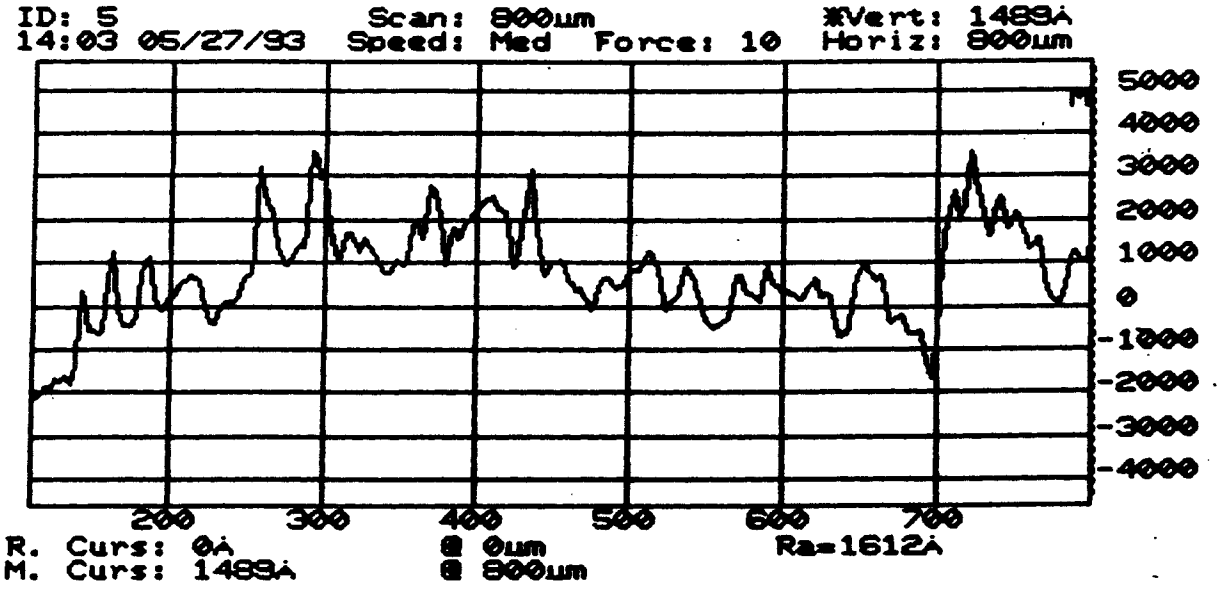

(b)

Fig. 3.26 - Surface Profiles of a Vespel SP-3 Shoe

(a) Before the Test, Surface Roughness = 9884 Å (0.99 µm) Ra, and (b) After 10 min. of Sliding on a Cast Iron Plate, Surface Roughness = 1612 Å (0.162 µm) Ra

Test Conditions: Env. Temperature = 245°F, Contact Pressure = 500 psi, Sliding Velocity = 100 fpm, Counterface Surface Roughness = 016 µm Ra.

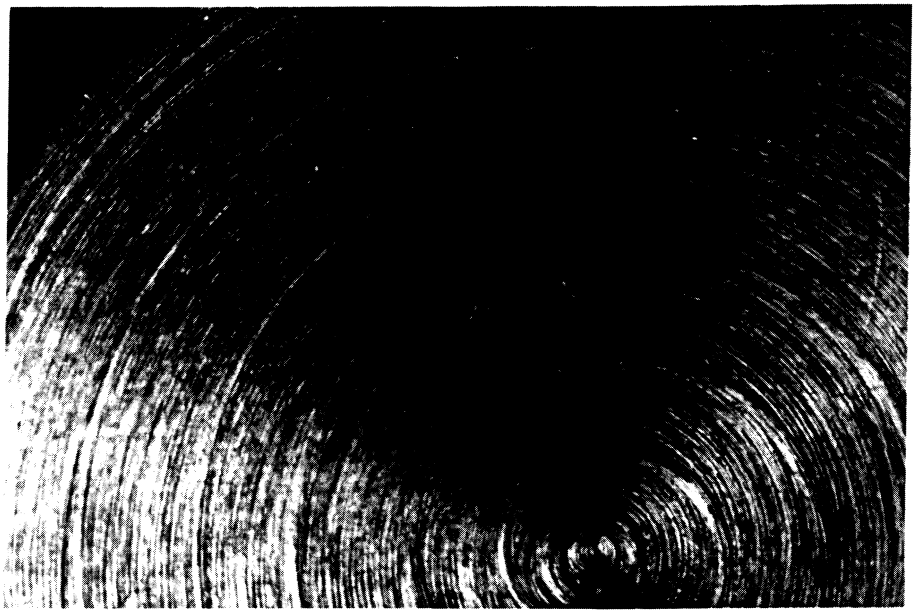

(a)

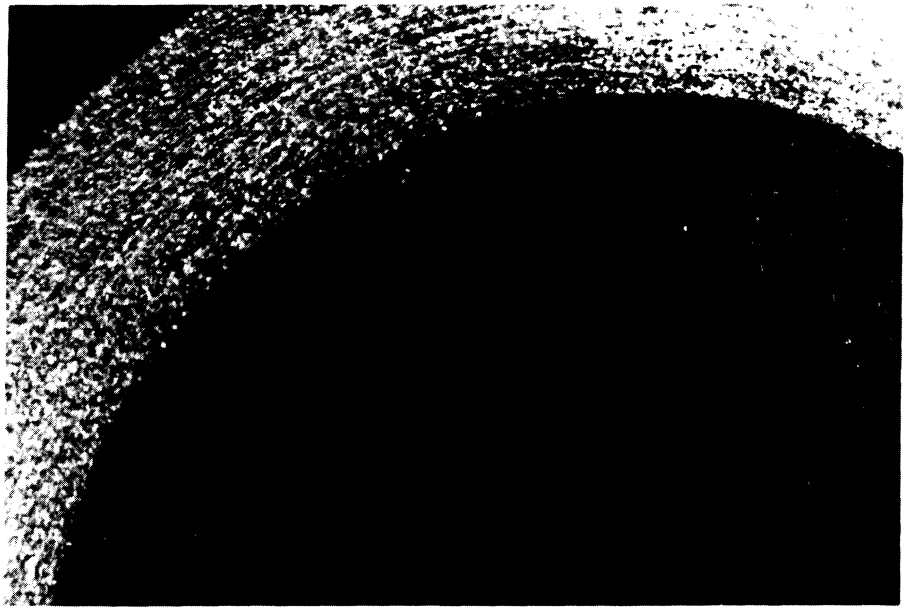

(b)

Fig. 3.27 - Surface Appearance of a Vespel SP-211 Shoe at 10x Magnification (a) Before the Test, and (b) After 10 min. of Sliding on a Cast Iron Plate. Test Conditions: Env. Temperature = 245°F, Contact Pressure = 500 psi, Sliding Velocity = 100 fpm, R134a Environment, Plate Surface Roughness = 0.16 μm Ra. Test Duration = 10 hours.

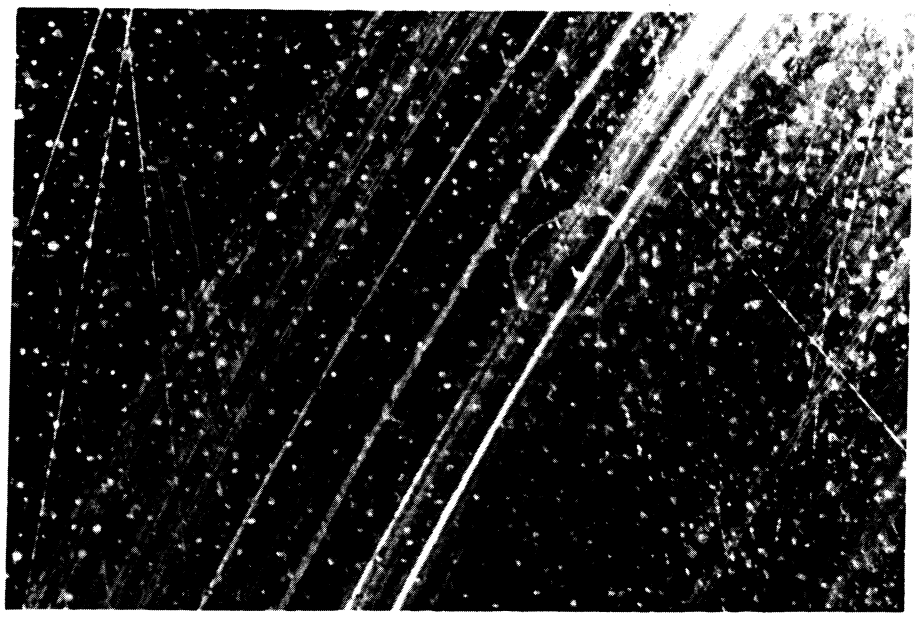

↑ Polymer Transfer ↑

(a)

Polymer Transfer Ridges ↑ ↑

(b)

Fig. 3.28 - Torlon 4301 Polymer Transfer at Different Environmental Temperatures. (a) Environmental Temperature = 73°F, and (b) Environmental. Temperature = 245°F. Test Conditions: Contact Pressure = 500psi, Sliding Velocity = 100 fpm, R134a Environment, Plate Surface Roughness = 0.15 μm Ra. Test Duration = 10 hours.

The specimen holder, described in section 3.2.1.2 of this chapter, allows tests at different contact diameters to be conducted. For a given test duration, the smaller diameter produced twice the overlapping passes than the larger diameter. Tests on both sliding diameters were conducted in order to study the effect of the number of passes on polymer transfer. When the number of passes is increased, the polymer transfer to the surface becomes more uniform over the whole sliding area. For a small number of overlaps, the transfer film consisted of thin platelets that were deposited in the valleys of the surface. As sliding is continued, the platelets tend to coalesce together and form ridges. Finally a uniform layer of transferred material can be formed. Typical surface appearances for tests run on the two different diameters are given in Fig. 3.29 and Fig 3.30. Note the "ridge-like" appearance of the polymer transfer on the larger diameter and the more uniform transfer, with ridges only at the ends of the contact area, for the smaller. This change in the film appearance did not lead to any changes in the friction and wear results, however. The transition from one type of polymer transfer to another with the number of passes has been reported in the literature as well [4].

Except for the polymer transfer, no other changes in the surface topography of the cast iron surfaces were observed (Fig. 3.31). With the thin uniform polymer film, all the surface irregularities were covered by the polymer transferred. More massive polymer transfer was observed only in the deepest valleys of the surface. When thick ridges were present (Fig. 3.30b), all the surface irregularities were covered by the ridge. These ridges could be detected and their thickness measured by the stylus of a surface profiler (Fig. 3.32). The two ridges seen in the picture correspond to the two characteristic heights on the surface profile. The rest of the surface was relatively flat and thus the thickness of the transfer film could be estimated. For this particular test, the thickness of the film transferred was about 1 μm.

Tests conducted in liquid refrigerant showed less polymer transfer to the surface. This can be attributed to the extremely low temperature at which these tests were run. They also were characterized by a low friction coefficient. The tests conducted in oil showed the same type of polymer transfer as those run in dry conditions. These tests were also characterized by very low (0.04) friction coefficients.

Examination of the surface of the plates with different initial surface roughness with an optical microscope did not reveal any significant change in the appearance of the polymer film. With the rougher surface, however, most of the polymer found on the surface was confined to the valleys of the surface roughness profile, and no uniform film formation was visible. In both smoother and rougher surfaces the "ridge-like" polymer transfer was predominant.

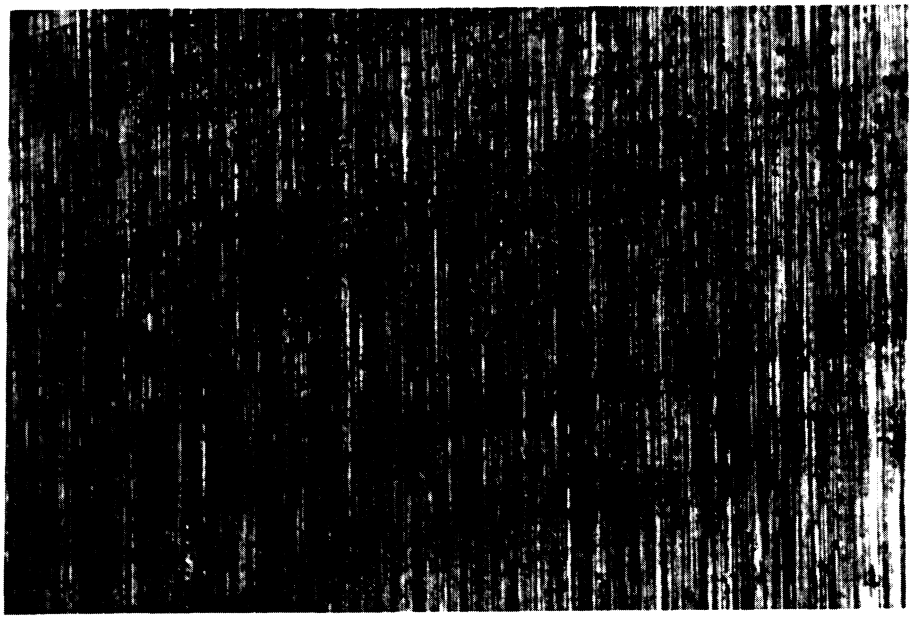

← Polymer Platelets and Ridges ←

(a)

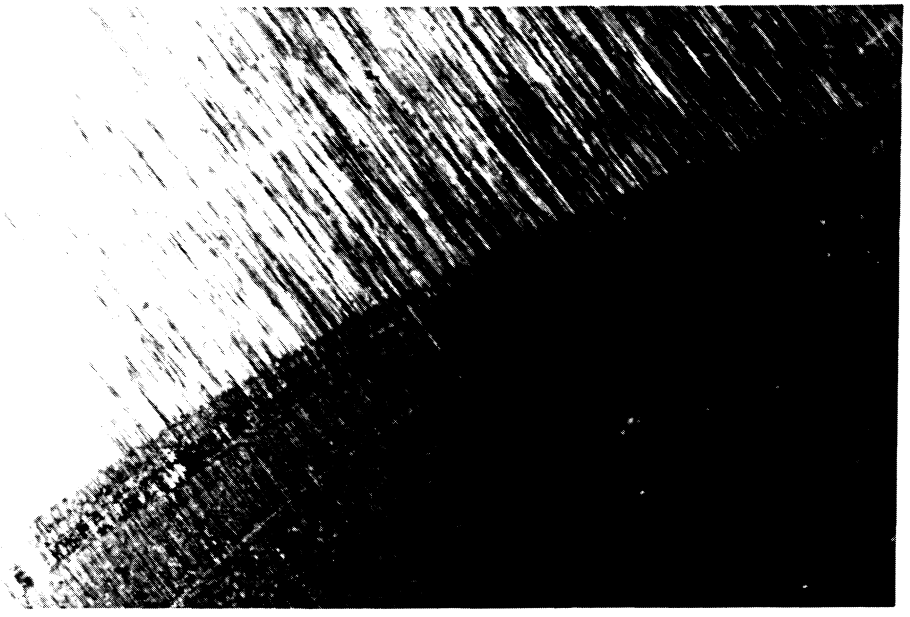

←Polymer Film

(b)

Fig. 3.29 - Torlon 4301 Transfer on a Cast Iron Plate at Magnification 10x
(a) Platelets and Ridges Transfer After 150,000 Overlapping Passes (on the Larger Diam.)
(b) Thin Uniform Film Transfer After 300,000 Overlapping Passes (on the Smaller Diam.)
Test Conditions: Env. Temperature = 245°F, Contact Pressure = 500psi,
Sliding Velocity = 100 fpm, R134a Environment, Plate Surface Roughness = 0.17 μm Ra.
Test Duration = 10 hours.

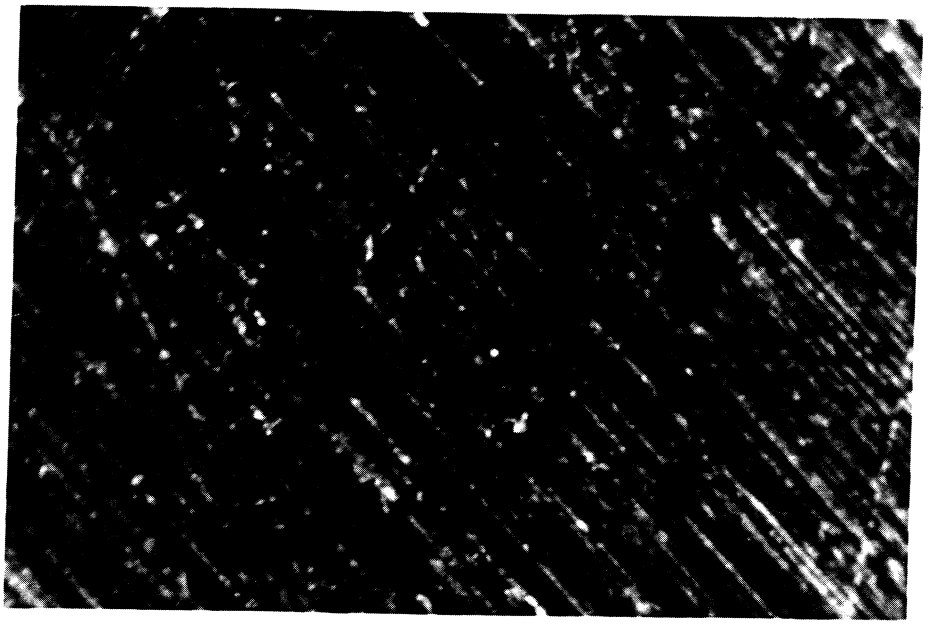

Polymer Platelets ↑ (a)

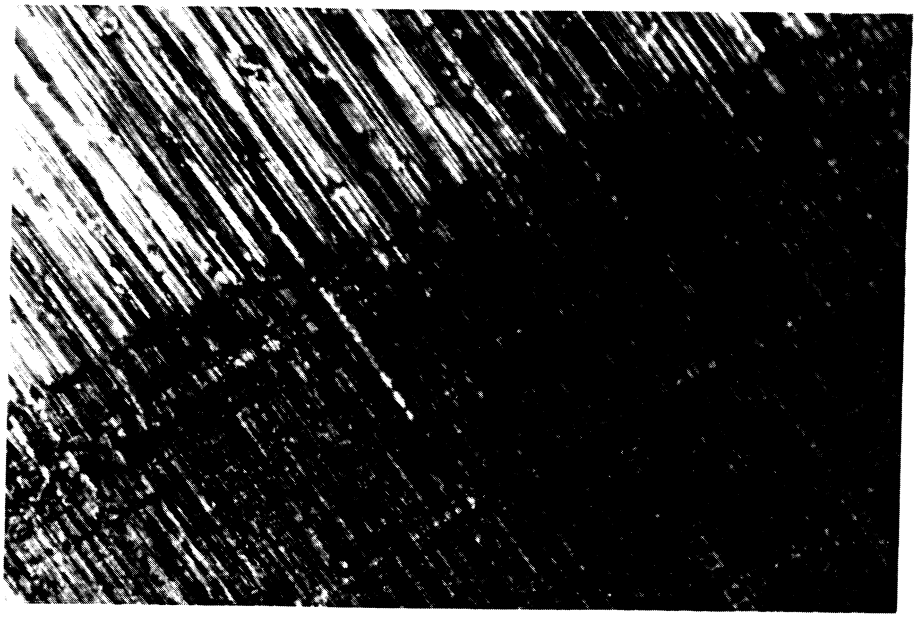

←Polymer Film

(b)

Fig. 3.30 - Torlon 4301 Transfer on a Cast Iron Plate at Magnification 63x
(a) Platelets and Ridges Transfer After 150,000 Overlapping Passes (on the Larger Diam.)
(b) Thin Uniform Film Transfer After 300,000 Overlapping Passes (on the Smaller Diam.)
Test Conditions: Env. Temperature = 245°F, Contact Pressure = 500psi,
Sliding Velocity = 100 fpm, R134a Environment, Plate Surface Roughness = 0.17 μm Ra.
Test Duration = 10 hours.

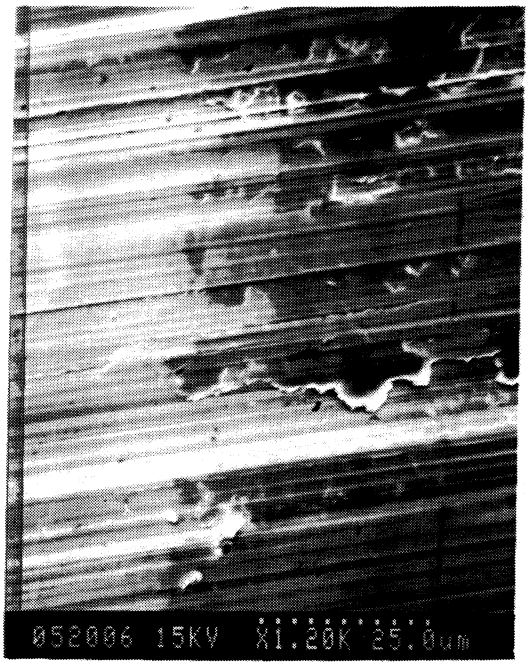

←Thin
Uniform
Film

(a)

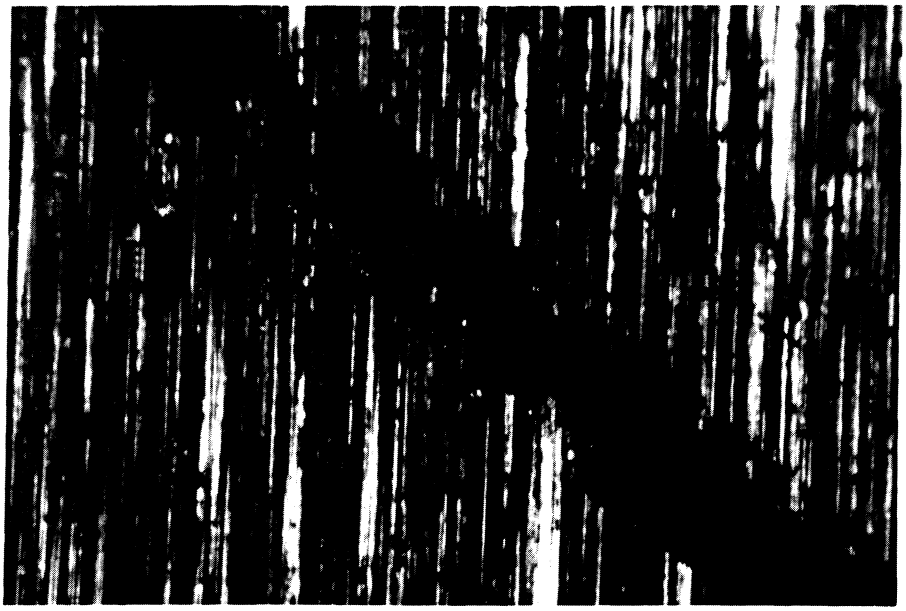

Thick
Polymer
Ridge
←

(b)

Fig. 3.31 - Changes in the Surface Topography of the Cast Iron Plates
With Various Types of Vespel SP-211 Polymer Transfer.
(a) SEM Picture of a Thin Uniform Film Transfer at Magnification 1,200x
(b) Optical Microscope Picture of a "Ridge-Like" Transfer at Magnification 63x
Test Conditions: Environmental Temperature = 245°F, Contact Pressure = 500psi, Sliding Velocity = 100 fpm, R134a Environment, Plate Surface Roughness = 0.12 μm Ra.

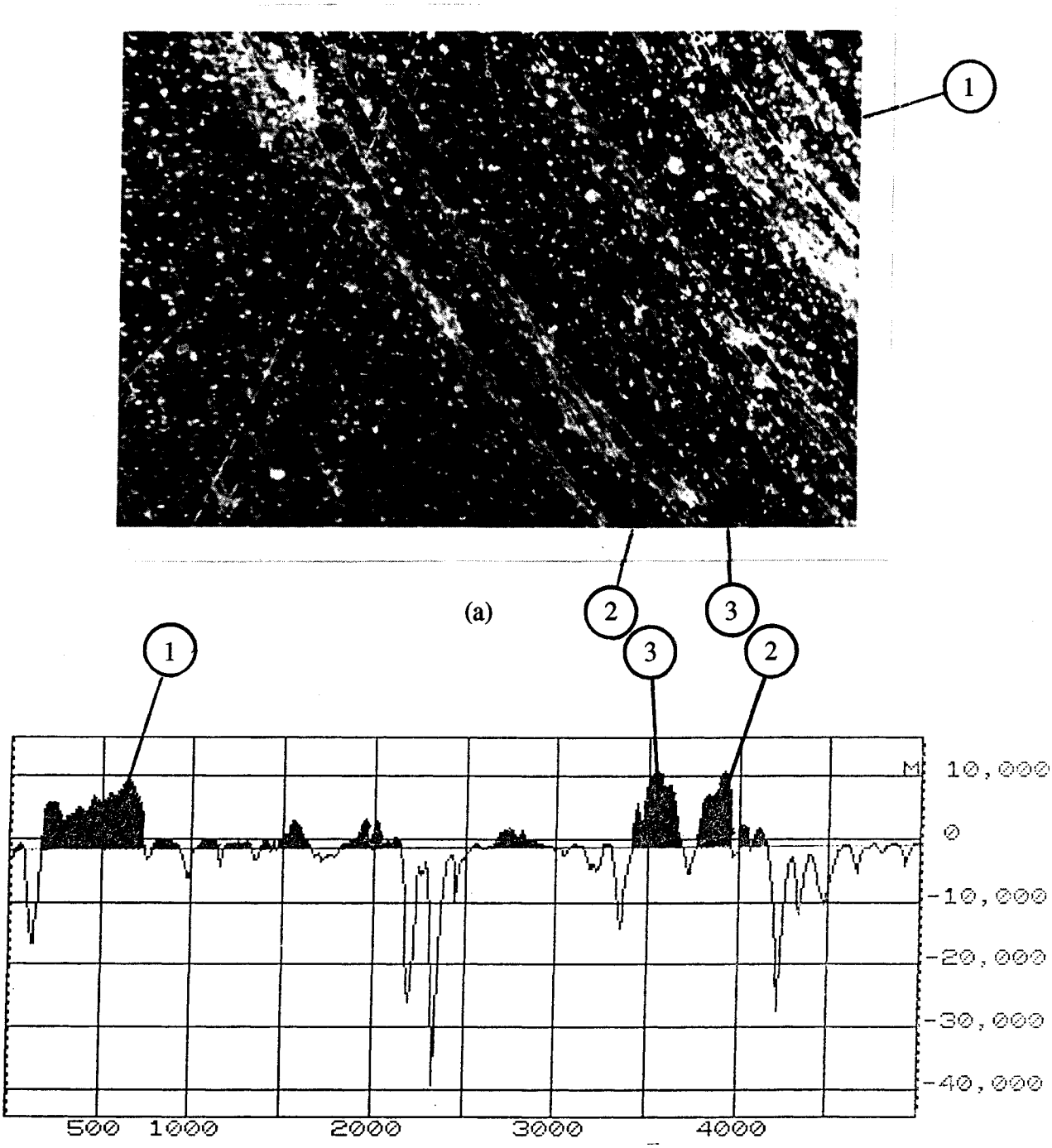

(b)

Fig. 3.32 - Polymer Ridges Transferred from a Vespel SP-211 Shoe Onto a Cast Iron Plate (a) Surface Appearance (Note the Polymer Ridges in the Middle and the Upper Right Corner of the Picture), and (b) Profile of the Same Surface Perpendicular to the Ridges Test Conditions: Env. Temperature = 245°F, Contact Pressure = 500psi, Sliding Velocity = 100 fpm, R134a Environment, Plate Surface Roughness = 0.12 μm Ra. Test Duration = 10 hours.

3.4.7.3 Surface of Bronze Shoe Before and After the Test

The polymer transfer film formed onto the bronze surface was more of the flattened particle, or "lump-type" rather than "ridge-type" (Fig. 3.33) This type of polymer transfer has been found to produce higher wear rates [11, 21]. After longer periods of sliding, however, the bronze shoes also tended to form a continuous thin film of polymer on the surface. A typical "lump-like" transfer and a transition from particulate to continuous polymer film on the surface of the bronze shoe is given in Fig. 3.33.

3.4.8 Comparison of the Friction and Wear Results With Data From Other Studies

Polyimide and poly(amide-imide) are among the polymers that have attracted most attention from tribologists. They have been tested as pure base polymers and in combination with different fillers and reinforcing materials. These polymers constitute a whole class of materials with quite different properties depending on their chemical structure and processing. Hence, comparison of results which were obtained with different polymer grades and under different conditions is difficult. Extrapolation of test data to conditions which are not the same as those used to obtain the data, can be very risky.

Most of the tests reported in the literature have been conducted in air and at ambient temperature. On the other hand, most of the test data obtained in this study were at 245 °F and in a refrigerant environment. Therefore, differences in the results were inevitable. The tribometer that was used to obtain the data presented in this study has the capability of keeping the environmental temperature virtually constant. The conventional tribometers usually lack this capability. Therefore, even tests reported to be conducted at ambient temperature may have been performed at higher environmental temperatures.

Still some comparison of test data can be done. The general trends in polymer behavior can also be expected to show some similarity.

The comparison of test data was further complicated by the differences in the presentation of the data. Test data in this study are presented in English units. The wear rate is given in inches per 1000 hours. The specific wear rate is given in in^3•min/ft/lbf/hr, which is obtained by simply dividing the wear rate by the PV value in psi•fpm. All data from other studies have been converted to the same units using the conversion factors given by Lancaster [14].

Test data obtained in this and other studies are summarized in Tables 3.22 and 3.23. In Table 3.22a, the data for polyimide grades at ambient temperature and dry sliding conditions are presented. In fact, most of the data available from the literature are for these test conditions. As seen from the table, the variation of the friction coefficient and the specific wear rate is very large.

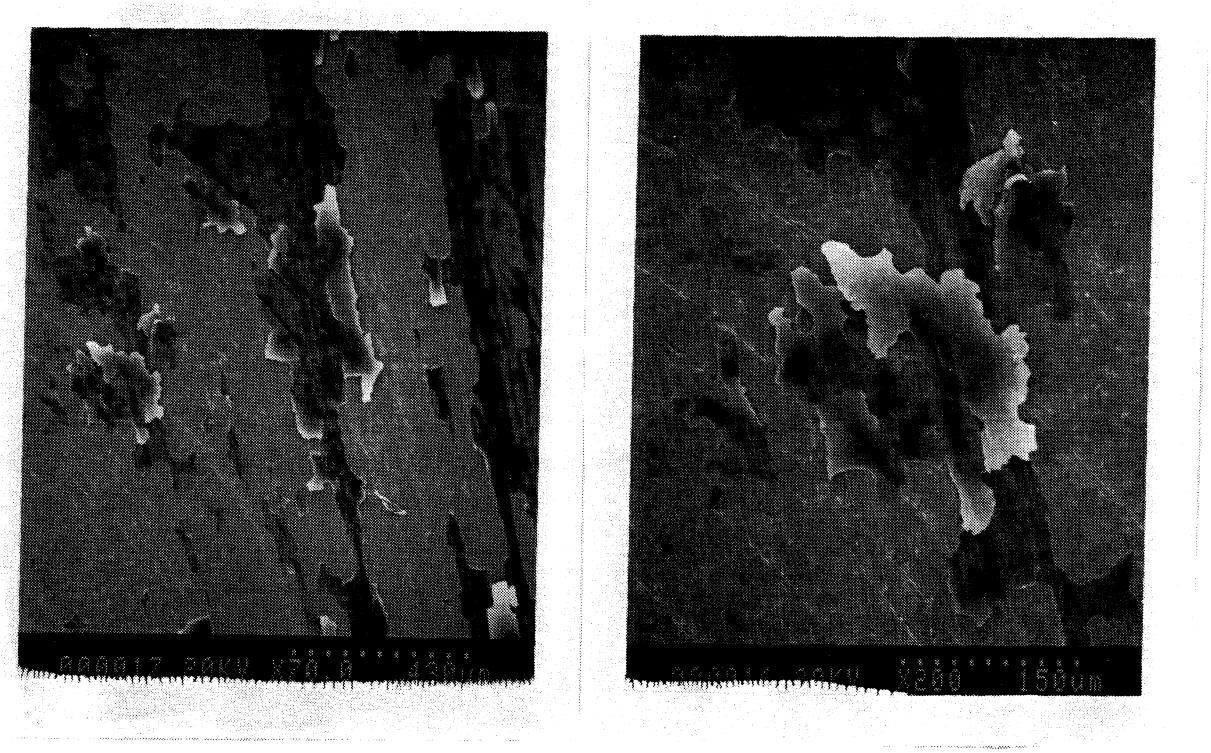

(a) (b)

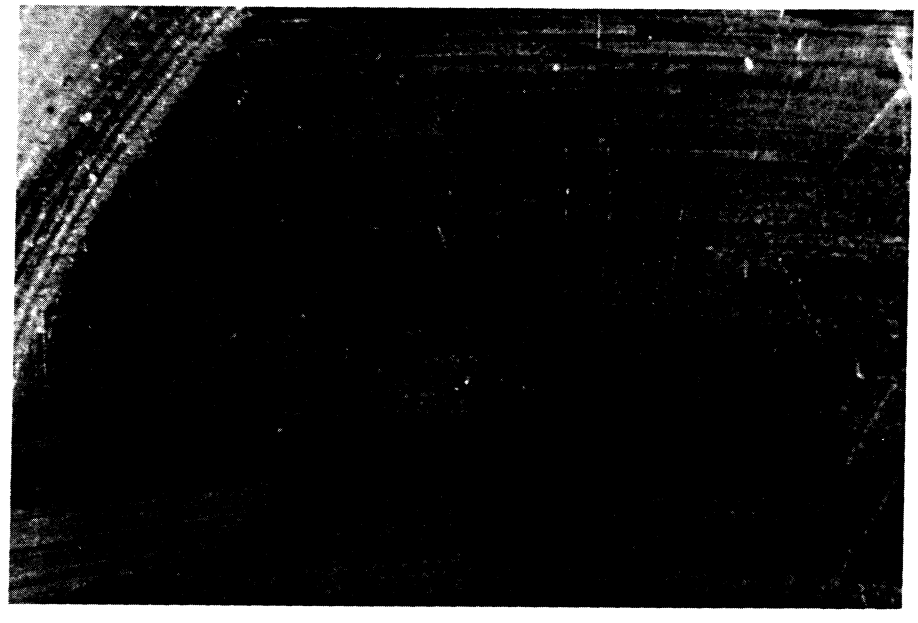

(c)

Fig. 3.33 - Vespel SP-21D Polymer Transfer on a Bronze Shoe
SEM Micrographs of Thick "Lump-Like" Particle Transfer at
(a) Magnification 70x, (b) Magnification 200x,
(c) Optical Microscope Photograph of Polymer Transfer at Magnification 63x.
Test Conditions: Environmental Temperature = 245°F, Contact Pressure = 500psi,
Sliding Velocity = 100 fpm, R134a Environment, Test Duration = 10 hours.

Table 3.22a - Comparison of the Friction and Wear Results for Polyimide With Data Obtained in Other Studies in Dry Sliding Conditions and Ambient Temperature

Source	Material	Contact Pressure, psi	Sliding Velocity, fpm	Environ. Temperature °F	Counterface Material and Surface Roughness	Environment	Friction Coefficient	Specific Wear Rate $10^{-10}\frac{in.^3 \bullet min.}{ft \bullet lbf \bullet hr}$
Jones et al [23]	Polyimide (Grade Not Specified)	---	32.5	73	Steel (Not Specified)	Dry Air	0.73 (0.33 - 0.80)	147
Fusaro [4]	Polyimide (Grade Not Specified)	---	570	Ambient	Haynes 6B 0.07 µm Ra	Air 50% Humidity	0.73	252
Fusaro [4]	Polyimide Graphite Powder Filler	---	570	Ambient	Haynes 6B 0.07 µm Ra	Air 50% Humidity	0.64	27
Friedrich [2]	Vespel SP-21D	83 - 1210	118 - 591	Ambient	Steel DIN 100Cr6 0.06 µm Ra	Dry Air	0.24	28 - 68
Friedrich [2]	Vespel SP-211D	83 - 1210	118 - 591	Ambient	Steel DIN 100Cr6 0.06 µm Ra	Dry Air	0.12	10 - 46
Gardos [10]	PTFE Filled Polyimide	10 - 140	100	Ambient	1020 Steel 0.5 µm Ra	Air	0.27 - 0.40	5 - 60
Anderson [3]	Polyimide with 15% Graphite Powder Filler Similar to SP-21D	145	2.56	Ambient	En3B	Air	---	39.5
Anderson [3]	Polyimide with 10% PTFE and 15% Graphite Similar to SP-211	145	2.56	Ambient	En3B	Air	---	15.8
Tewari and Bijwe [7]	Vespeel SP-22 40% Graphite Powder	---	413	Ambient	Mild Steel 0.2 µm Ra	Air	0.1 - 0.2	5 - 15
Du Pont [13]	Vespel SP-21D	---	---	73	---	Air	0.12 - 0.24	3.99
Du Pont [13]	Vespel SP-211	---	---	73t	---	Air	0.08 - 0.12	3.10
Du Pont [13]	Vespel SP-3	---	---	73	---	Air	0.17 - 0.25	11.1 - 14.6
Amoco [9]	Vespel SP-21	50 - 1000	50 - 900	Ambient	C1018 Steel	Air	---	32 - 35
This Study	Vespel SP-211	500	100	73	Ductile CI 0.15 µm Ra	R134a Refrigerant	0.40	13

Table 3.22b - Comparison of the Friction and Wear Results for Polyimide With Data Obtained in Other Studies in Dry Sliding Conditions and Temperature Above Ambient

Source	Material	Contact Pressure, psi	Sliding Velocity, fpm	Environ. Temperature °F	Counterface Material and Surface Roughness	Environment	Friction Coefficient	Specific Wear Rate $10^{-10}\ \frac{in.^3 \bullet min.}{ft \bullet lbf \bullet hr}$
Jones et al [23]	Polyimide (Grade Not Specified)	---	32.5	500	Steel (Not Specified)	Dry Air	0.30 (0.15 - 0.60)	323
Fusaro [4]	Polyimide (Grade Not Specified)	---	570	212	Haynes 6B 0.07 µm Ra	Air 50% Humidity	0.62	252
Anderson [3]	Polyimide with 15% Graphite Powder Filler Similar to SP-21D	145	2.56	212	En3B	Air	---	184
Anderson [3]	Polyimide with 10% PTFE and 15% Graphite Similar to SP-211	145	2.56	212	En3B	Air	---	94
This Study	Vespel SP-21D	1000	800	245	SiPb Bronze	R134a, R22, Air, Argon	0.1	10
This Study	Vespel SP-211	250 - 2000	100 - 664	245	Ductile Cast Iron, Ra 0.06 - 0.22 µm	R134a, R22, Air, Argone	0.29	59
This Study	Vespel SP-3	500	50 - 800	245	Ductile Cast Iron, Ra 0.06 - 0.22 µm	R134a, R22, Air, Argone	0.29	107

Table 3.22c - Comparison of the Friction and Wear Results for Polyimide With Data Obtained in Other Studies in Lubricated Sliding Conditions and Temperature Above Ambient

Source	Material	Contact Pressure, psi	Sliding Velocity, fpm	Environ. Temperature °F	Counterface Material and Surface Roughness	Environment	Friction Coefficient	Specific Wear Rate $10^{-10}\ \frac{in.^3 \bullet min.}{ft \bullet lbf \bullet hr}$
Jones et al [23]	Polyimide (Grade Not Specified)	---	32.5	500	Steel (Not Specified)	Dry Air Mineral Oil	0.13 (0.07 - 0.23)	35
This Study	Vespel SP-21D	500 - 12900	40 - 664	245	SiPb Bronze	R134a PAG Oil	0.052 (0.03 - 0.08)	1.2
This Study	Vespel SP-3	500 - 1500	664	245	Ductile Cast iron, Ra 0.06 - 0.22 µm	R134a PAG Oil	0.052 (0.03 - 0.08)	0.67

Table 3.23a - Comparison of the Friction and Wear Results for Poly(amide-imide) With Data Obtained in Other Studies in Dry Sliding Conditions and Ambient Temperature

Source	Material	Contact Pressure, psi	Sliding Velocity, fpm	Environ. Temperature °F	Counterface Material and Surface Roughness	Environment and Lubricant	Friction Coefficient	Specific Wear Rate $10^{-10}\ \frac{in.^3 \bullet min.}{ft \bullet lbf \bullet hr}$
Fusaro [4]	Poly(amide-imide) with 10% PTFE and 15% Graphite Filler Similar to Torlon 4301	---	570	Ambient	440C HT Stainless Steel 0.07 µm Ra	Air 50% Relative Humidity No Lubricant	0.37	96.7
Jones et all [23]	Poly(amide-imide)	---	32.5	73	Steel	Air No Lubricant	0.62 (0.30 - 0.73)	17.5
Amoco [9]	Torlon 4301	50	200	73	C1018 Hardened	Air No Lubricant	0.27	17
Amoco [9]	Torlon 4301	50	900	73	C1018 Hardened	Air No Lubricant	0.14	53
Amoco [9]	Torlon 4301	1000	50	73	C1018 Hardened	Air No Lubricant	0.12	41
This Study	Torlon 4301	500	100	73	Ductile Cast Iron 0.17 µm Ra	R134a Refrigerant No Lubricant	0.40	16.7

Table 3.23b - Comparison of the Friction and Wear Results for Poly(amide-imide) With Data Obtained in Other Studies in Dry Sliding Conditions and Temperature Above Ambient

Source	Material	Contact Pressure, psi	Sliding Velocity, fpm	Environ. Temperature °F	Counterface Material and Surface Roughness	Environment and Lubricant	Friction Coefficient	Specific Wear Rate $10^{-10}\frac{in.^3 \bullet min.}{ft \bullet lbf \bullet hr}$
Jones et all [23]	Poly(amide-imide)	---	32.5	500	Steel	Air No Lubricant	0.43 (0.20 - 0.65)	137
This Study	Torlon 4301	100 - 1000	25-800	245	Ductile Cast Iron and SiPb Bronze 0.06 - 0.22 µm Ra	R134a R22 Air Argon No Lubricant	0.31 (0.19 - 0.52)	27.8 (10.2 - 120)

Table 3.23c - Comparison of the Friction and Wear Results for Poly(amide-imide) With Data Obtained in Other Studies in Lubricated Sliding Conditions

Source	Material	Contact Pressure, psi	Sliding Velocity, fpm	Environ. Temperature °F	Counterface Material and Surface Roughness	Environment and Lubricant	Friction Coefficient	Specific Wear Rate $10^{-10}\frac{in.^3 \bullet min.}{ft \bullet lbf \bullet hr}$
Amoco [9]	Torlon 4301	50	900	73	C1018 Hardened	Air Hydraulic Fluid	0.08	1.0
This Study	Torlon 4301	500	100	245	SiPb Bronze 0.12 µm Ra	R134a PAG Oil	0.024	0.87

The lower range of these values is represented by data given in the manufacturers manuals [13]. The higher values are those reported by Fusaro [4] for an unfilled polyimide, which is expected to provide worse tribological properties. Data from this study are closer to the lower end of the range.

Friction and wear differences are larger for tests conducted at higher temperatures and under lubricated conditions. Polymer wear rates at different temperatures obtained by Anderson [3] are probably the most complete. A comparison of data from this study with those obtained by Anderson is also given in Fig 3.21. As previously stated, the discrepancies in the results are due mainly to the difference in the PV values used by Anderson and in this study.

The lubricated condition results are even less consistent. This, however could be expected because the tribological phenomena in the interface are to a great extend determined by the properties of the lubricant used.

Table 3.23 presents data for the poly(amide-imide) polymers. These have been less extensively studied, and the most complete reference for their tribological behavior is the manufacturers manual [9]. Data from this study are close to those given in the manual and also close to those reported by Jones [23]. The higher wear rates given in the manual for the higher PV values can be attributed to the frictional heating of the interface.

In general, the data from this study display approximately the same range of change and average values as those presented in other studies.

3.5 Summary of the Results

The results from the friction and wear tests and surface analyses conducted on polyimide and poly(amide-imide) polymer grades can be summarizes as follows:

• Polyimide and poly(amide-imide) polymer grades do not chemically degrade in chlorodifluoromethane (R22) and tetrafluoroethane (R134a). These refrigerants may therefore be considered to provide inert environment for the polymer operation. The lack of water vapor in this environment may produce slightly higher friction coefficients than in air for polymer grades with graphite filler.

• The combination of graphite and PTFE as filler materials provides the best friction and wear characteristics in a refrigerant environment. These fillers also make the polymer grades capable of operating in a variety of environments without losing their outstanding tribological properties.

• Molybdenum disulfide-filled polymers perform better in refrigerant environment than in air. The wear rates for these polymer grades, are on the average, higher than those obtained with other fillers.

• Polyimide and poly(amide-imide) are both extremely good materials for dry bearing applications. Some grades can perform in dry conditions without any signs of thermal degradation at PV values as high as 800,000 psi•fpm.

• The friction coefficient and the wear rate for polyimide and poly(amide-imide) are very similar at moderate PV values (up to 100,000 psi•fpm) and at environmental temperatures of up to 245°F. Since the poly(amide-imide) has some advantages in cost and ease of processing, it should probably be used if performance at higher PV values is not necessary.

• Polyimide grades should be preferred at PV values above 100,000 psi•fpm because they have higher degradation temperatures and produce lower flash temperatures.

• Counterface surface roughness should be kept below 0.2 μm Ra, if low wear rates are desired. For exceptionally lower wear rates, a further decrease in the surface roughness may be very beneficial since the roughness to wear rate curve is steeper for the lower roughnesses. The manufacturing process for the counterface surface should be chosen in such a way as to reduce asperity peaks. The presence of deep valleys on the surface does not have detrimental effects on the wear rate.

• The environmental temperature has a strong effect on both the friction coefficient and wear rate. The wear rate can change by an order of magnitude if the temperature is increased from 73°F to 245°F. The friction coefficient is lower at the higher temperatures.

• The tribological behavior of polyimide and poly(amide-imide) is governed by the process of polymer transfer to the counterface surface. Typically, these polymers form thick ridges on the mating surface. Counterface surface roughness and material may affect the morphology of polymer transfer. Temperature is the decisive factor for the appearance, rate, and adhesive strength of the polymer transferred. Larger number of overlapping passes produce more uniform polymer films on the interface.

• The wear rates under lubricated conditions are one order of magnitude lower than those under dry conditions.

3.6 References

1. **Davis B., Sheiretov T., and Cusano C.,** Tribological Evaluation of Contacts Lubricated by Oil-Refrigerant Mixtures, Proceedings of the 1992 International Compressor Engineering Conference at Purdue, Purdue University, West Lafayette, IN, USA, 1992, pp. 477-487.

2. **Friedrich K.,** Sliding Wear Performance of Different Polyimide Formulations, *Tribology International,* 1989, **22** (1), pp. 25-31, 1989.

3. **Anderson J. C.,** Wear of Commercially Available Plastic Materials, *Tribology International,* 1982, **5** (5), pp. 255-263.

4. **Fusaro R. L. and Hady W. F.**, Low-Wear Partially Fluorinated Polyimides," *ASLE Transactions,* 1984, **28** (4), pp. 542-552.

5. **Play D. F.**, Counterface Roughness Effect on the Dry Steady State Wear of Self-Lubricating Polyimide Composites, *ASME Journal of Tribology,* 1984, **106** (4), pp. 177-184.

6. **Evans D. C., and Senior G.S.**, Self-Lubricating Materials for Plain Bearings, *Tribology International,* 1982, **15** (4), pp. 243-248, 1982.

7. **Tewari U. S. and Bijwe. J.**, On the Abrasive Wear of Some Polyimides and Their Composites, *Tribology International,* 1991, **24** (4), pp. 247-254.

8. **Sliney H. E.**, Some Load Limits and Self-Lubricating Properties of Plain Spherical Bearings with Molded Graphite Fiber-Reinforced Polyimide Liners to 320 C, *Lubrication Engineering,* 1978. **35** (9), pp. 497-502.

9. **Amoco Performance Products,** TORLON Engineering Polymers / Design Manual

10. **Gardos N.**, Self-Lubricating Composites for Extreme Environment Applications, *Tribology International,* 1982, **15** (5), pp. 273-283, 1982.

11. **Fusaro R. L.**, Counterface Effects on the Tribological Properties of Polyimide Composites, *Lubrication Engineering,* 1985, **42** (11), pp. 668-676.

12. **Sliney H. E. Jacobson T. P.**, Performance of Graphite Fiber-Reinforced Polyimide Composites in Self-Aligning Plain Bearings to 315 C, *Lubrication Engineering,* 1975, **31** (12) , pp. 609-613.

13. **Du Pont Company**, Start with Du Pont. Properties of Du Pont VESPEL Parts.

14. **Lancaster J. K.**, Estimation of the Limiting PV Relationships for Thermoplastic Bearing Materials, *Tribology,* 1971, **4** (2), pp. 82-87.

15. **Jaeger J. C.**, Moving Sources of heat and the temperature at sliding contacts, *Proceedings of the Royal Society of New South Wales,* 1942, **76**, pp. 203.

16. **ASM International**, ASM Handbook. Tenth Edition. Vol. 1: Properties and Selection: Irons, Steels, and High Performance Alloys.

17. **ASM International**, ASM Handbook. Tenth Edition. Vol. 2: Properties and Selection: Nonferrous Alloys and Special Purpose Materials.

18. **Fusaro R. L.**, Effect of Atmosphere and Temperature on Wear, Friction, and Transfer of Polyimide Films, *ASLE Transactions,* 1976, **21** (2), pp. 125-133.

19. **Lancaster J. K.**, Dry Bearings: a Survey of Materials and Factors Affecting Their Performance, *Tribology,* 1973, **6** (6) , pp. 219-251.

20. **Sviridyonok A. I.**, Self-Lubrication Mechanisms in Polymer Composites, *Tribology International,* 1991, **24** (1), pp. 37-42.

21. **Clarke C. G. and Allen C.**, The Water Lubricated, Sliding Wear Behaviour of Polymeric Materials Against Steel, *Tribology International*, 1991, **24** (2), pp. 109-118.

22. **Fusaro R. L., and Sliney H. E.**, Lubricating Characteristics of Polyimide Bonded Graphite Fluoride and Polyimide Thin Films, *ASLE Transactions,* 1972, **16** (3) pp. 189-196.

23. **Jones W. R., Hady W. F., and Johnson R. L.**, Friction and Wear of Poly(amide-imide), Polyimide, and Pyrrone polymers at 260 C (500 F) in Dry Air," *National Aeronautics and Space Administration,* NASA TN D-6353, 1971, pp. 1-17.

24. **Giltrow J. P. and Lancaster J. K.**, The Role of the Counterface in the Friction and Wear of Carbon Fiber Reinforced Thermosetting Resins, *Wear,* 1970, **16** (5) pp. 359-374.

25. **Briscoe A.**, Wear of Polymers: An Essay on Fundamental Aspects, *Tribology International,* 1981,**14** (4), pp. 231-243.

26. **Fusaro R. L.**, Molecular Relaxations, Molecular Orientation and the Friction Characteristics of Polyimide Films, *ASLE Transactions,* 1975, **20** (1), pp. 1-14.

27. **Mens, J. W. M. and de Gee, A. W. J.**, Friction and Wear Behaviour of 18 Polymers in Contact with Steel in Environments of Air and Water, *Wear,* 1991 **149** (1), pp. 255-268.

CHAPTER 4

Tribological Evaluation of Various Surface Treatments for M2 Tool Steel

4.1 Introduction

M2 tool steel is representative of a class of materials which are used in conditions characterized by a rapid application of loads and high temperatures, such as machining tools, high temperature springs, and bearings. The application of interest in this study is for the vane material in rolling piston compressors. In this application, the vane slides on a gray cast iron piston. This is the critical tribological contact in the rolling piston compressor. The vane has a cylindrical surface which makes contact with the piston. This line contact can experience maximum contact pressure of about 150,000 psi. In a previous study [1], it was found that the wear rate of a hardened M2 tool steel sliding on cast iron in a refrigerant R12-mineral oil environment can be 3-7 times lower than the wear rate of the same contact pair in a refrigerant R134a-polyolester oil environment. Since R134a will replace R12 in the near future, some measures should be taken to improve the tribological characteristics of the vane-piston interface when operated in a R134a-polyolester oil environment. One solution to this problem may be to increase the wear resistance of the vane by applying various wear resistant treatments or coatings to its surface. For example, it has been reported in the literature [2], that ion nitriding treatment improves the wear resistance of steel parts in a refrigerant environment. Hence, the tribological evaluation of various surface treatments for M2 steel in refrigerant environments is the major goal of this study.

4.2 Surface Treatments for M2 Tool Steel

All tool steels must be heat treated to develop specific combinations of wear resistance, resistance to deformation or breaking at high loads, and resistance to softening at elevated temperatures. In addition to the heat treatment, some surface processes may further enhance the wear resistance of the material. The tool steels constitute a wide class of materials, and different surface treatments are recommended depending on the chemical composition of the base material.

4.2.1 Chemical Composition of the M2 Tool Steel

M2 steel belongs to the class of high speed steels. These are subdivided into T and M series depending on the major alloying element - tungsten for the T series and molybdenum for the M series. Group M steels have slightly greater toughness than the T steels at the same hardness. Other alloying elements in M steels are tungsten, chromium,

vanadium, cobalt, and carbon. M2 steel alloying elements and their percentages are given in Table 4.1.

Table 4.1 - Chemical Composition of M2 Tool Steel

Element	C	Mn	Si	Cr	Ni	Mo	W	V
%	0.95 - 1.05	0.15- 0.40	0.20 - 0.45	3.75 - 4.50	0.30 max.	4.50 - 5.50	5.50 - 6.75	1.75 - 2.20

M2 steel, in particular, has unusually high resistance to softening at elevated temperatures. Several types of surface treatments for M2 steel are recommended in the literature [3, 4, 5, 6, 7, 8]. These surface treatments are: various nitrogen treatments (nitriding), boron treatment (boronizing), and vapor deposition processes (CVD and PVD). All these processes may be expected to improve the wear resistance of tool steels. A brief description of these surface treatment processes is given below.

4.2.2 Nitriding

Nitriding has been used as a surface treatment for high speed steel for four decades. It is particularly suited for high speed steels because they contain elements that readily form nitrides, such as chromium, vanadium, tungsten, and molybdenum. Moreover, this thermochemical treatment lies within the range of tempering temperatures used for high speed steel, so that it can be applied as a final stage of the heat treatment process [7].

Nitrogen diffusing into the steel surface at a temperature of about 550°C combines with the constituent elements to form nitrides, the precipitation of which is accompanied by hardening of the surface layers. The actual nature of the surface layer depends on the nitrogen potential of the nitriding medium and on the composition of the substrate. At low nitrogen potential, the hardness increase is in the surface layer of martensite, but at higher potentials, iron nitrides may form with a characteristic white layer on the surface. This white layer is unwanted in most cases, because it is extremely brittle. But it has some advantages such as reduction of both friction and possibly adhesion or galling [3, 5].

The hardness of a diffusion layer depends on the concentration of the nitride-forming element and the operating temperature. M2 samples nitrided at 450°C and 550°C are found to give hardness values of 1440-1500 and 1380-1450 HV, respectively [1]

There are three basic method of nitriding: gas, liquid, and plasma (ion) nitriding. Each of these is discussed below.

4.2.2.1 Gas Nitriding

4.2.2.1 Gas Nitriding

Gas nitriding is a case-hardening process whereby nitrogen is introduced into the surface of a solid ferrous alloy by holding the metal at suitable temperature in contact with nitrogenous gas, usually ammonia. It is usually performed in a temperature range of about 900° to 1100°F (480° to 590°C). Ammonia dissociates into nitrogen and hydrogen when it contacts the heated metal surface. Nitrogen then diffuses into the metal surface, forming nitrides, which harden the surface.Gas nitriding usually produces comparatively thick cases (0.004 in. or greater). This thick case tends to be brittle. Therefore, gas nitriding is not often used with M2 steel [9].

4.2.2.2 Liquid Nitriding

Liquid nitriding employs the same temperature range as gas nitriding, that is, 510° to 580°C. The case-hardening medium is a molten, nitrogen bearing fused-salt bath containing either cyanides or cyanates. These same substances are used in processes like liquid carburizing and nitro-carburizing. Because nitriding is performed at a lower temperature than carburizing, the process adds more nitrogen than carbon to the surface. The depth of the nitrided case is typically 0.002 in. or less, and the operation is usually carried out in such a way as to avoid the white layer which is normally considered undesirable [3].

There are several proprietary modifications of the same process, e.g. 'Tuffriding', 'Sulfinuz', and others [8].

An increase of machine cutting tool life up to 500% by the application of this process has been reported [5].

4.2.2.3 Plasma Nitriding

The principle of plasma (ion) nitriding comprises the use of a glow discharge in a nitrogen atmosphere, which concentrates the available energy near the surface of the material to be treated. The workpiece to be nitrided is contained in a vacuum chamber and is heated to a temperature of between 400°C and 600°C. It is subjected to a negative DC potential of between 100 and 1500 V relative to the chamber wall which is earthed. The gas in the chamber is ionized. If the atmosphere is nitrogen, this results in a rapid increase in nitrogen concentration at the surface of the specimen, and rapid nitriding takes place. The temperature range of the process is convenient for the treatment of hardened and tempered high speed steels. The process produces a very hard surface without changing the properties of the substrate. The hardened layer usually is very thin. An illustration of the

latter is the hardness gradient of a plasma nitrided surface of M2 steel, given in Fig. 4.1. In the figure the three curves correspond to three different specimens tested.

Plasma nitriding has one additional important effect. The impact of ions on the surface of the workpiece results in sputtering, or ejection of atoms from the metal surface. This sputtering removes any impurities from the metal surface, thus making it highly suitable for the subsequent diffusion process. Also the ejected metal atoms react with the nitrogen atmosphere and then condense on the surface increasing the nitrogen content. These effects are said to give the process some advantages compared to the other nitriding processes.

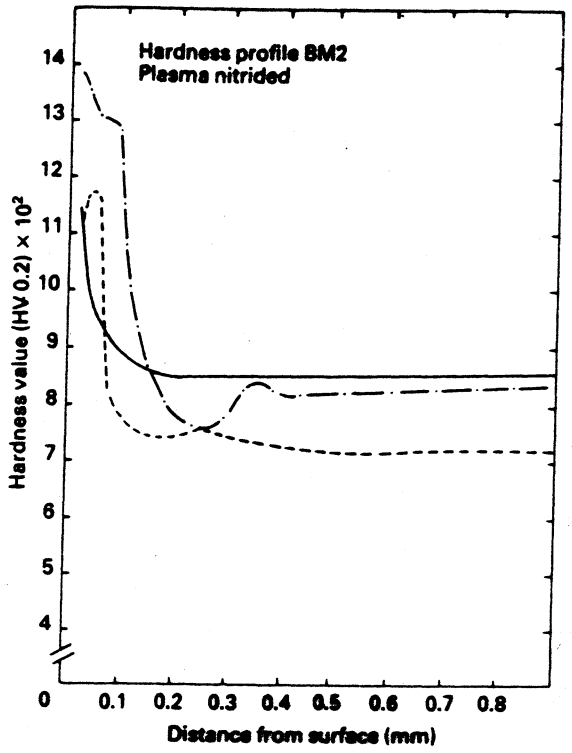

Fig. 4.1 - Hardness Gradient in Nitrided Surface [10]

4.2.3 Boronizing

Boronizing (boriding) is a thermochemical surface hardening process that can be applied to a wide variety of ferrous, nonferrous, and cermet materials. The process involves heating in the range of 700 to 1000 °C in contact with a boronizing compound, which can be paste, liquid or gaseous. The boron atoms diffuse into the metal forming either a single, or multiphase boride layer. The structure and the depth of the boride layer depends on the substrate treated, the presence of alloying elements, and the process temperature. Typically, the boride layer thickness is in the range of 0.0005 to 0.002 in. The boride layer is usually very hard (1500 - 2000 HV) [3, 4].

According to Budinski [4], tool steels provide a very suitable substrate for the boronizing process. The boronizing process can be performed either before or after the heat treatment. If the boronizing process is conducted first, then the subsequent hardening should be performed in an inert environment. If the heat treatment is first, then the boronizing should be performed at lower temperature, e.g. 540°C. In any case, if any increase in the wear resistance is desired the substrate should be heat treated to the same condition that would be acceptable if the material were to perform without the boronizing treatment.

The necessity to perform heat treatment in an inert environment is one of the disadvantages of the process. Another disadvantage is that the rolling contact fatigue properties of borided alloy steel parts are worse than those of carburized or nitrided steels [3, 11].

4.2.4 Vapor Deposition Processes

One of the most significant advances in high speed steel technology in recent years has been the introduction of commercial processes for deposition of hard coatings such as titanium nitride or carbide, alumina, or even diamond on the surface of steel [5]. The unique feature that distinguishes these methods from the more traditional methods discussed above is that the reaction at the surface causes deposition of the coating compound without involvement of the elements present in the steel substrate. The vapor deposition processes include the chemical vapor deposition (CVD) and the physical vapor deposition (PVD) processes.

4.2.4.1 Chemical Vapor Deposition

Titanium nitride coatings are probably among the most common for high speed tool steels. Titanium carbide, or carbonitride coatings are used as well. There is a growing tendency to use multiple layer deposition, varying the composition of the coating to optimize the adhesion of the coating to the substrate, and to create a surface with the desired properties.

The basic reaction in the CVD of titanium nitride (TiN) is:

$2TiCl_4 + N_2 + 4H_2 \rightarrow 2TiN + 8HCl$

The reaction takes place at a temperature between 850°C and 1000°C. Because the treatment temperature is above the tempering temperature range normally used for high speed steel but below the austenitizing range, the coating has to be applied before hardening, which means that vacuum hardening is required in order to preserve the coating.

The thickness of the coatings is typically 0.20 - 0.40 micro inches.

4.2.4.2 Physical Vapor Deposition

This process has the advantage that it takes place at a temperature below the tempering temperature of the high speed steel, so that fully hardened, tempered and finished parts can be treated. In the PVD process, a reaction between the gas atmosphere and the ions of some other metal takes place to produce a compound which is deposited on the steel surface. The thickness of the coating is usually in the range of 0.15 - 0.25 micro inches.

4.2.5 Layer Thickness and Hardness for Various Surface Treatments

There is an optimal case or coating thickness for each surface treatment process. If the coating is very thin, it may easily be worn out. On the other hand, if the coating is thicker than a certain limit, its intrinsic brittle nature begins to dominate. The cases or coatings may then be cracked and easily chipped from the surface. With tool steels, thinner coatings and cases are usually preferred. The preferred ranges of the case or coating thickness for various surface treatment processes are given in Table 4.2. The ranges of the surface hardness values obtainable by the various surface treatments are also given in Table 4.2 and Fig. 4.2. Data given in the table and the figure have been obtained by Hoyle [5].

Table 4.2 - Layer Thickness and Hardness for Various Surface Treatments

Heat Treatment	Hard Layer Thickness 10^{-6} in.	Hard Layer Hardness HV
Gas Nitriding	> 4.00	800 - 1500
Liquid Nitriding	< 2.00	800 - 1500
Plasma Nitriding	< 2.00	800 - 1500
Boronizing	0.50 - 2.00	1500 - 2000
TiN Coating (CVD)	0.20 - 0.40	1900 - 2500
TiN Coating (PVD)	0.15 - 0.25	2000 - 3000

4.2.6 Other Surface Treatment Processes for High Speed Steels.

In addition to the treatments described above, there are other processes that have provided improvement in the tribological properties of high speed steels. A brief description of the most popular of these processes is given below.

4.2.6.1 Carburizing

Carburizing, at least in its traditional form, is not widely used for high speed steels because the cases on such steels are extremely brittle. Carburizing may be useful in applications which require extreme wear resistance, but are not subjected to impact or highly concentrated loading [3].

There is, however, renewed interest in this treatment as a result of the introduction of vacuum and plasma carburizing [5]. With these processes, the carburizing can be better controlled, and a carbon content between 1.0 and 2.4% may be attained. Carburized high speed steels must be hardened after carburizing.

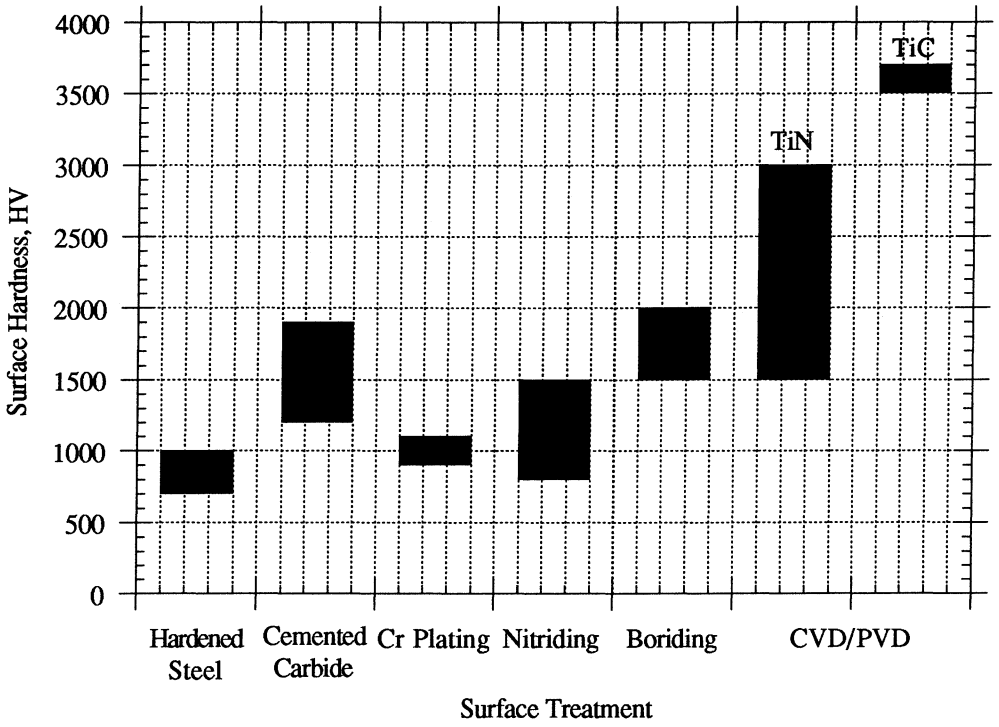

Fig. 4.2 Hardness of Various Surface Treatments

4.2.6.2 Toyota Diffusion Process

The Toyota Diffusion (TD) process was introduced in the early 1970s, and is designed to produce a layer of alloy carbides on the surface of steels, using a borax bath containing ferro-alloys which combine with carbon in the steel surface. Layers of vanadium, titanium, niobium or chromium carbides can be formed on the surface. TD treated parts can be heat treated to obtain desired core properties without detriment to the quality or adhesion of the carbide layers, provided the TD operation is carried out under strictly controlled conditions [5].

4.3 Experimental Procedure

All tests in this study were conducted with a high pressure tribometer. A complete description of the capabilities and the operation of this test facility is given in [1].

4.3.1 Simulation of Critical Contact

The critical tribological contact in a rolling piston compressor is that between the vane and the piston. The vane tip and the piston have cylindrical shapes. In the tests conducted, this contact was simulated by a cylindrical pin sliding on a flat plate. The radius of the pin is equal to the equivalent radius calculated by Hertz's contact stress formulae. Hence, the maximum Hertzian stress in the simulated contact is equal to the stress in the real compressor. More detailed information about the critical contact simulated is given in [1]. The pin and plate dimensions are the same as those given in Table 2.1. The specimen holders used are the same as those used in [1]. Specimen materials are the same as those given in Table 2.1.

4.3.2 Surface Treatments for the M2 Steel Tool Pin.

Various surface treatments for the M2 tool steel pin were tested. These were: gas nitriding with two different case thicknesses, liquid nitriding, boronizing, and a CVD TiN coating. All specimens were heat treated at the same time and under the same conditions, to an average surface hardness of about 900 HV before the application of the surface treatment. The TiN coated specimens were heat treated after the CVD process. All surface treatments were done by commercial surface treating companies. Data for the various surface treatments tested are given in Table 4.3. They are representative of the condition after the treatment.

Table 4.3 - Characteristics of Various Surface Treatments for the M2 Tool Steel Pins

Surface Treatment	Hard Layer Thickness in.	Surface Hardness HV	Substrate Hardness HV	Surface Roughness μm Ra
Gas Nitriding	0.008	1450	914	0.28
Gas Nitriding	0.012	1500	936	0.27
Liquid Nitriding	0.001	1540	938	0.29
Plasma Nitriding	---	1690	918	0.26
Boronizing	---	1261	730	0.25
TiN Coating (CVD)	---	2631	1100	0.32
Hardened	---	913	910	0.29

The surface roughness of the pins varied in the range from 0.25 to 0.32 μm Ra. This variation was due to the slight changes to the surface caused by the various surface treatments applied. In fact, most of the surface treatments did not alter the initial surface roughness. Since the surface roughnesses of the pins fell within a narrow range of values, their effects on the results are believed to be insignificant.

The hardness of the pins, both surface and substrate, is an important tribological parameter. From Table 4.3 and Fig. 4.2, it is evident that the surface hardnesses of the specimens used for this study are typical for the surface treatment applied. The only substantial discrepancy is with the boronizing treatment for which the hardness of the surface is below the values usually achieved with this surface treatment process. All the substrate hardness values are close to the hardness of the hardened steel specimen, again with the exception of the boronizing process. The reason for these lower hardness values is that the boronized specimens were not heat treated after the boronizing process. Since the process temperature lies above the tempering temperature for M2 steel, the substrate lost some of its hardness.

4.3.3 Surface Characteristics of the Cast Iron Plates

The surface roughness and surface hardness of both the plates and the pins were measured for each test. The gray cast iron plates were ground to an average surface roughness of 0.58 μm Ra. The range of the surface roughness readings for the whole set of plates used in the tests was from 0.43 to 0.73 μm Ra. The distribution of the surface roughness of the plates is given in Fig. 4.3. From the figure, it is evident that surface roughness range is relatively narrow. Therefore, it was assumed that the small differences in roughness would not significantly influence the friction and wear results. The surface hardness of the plates was measured as well. The average surface hardness was about 573 HV and the scatter of the surface hardness readings is given in Fig. 4.4.

4.3.4 Test Conditions and Test Duration

Two maximum contact pressures were used in the tests: 150,000 psi and 200,000 psi. The sliding motion was oscillatory with 100 fpm amplitude and 5 Hz frequency. The environmental temperature was 177°F. The test conditions were essentially the same as those given in Table 2.2.

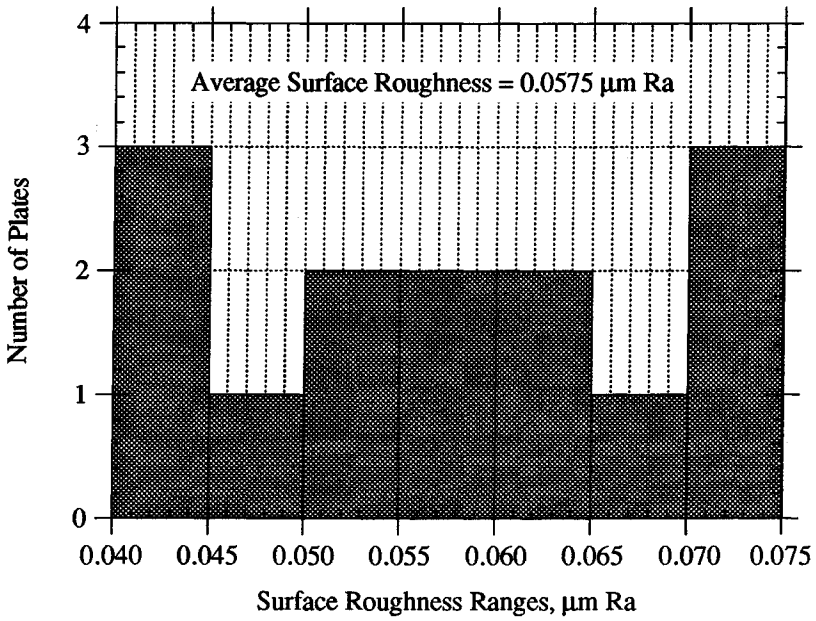

Fig. 4.3 - Surface Roughness Of the Gray Cast Iron Plates

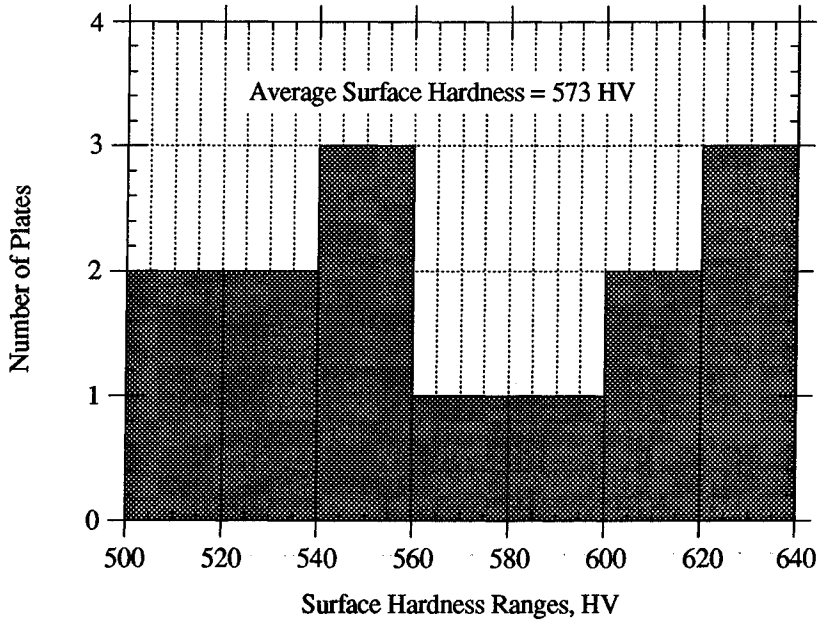

Fig. 4.4 - Surface Hardness of the Gray Cast Iron Plates

The duration of the tests was varied over a broad range in order to monitor the wear rate on the surfaces of the specimens. There were some indications that the wear rate was not constant throughout the test. There was an initial run-in period in which the wear rate was relatively high. The duration of this initial period was found to differ with the various surface treatments. To monitor the wear rate on surfaces of the specimens, testing was stopped occasionally and measurements of the wear were made. Wear measurements were taken at the following times: 15 min., 1 hour, 5 hours, and 10 hours. The total duration of these tests was 16 hours and 15 min. These were tests at 150,000 psi maximum contact pressure. Most of the tests at 200,000 psi were 10 hours long. A small number of 24-hour-long tests were conducted with the TiN coating in order to obtain measurable wear. The tests were conducted either in a R134a refrigerant-polyolester oil mixture, or in polyolester oil without the refrigerant. Data for the polyolester oil are given in Table 2.3.

4.3.5. Friction and Wear Measurements

The friction coefficient was monitored and recorded constantly throughout the test by a computer controlled Data acquisition system. The latter is described in more detail in Chapter 5 of this study.

The wear on the tool steel pin was obtained by measuring the width of the wear scar by an optical microscope. The wear volume was then calculated using simple geometry, as described in Chapter 1.

The wear of the plates was measured by taking surface profiles of the plate perpendicular to the wear scar, as described in Chapter 1. With the shorter test durations (15 min. and one hour) this method could not be used for quantitative measurements because the depth of the wear scars was too small.

Additional qualitative information on the nature of wear was obtained with optical and electron microscopes.

4.4 Results and Discussion

4.4.1 Friction and Wear Results for the Tests Conducted at 200,000 psi Maximum Contact Pressure

All the surface treatments were initially tested at 200 ksi maximum contact pressure in R134a -polyolester oil mixture. The duration of these tests was 10 hours. The results from these tests are given in Table 4.4. The same results are presented in graphical form in Fig 4.5 through 4.7. Since the behavior of the two gas nitriding treatments was very similar, only the data for the 0.008 in. thick case are given in the graphs.

Table 4.4 - Friction and Wear Results for the Tests Conducted at 200 ksi Max. Contact Pressure in R134a-Polyolester Oil Mixture. Test Duration = 10 hours.

Surface Treatment	Ave. Friction Coefficient	Pin Wear Scar Width mm	Pin Volume Worn 10^{-3} mm^3	Ave. Plate Wear Depth μm	Pin Hard Layer Surface Morphology
Gas Nitriding, Case 0.08 in.	0.039	0.32	8.20	0.50	Cracked and Chipped
Gas Nitriding, Case 0.12 in.	0.040	0.32	8.20	0.50	Cracked and Chipped
Ion Nitriding	0.048	0.27	4.92	0.70	Smooth and Continuous
Liquid Nitriding	0.044	0.25	3.91	0.70	Smooth and Continuous
Boronizing	0.041	0.39	14.8	0.40	Flattened Oval Asperities
TiN Coating	0.084	0.12†	0.43	1.00	Flattened Sharp Asperities
Hardened	0.040	0.26	4.40	0.80	Smoothened Surface

† Value is only approximate due to the irregularity and discontinuity of the wear scar

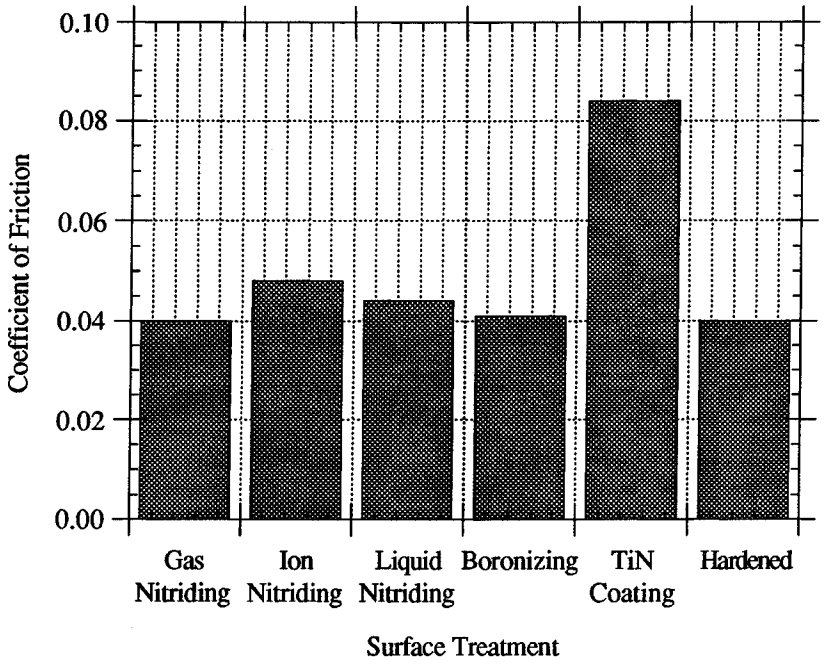

Fig. 4.5 - Average Coefficient of Friction for Various Surface Treatments Tested in R134a-Polyolester Oil Mixture
Contact Pressure = 200 ksi. Test Duration = 10 hours.

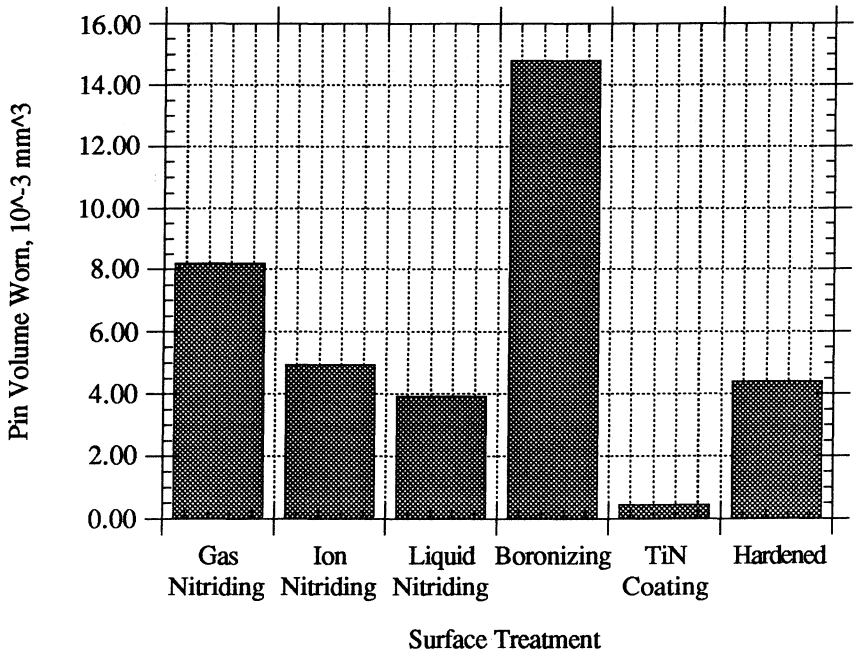

Fig. 4.6 - Pin Wear Volume for Various Surface Treatments Tested in R134a-Polyolester Oil Mixture Contact pressure = 200 ksi. Test Duration = 10 hours.

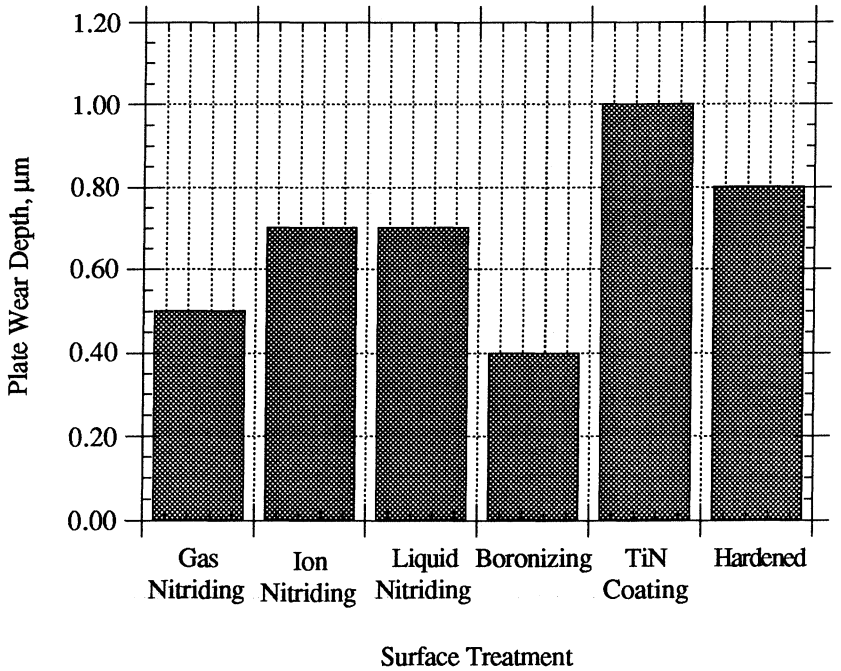

Fig. 4.7 - Plate Wear Depth for Various surface Treatments Tested in R134a-Polyolester Oil Mixture Contact pressure = 200 ksi. Test Duration = 10 hours.

Some of the results obtained were somewhat unexpected. The TiN coating was expected to give the least wear on the pins, and this was confirmed by the tests. It showed wear volumes an order of magnitude less than the other surface treatments. Due to their higher surface hardness, the other surface treatments were expected to provide lower wear volumes on the pin compared to the hardened pin. Two of the surface treatments, namely the liquid and the ion nitriding, produced almost the same wear volumes as the hardened specimen. The other two, the gas nitriding and the boronizing produced twice and three times larger wear, respectively. In the case of the gas nitriding, the high wear could be explained by the relatively thick and brittle case. The boronizing treatment was expected to produce the second smallest wear after the TiN coating, but it gave the worst wear results. This behavior is probably due to the fact that the boronized specimens were not heat treated after the surface treatment. Hence the substrate of the specimen remained relatively soft (see Table 4.3). The thickness of the hard layer, though not measured, is typically very small for this surface treatment, and without the support from the substrate it obviously could not perform well under the high contact pressures used in this study. SEM examination of the surface showed that, regardless of the high volume worn, the case was not completely worn off.

The coefficient of friction was similar for all specimens with the exception of the TiN coating, which produced friction coefficients twice as large as the others treatments. The boronizing specimens consistently showed the lowest friction coefficients.

The wear on the gray cast iron plates was inversely proportional to the wear on the pins. The highest wear on the plate occurred with TiN coated specimens, and the lowest plate wear occurred with the boronized specimen.

In order to better understand the friction and wear behavior of the specimens, the worn surfaces were examined with optical and scanning electron microscope (SEM).

4.4.2 Wear Surface Morphology for the Various Surface Treatments

Micrographs of the pin wear scar are shown in Fig. 4.8 and Fig 4.9. The photographs given in Fig. 4.8 were taken with an optical microscope, while those in Fig. 4.9 are SEM micrographs.

Figures 4.8(a) and (b) show the surface of the wear scar of the gas nitrided pin. This surface has the same appearance for both case thicknesses tested. Typical for this type of wear were the two lighter color bands adjacent to the dark colored wear scar. Examination of these bands with the SEM (Fig. 4.9 (a) and (b)) revealed that this appearance was due to the chipping of the hard layer, thus exposing the lighter substrate.

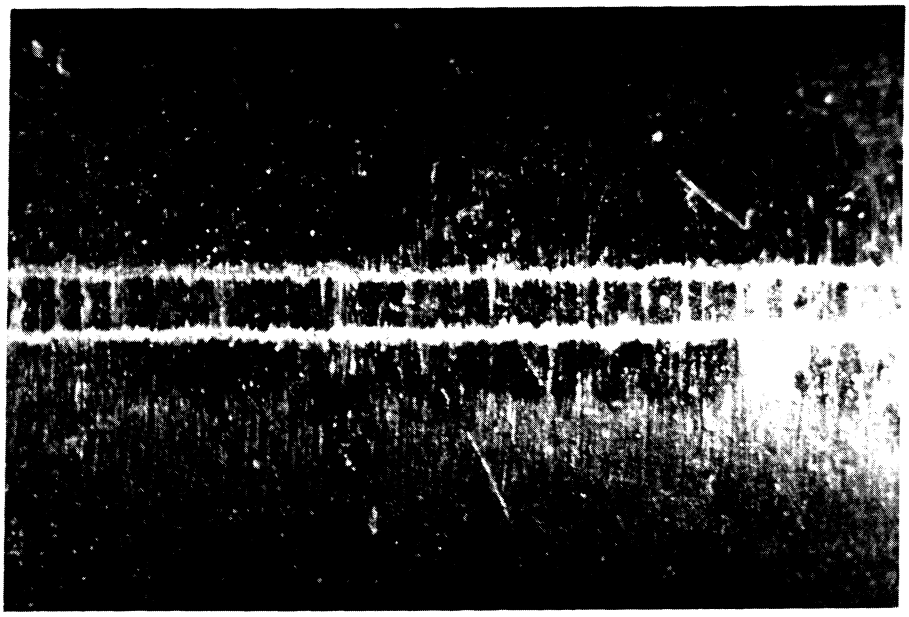

(a)

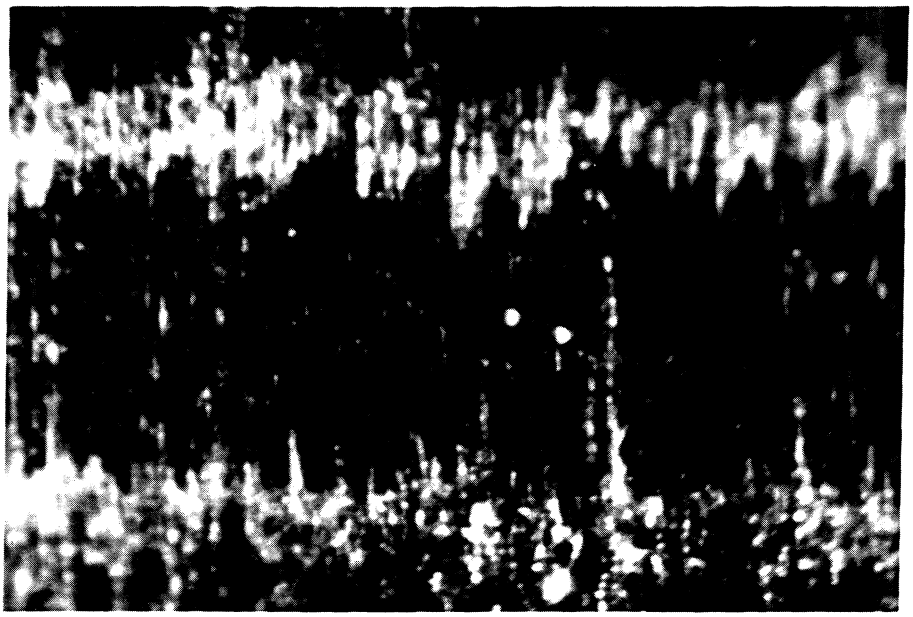

(b)

Fig. 4.8 - Wear Scar on the M2 Tool Steel Pin Tested In R134a-Polyolester Oil Mixture
(a) Gas Nitrided, Magnification 10x (b) Gas Nitrided, Magnification 63x.
Contact Pressure = 200 ksi. Test Duration = 10 hours

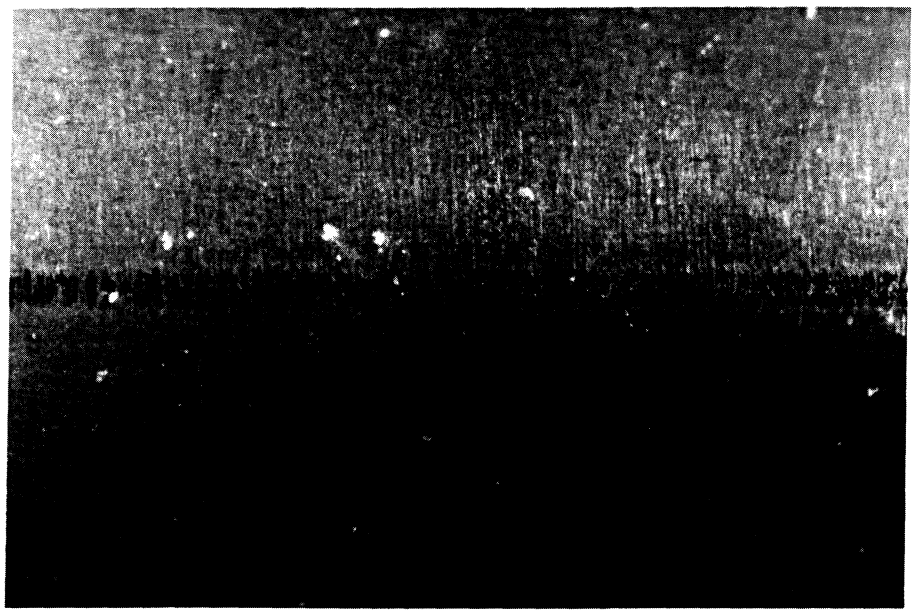

(c)

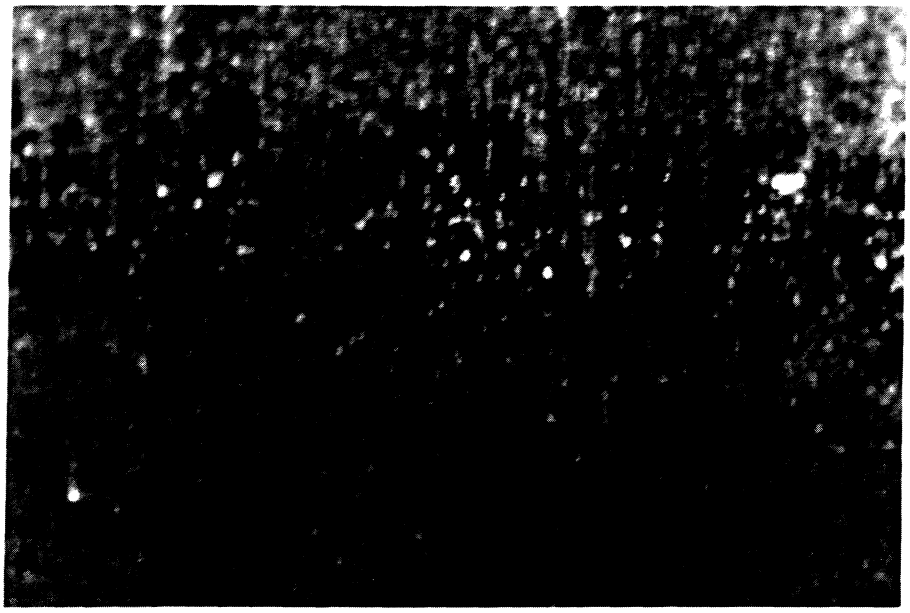

(d)

Fig. 4.8 (cont.) - Wear Scar on the M2 Tool Steel Pin Tested In R134a-Polyolester Oil Mixture (c) Ion Nitrided, Magnification 10x, (d) Ion Nitrided, Magnification 63x. Contact Pressure = 200 ksi. Test Duration = 10 hours

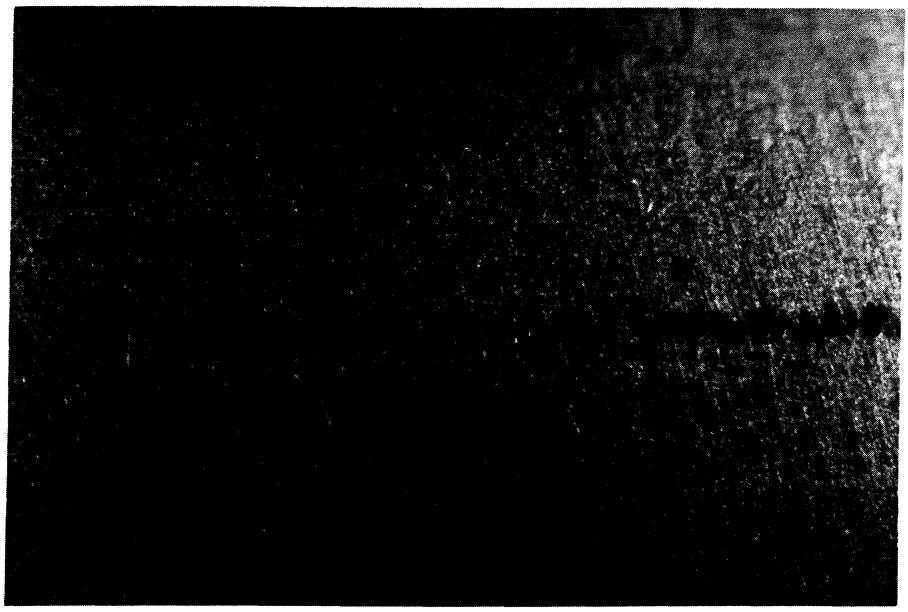

(e)

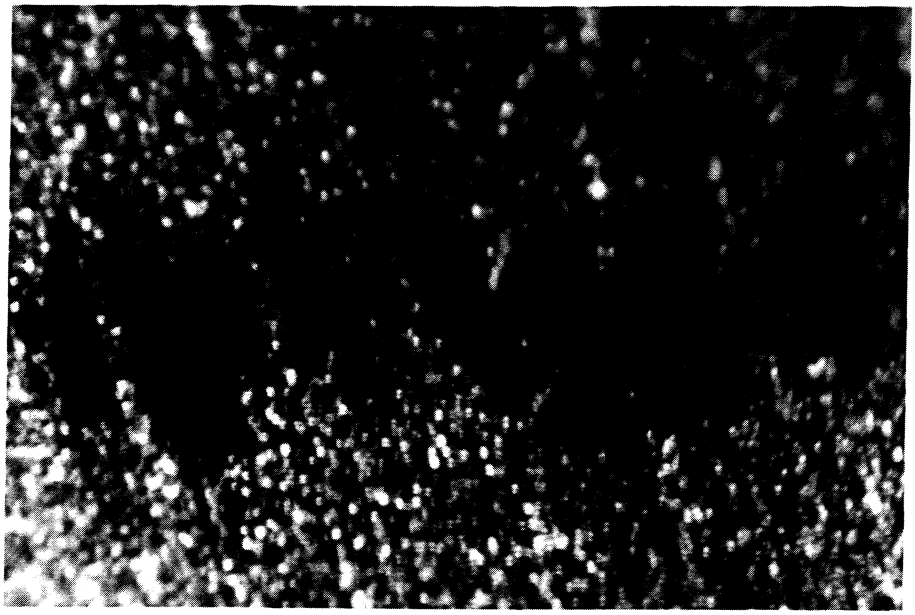

(f)

Fig. 4.8 (cont.) - Wear Scar on the M2 Tool Steel Pin Tested In R134a-Polyolester Oil Mixture (e) TiN Coated, Magnification 10x, (f) TiN Coated, Magnification 63x. Contact Pressure = 200 ksi. Test Duration = 24 hours

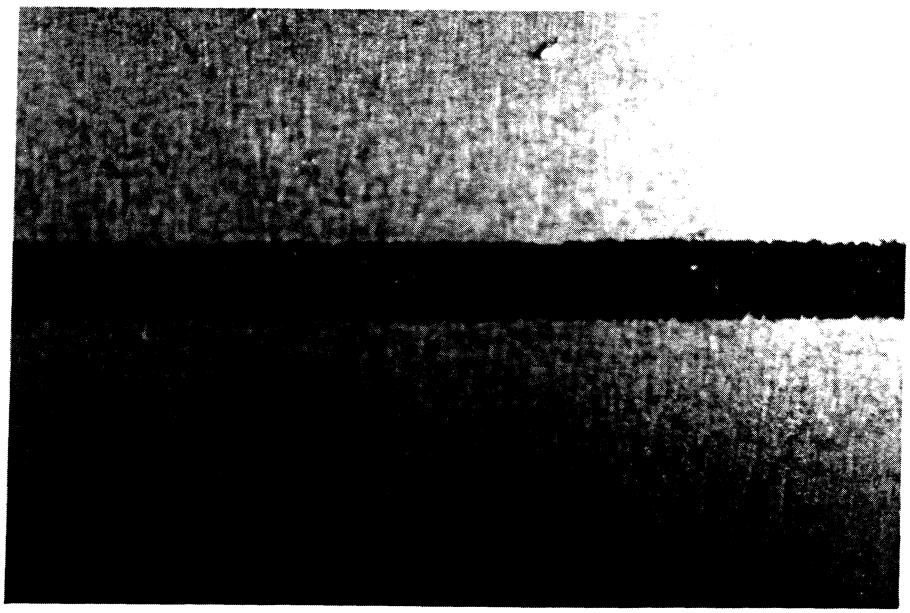

(g)

(h)

Fig. 4.8 (cont.) - Wear Scar on the M2 Tool Steel Pin Tested In R134a-Polyolester Oil Mixture (g) Boronized, Magnification 10x, (h) Boronized, Magnification 63x. Contact Pressure = 200 ksi. Test Duration = 10 hours

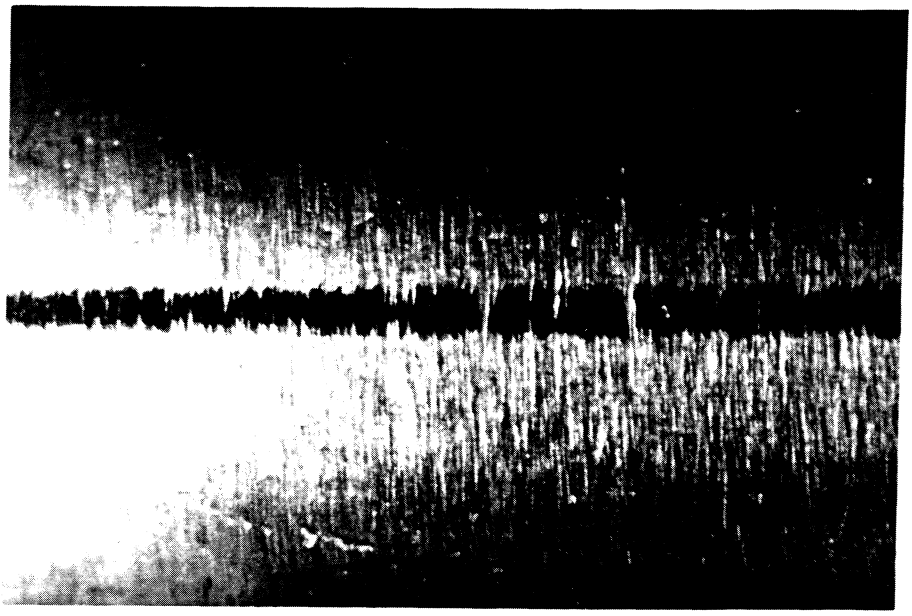

(i)

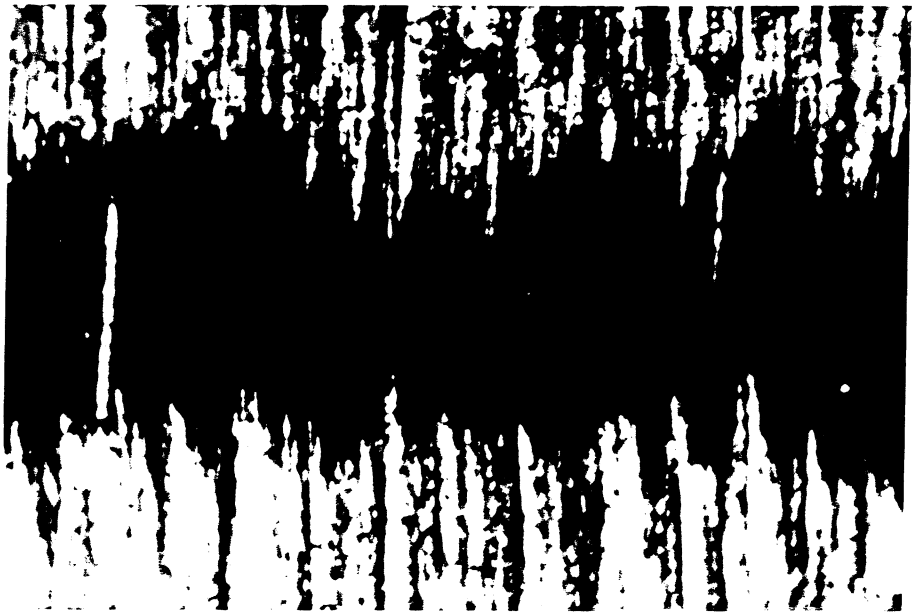

(j)

Fig. 4.8 (cont.) - Wear Scar on the M2 Tool Steel Pin Tested In R134a-Polyolester Oil Mixture. (i) Liquid Nitrided, Magnification 10x, (j) Liquid Nitrided, Magnification 63x. Contact Pressure = 200 ksi. Test Duration = 10 hours

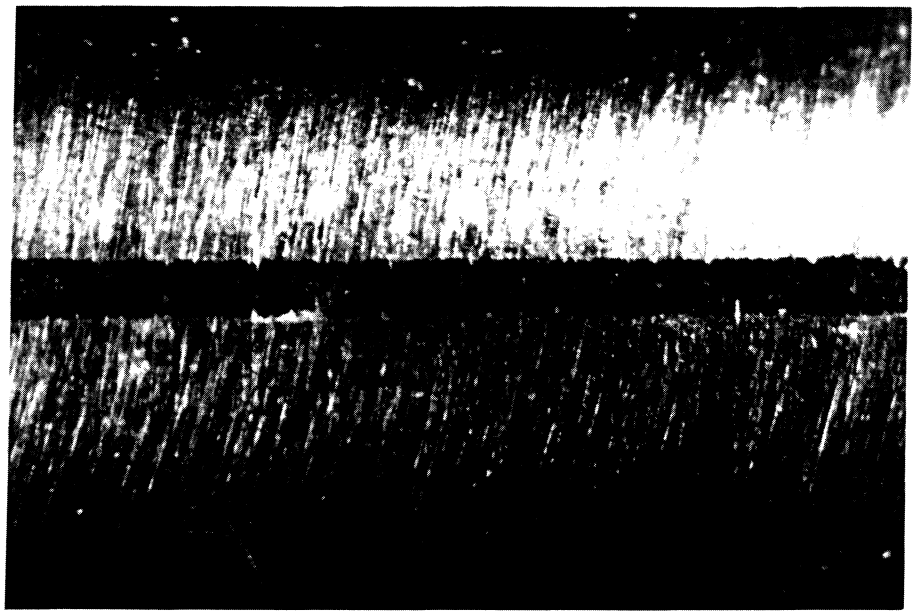

(k)

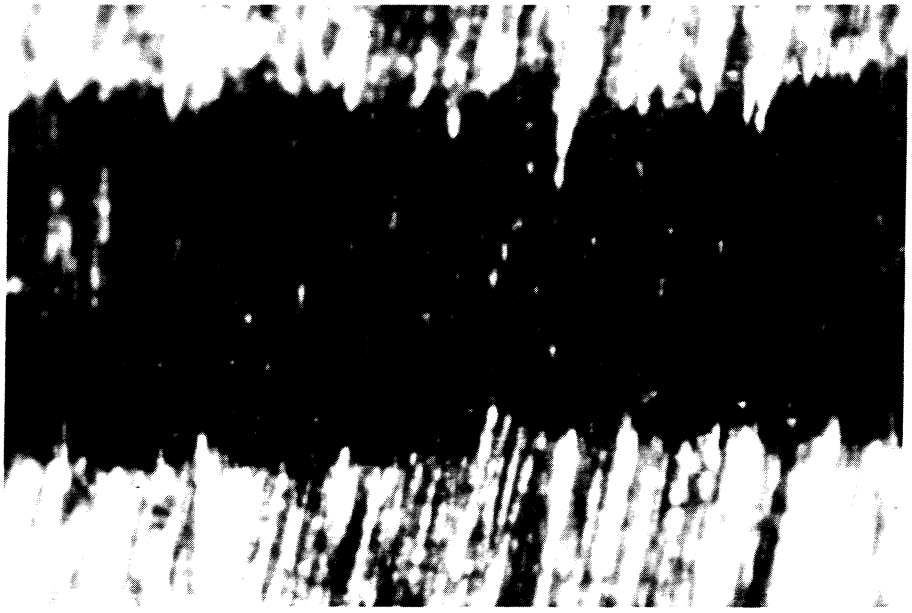

(l)

Fig. 4.8 (cont.) - Wear Scar on the M2 Tool Steel Pin Tested In R134a-Polyolester Oil Mixture (k) Hardened, Magnification 10x, (l) Hardened, Magnification 63x. Contact Pressure = 200 ksi. Test Duration = 10 hours

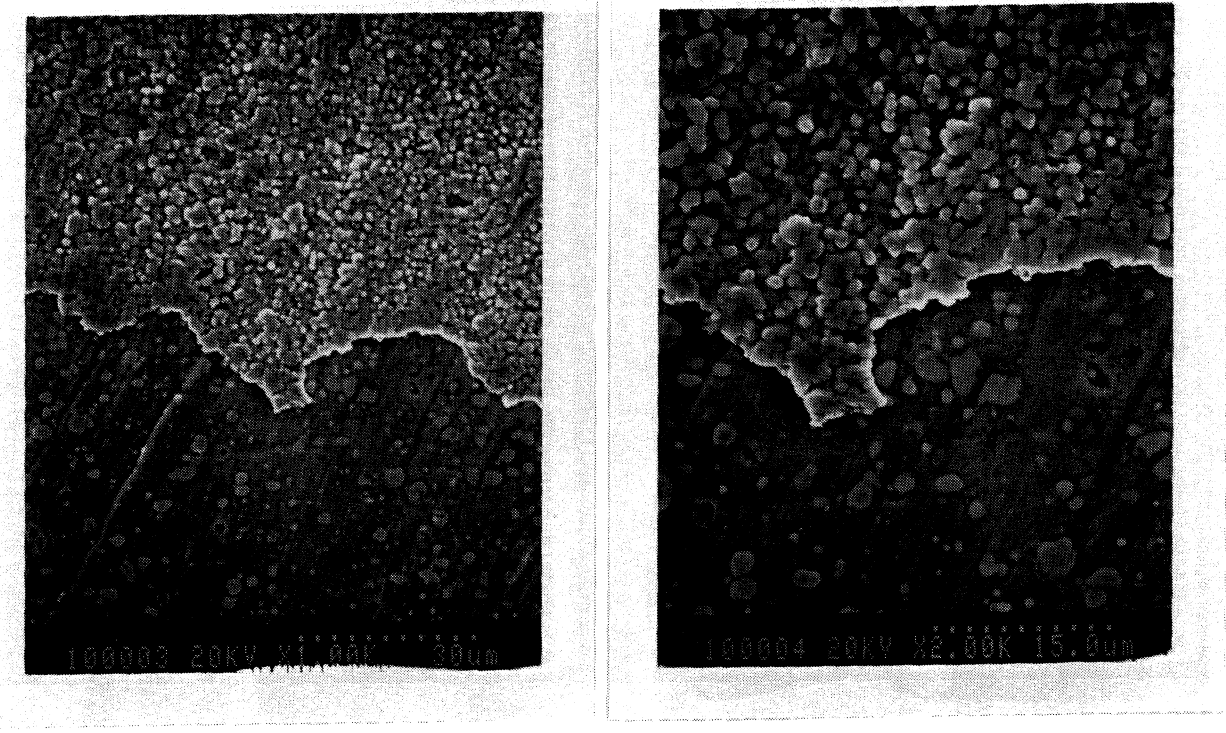

(a) (b)

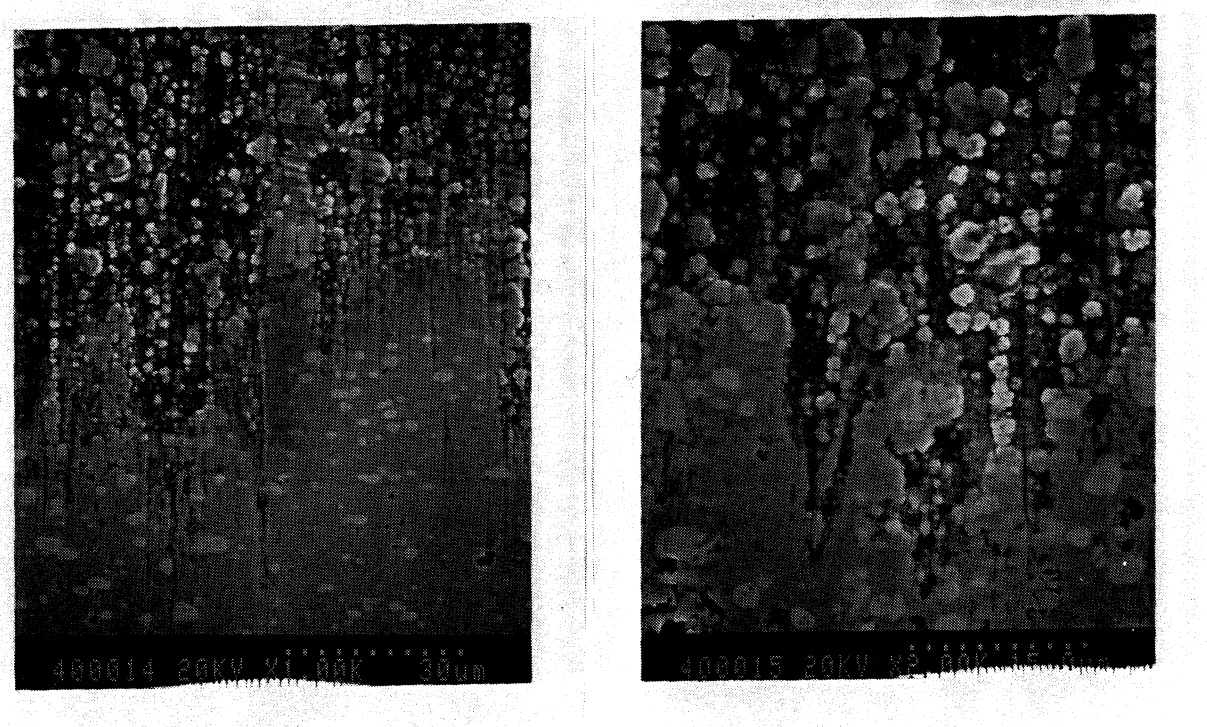

(c) (d)

Fig. 4.9 - SEM Micrographs of Pin Wear Scar for Various Surface Treatments
(a) Gas Nitrided at Magnification 1K, (b) Gas Nitrided at Magnification 2K,
(c) Ion Nitrided at Magnification 1K, (d) Ion Nitrided at Magnification 2K.

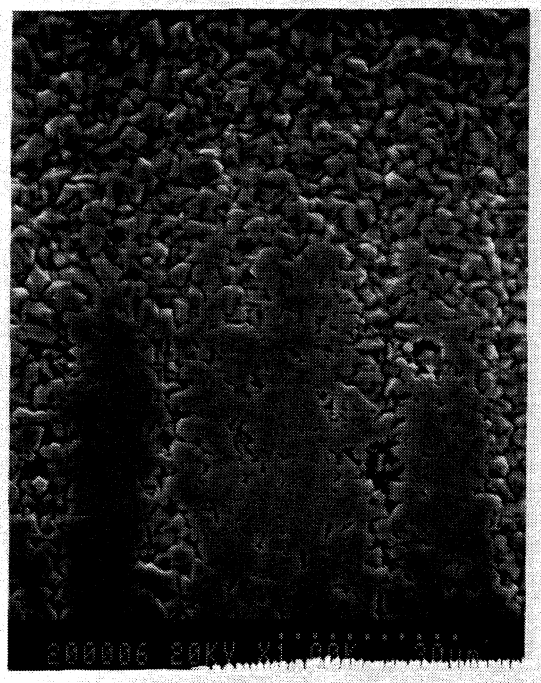

(e)

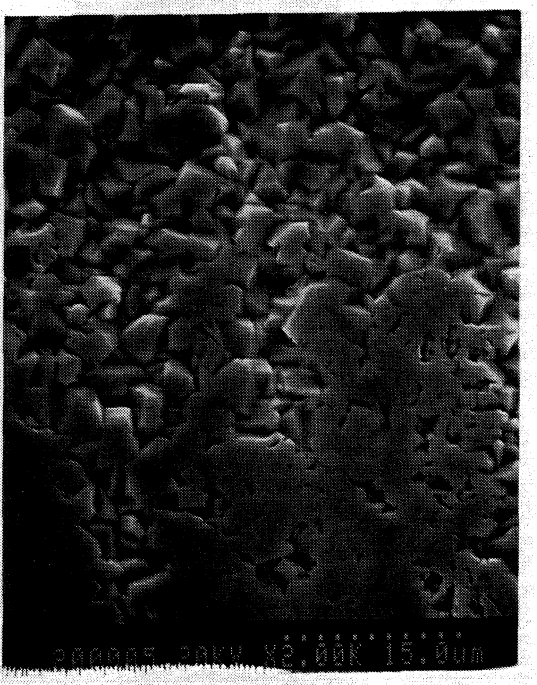

(f)

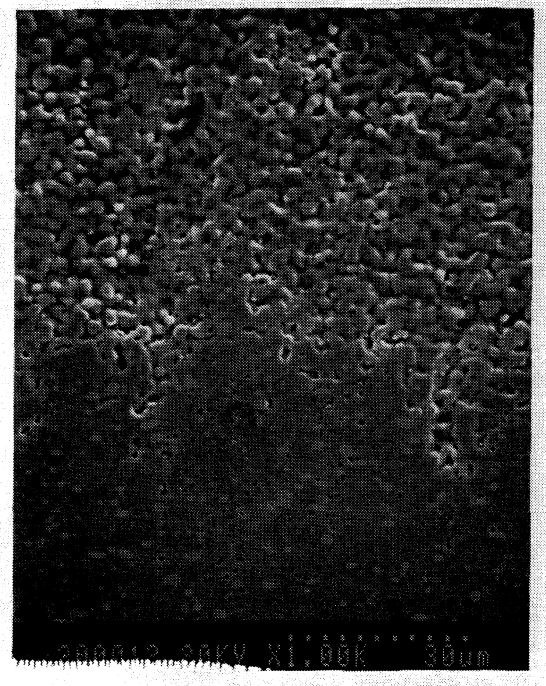

(g)

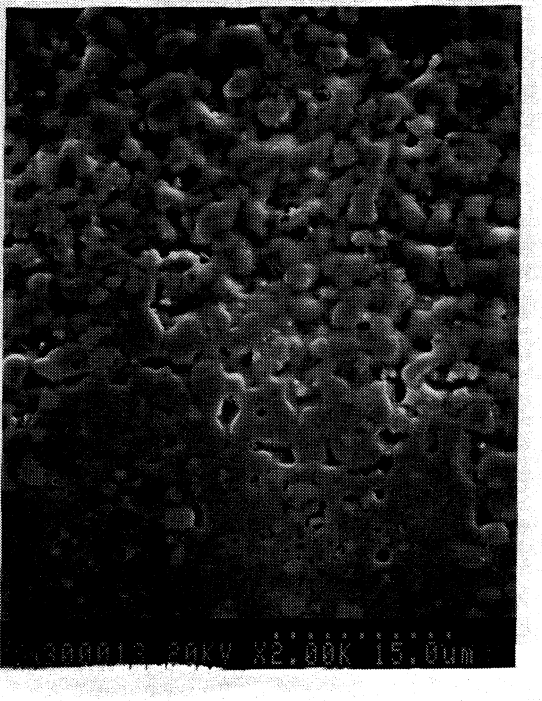

(h)

Fig. 4.9 (cont.) - SEM Micrographs of Pin Wear Scar for Various Surface Treatments
(e) TiN Coated at Magnification 1K, (f) TiN Coated at Magnification 2K,
(g) Boronized at Magnification 1K, (h) Boronized at Magnification 2K.

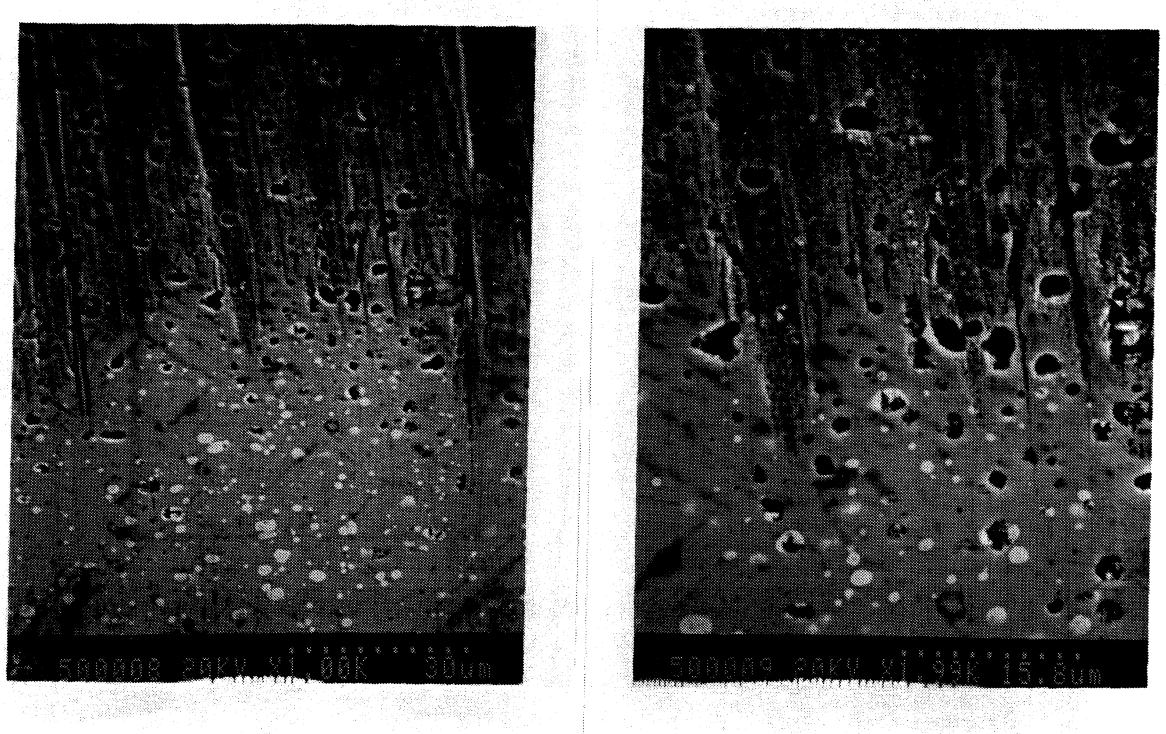

(i) (j)

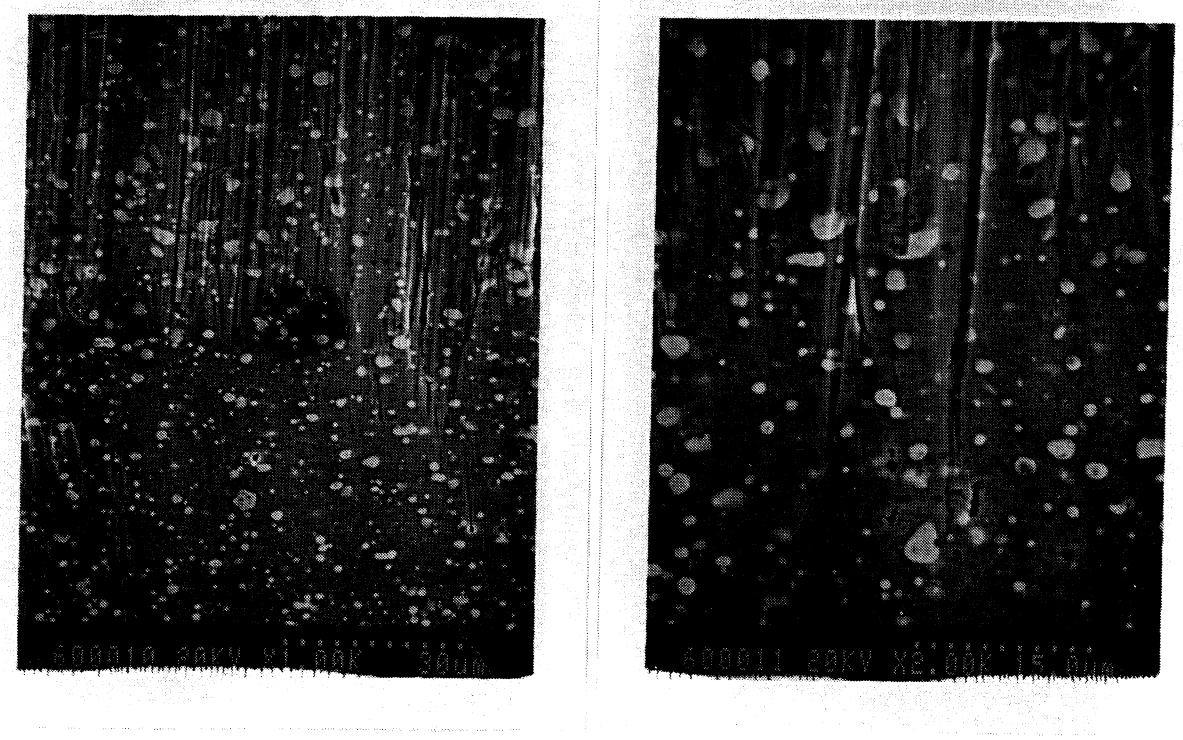

(k) (l)

Fig. 4.9 (cont.) - SEM Micrographs of Pin Wear Scar for Various Surface Treatments
(i) Liquid Nitrided at Magnification 1K, (j) Liquid Nitrided at Magnification 2K,
(k) Hardened at Magnification 1K, (l) Hardened at Magnification 2K.

The regions which can be distinguished on the picture are the nitrided layer, which has a granular appearance, and the substrate, on which machining marks are visible. These marks are partially smoothened by the wear process (the bottom portion of the photographs). From the pictures, it is evident that this surface treatment did not work well and that the hard layer was worn out fairly quickly. This result was expected. Gas nitriding for tool steels is not recommended in the literature [3].

The ion nitrided pin has a wear scar quite different from that of the gas nitriding. It is dark in color and quite well distinguished (Fig. 4.8 (c) and (d)). The SEM shows that the hard layer was not completely worn off during the test, and the different color of the wear scar compared to the unworn surface is due to a smoothening and gradual wear of the surface (see Fig. 4.9 (c) and (d)).

The wear scar produced on the TiN coated pin is given in Fig. 4.8 (e) and (f). It is discontinuous and appears more like isolated wear patches. The SEM examination, given in Fig. 4.9 (e) and (f), shows some smoothening of the surface in the areas of contact. The surface is characterized by asperities with sharp edges. It is possible that these asperities were causing abrasion of the mating surface. This larger abrasion component was probably the reason for the recorded high friction coefficient and wear on the plate surface. This type of surface texture might not be suitable for sliding contact applications when low wear on both surfaces is desired. In refrigerator compressors in particular, it can cause higher energy consumption and shorter service life of the piston. It is possible, however, to produce TiN coatings with a smooth surface by controlling the deposition process. These will cause minimal abrasion of the mating surface and can produce friction coefficient even lower than those for the uncoated steel due to reduced adhesion component of the friction force [7].

The boronized surface gave the largest wear scars. The appearance of the wear scar is given in Fig. 4.8 (g) and (h). The surface of the specimen is grayish in color while the wear scar appears as a black band. Examination with the SEM (see Fig. 4.9 (g) and (h)) shows wear and smoothening of the asperities on the surface of the specimens The surface looks more like one produced by a deposition, rather than a diffusion process. It is to some extent similar to the one produced by the CVD process. According to the heat treating company which made the coating, there is always some growth of boride compounds on the surface, while the hardest and the most wear resistant layer lies deeper below the surface. Even though the cases produced by the boronizing treatment are in general very thin (see Table 4.2), the hard layer does not seem to be completely worn anywhere on the surface of the pin. The asperities for this treatment are rounded, and therefore, they probably did not abrade the counterface as much as the TiN coating.

Pictures of the liquid nitrided pin are given in Fig 4.8 (i) and (j), and Fig. 4.9 (i) and (j). In this case, the type of wear observed is very much similar to that observed on the hardened surface (Fig. 4.8 (k) and (l) and Fig. 4.9 (k) and (l)). This is due to the fact that the case is much thinner than those produced by the gas and ion nitriding, and there is less growth of nitrides on the surface. For both the liquid nitriding and the hardened steel, the observed difference in the surface appearance of the wear scar compared to the virgin surface is due to the smoothening of the grooves left from the machining of the specimens.

The surface morphology of the plates was studied with the DEKTAK stylus profiler. Traces of the wear scars on the plates for the various surface treatments are given in Fig. 4.10. The average depths of the wear scars shown in the figure correspond to those given in Table 4.2.

4.4.3 Wear Rate on the Pin Surface

Records of the friction coefficient throughout the test showed that it was higher at the beginning of the test and then gradually decreased to a steady-state value. The characteristic decrease in the friction coefficient in the beginning was an indication of a transition period, during which the wear rate might be higher as well. A typical record of the friction coefficient for a ten-hour-long tests is given in Fig. 4.11.

The globular appearance of the surface for most of the surface treatments also suggested that the wear rate on the pin may be relatively high during the run-in period when an initial smoothening of the surface asperities takes place, and decrease substantially after this period. In order to verify this hypothesis, tests were conducted where the wear scar was periodically measured by stopping the test. The intervals between the measurements were gradually increased. The first measurement was taken after only 15 minutes of testing. The following measurements were taken in intervals of one hour, five hours, and ten hours, respectively. The surface treatments tested were ion nitriding, liquid nitriding, boronizing and hardened steel. The gas nitriding was not tested because of the cracking in the hard layer. The TiN coating was not tested as well, because no measurable wear could be obtained in the first three runs. All tests were conducted at 150,000 psi contact pressure and in R134a-polyolester oil mixture. Data from this set of tests are given in Table 4.5.

The friction coefficient shown in the table follows the general trend of constant decrease throughout the test. The fastest decrease occurs in the first hour and the curve levels off thereafter, as shown in Fig. 4.11.

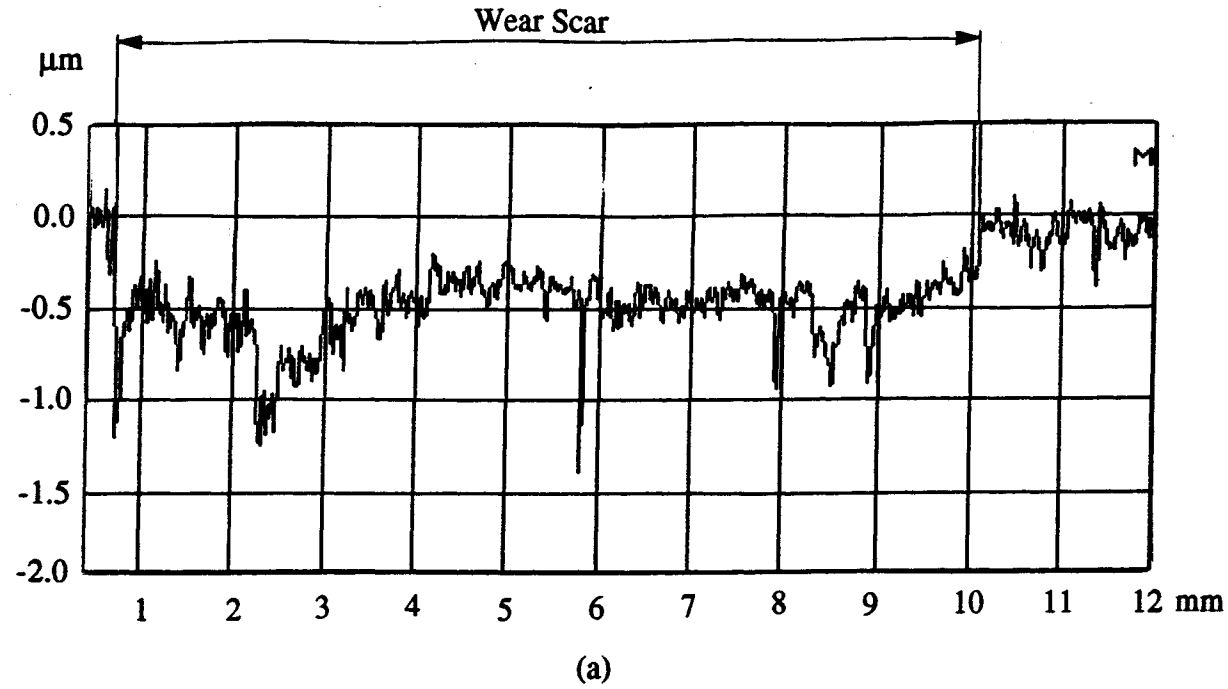

(a)

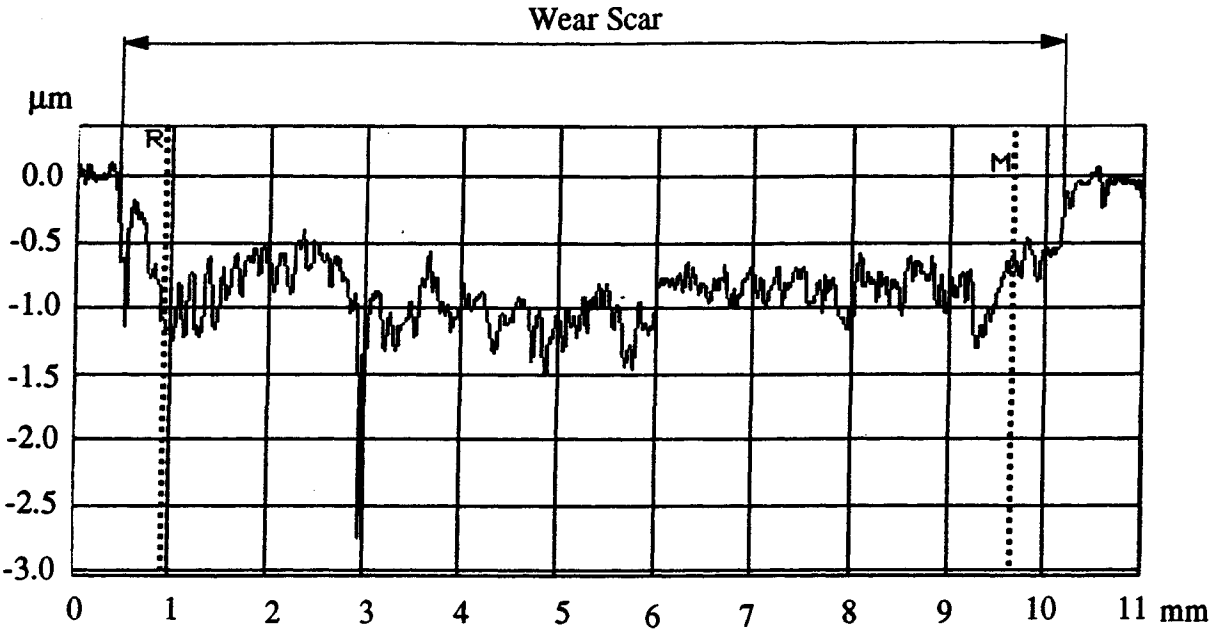

(b)

Fig. 4.10 - Wear Scar on the Grey Cast Iron Plates Tested in R134a-Polyolester Oil Mixture. (a) Tested Against Gas Nitrided Pin (b) Tested Against Ion Nitrided Pin Contact Pressure = 200 kpsi. Test Duration = 10 hours

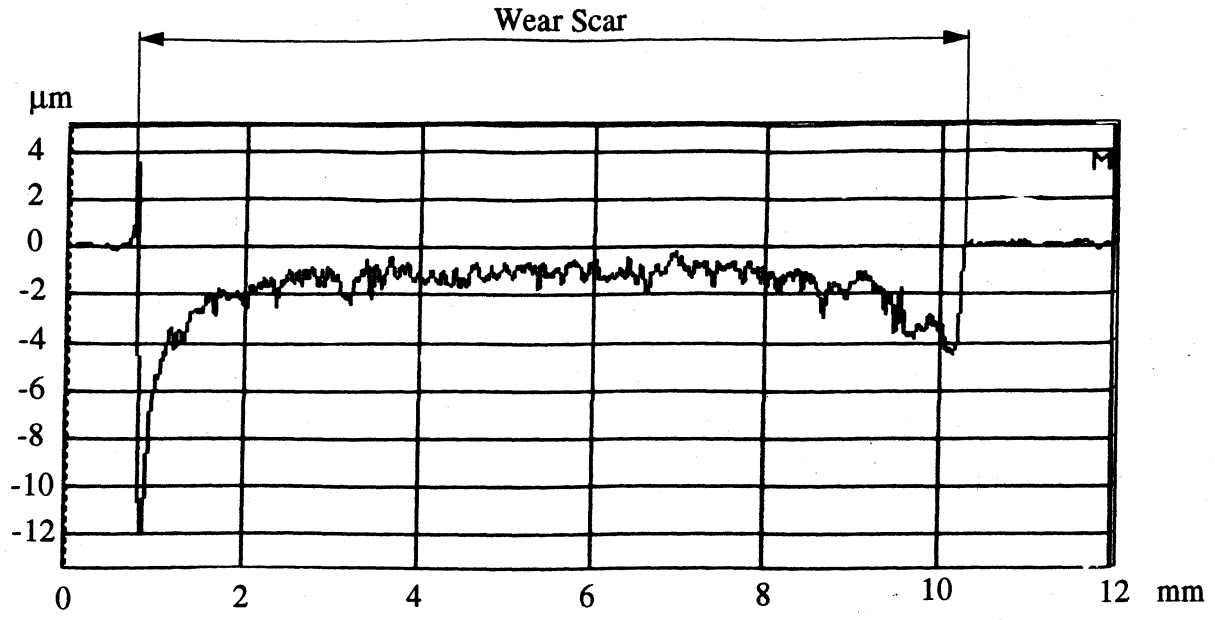

(c)

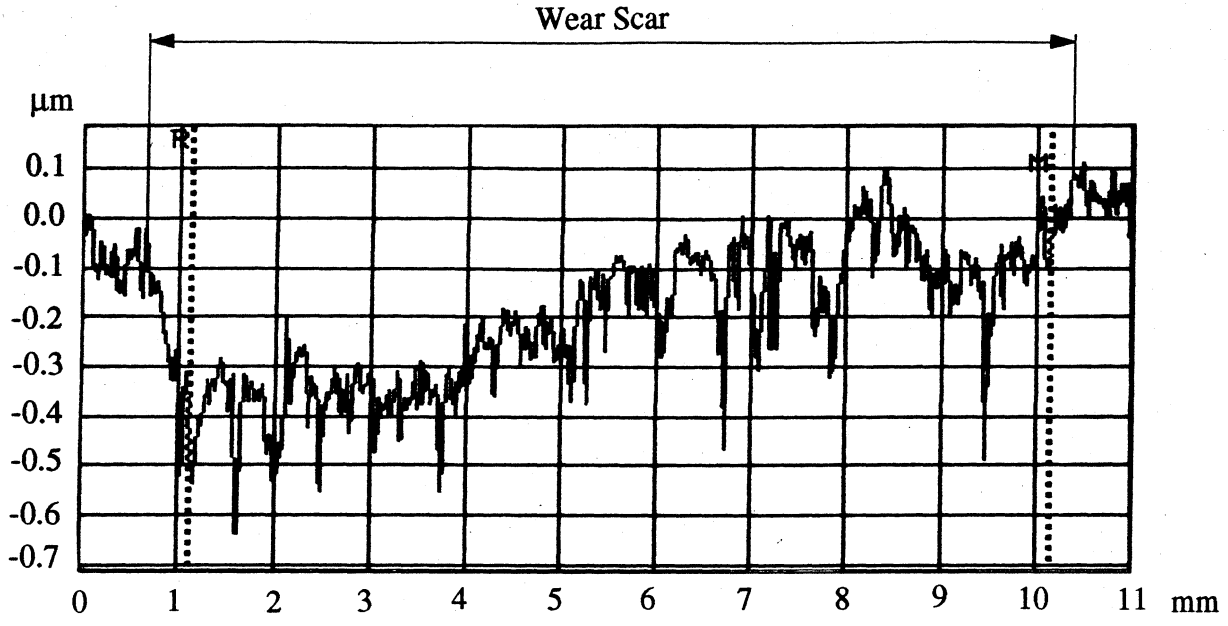

(d)

Fig. 4.10 (cont.) - Wear Scars on the Gray Cast Iron Plates Tested in R134a-Polyolester Oil Mixture. (c) Tested Against TiN Coated Pin (d) Tested Against Boronized Pin Contact Pressure = 200 ksi. Test Duration = 10 hours

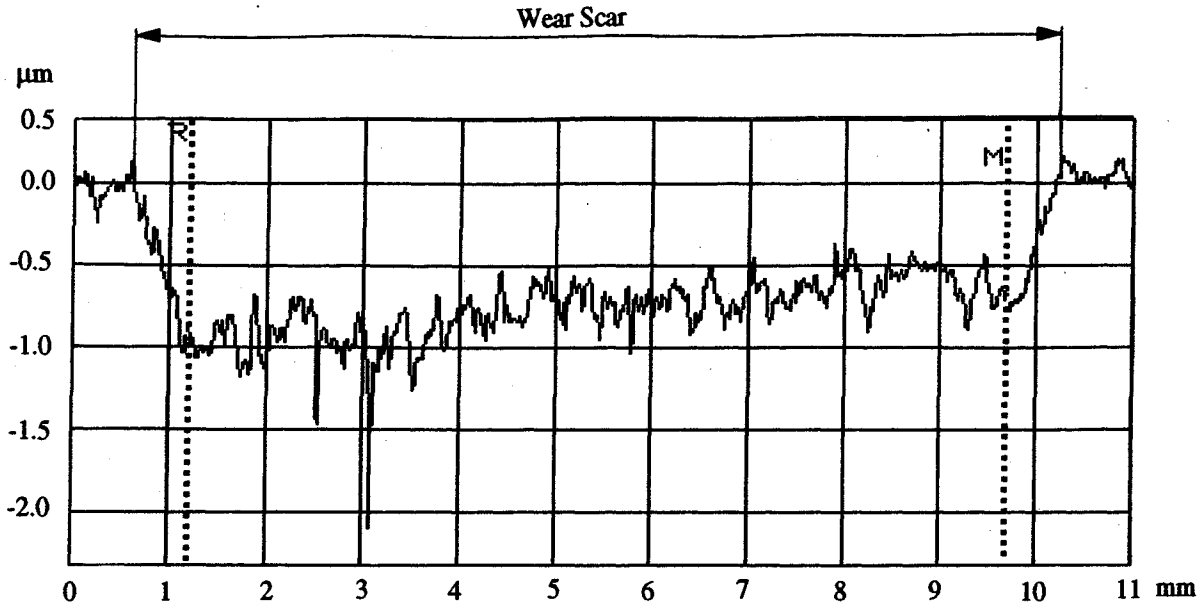

(e)

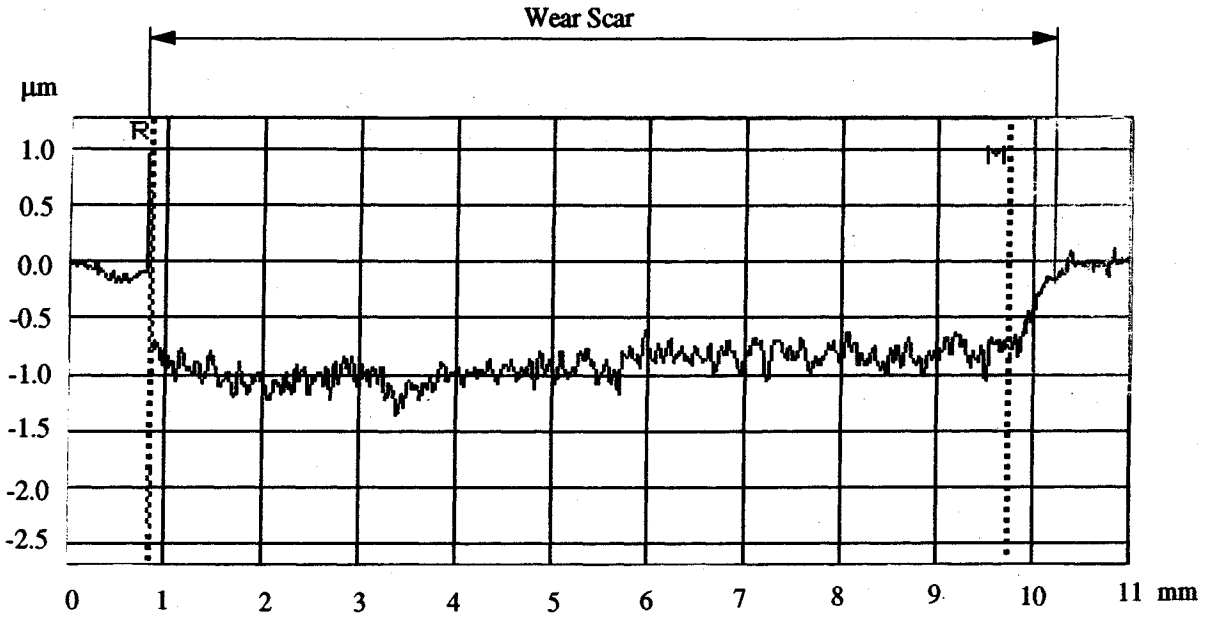

(f)

Fig. 4.10 (cont.) - Wear Scars on the Gray Cast Iron Plates Tested in R134a-Polyolester Oil Mixture. (e) Tested Against Liquid Nitrided Pin (f) Tested Against Hardened Pin Contact Pressure = 200 ksi. Test Duration = 10 hours

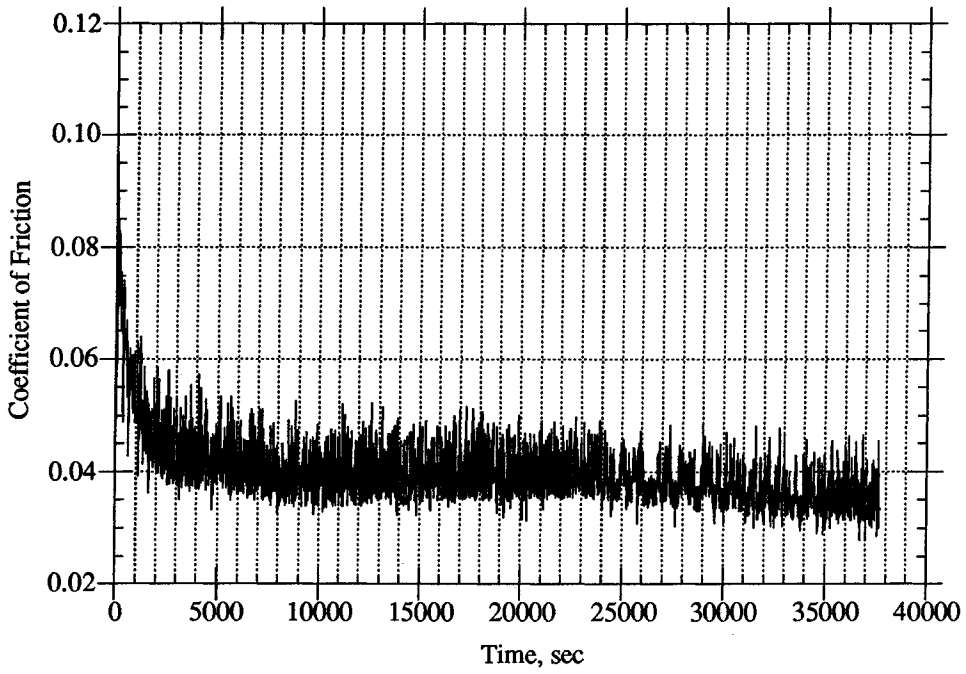

Fig. 4.11 - Typical Record of the Coefficient of Friction in R134a-Polyolester Oil Mixture. Boronized Pin. Contact Pressure = 200 ksi. Test Duration = 10 hours.

Table 4.5 - Change of Friction and Wear with Time for Various Surface Treatments

Surface Treatment	Parameter	Time From the Beginning of Test When Measurements Were Taken, min.			
		15	75	375	975
Liquid Nitriding	Wear Scar Width, mm	0.133	0.205	0.238	0.269
	Volume Worn, 10^{-3} mm^3	0.583	2.16	3.37	4.87
	Ave. Friction Coefficient	0.089	0.069	0.055	0.044
Ion Nitriding	Wear Scar Width, mm	0.148	0.174	0.211	0.273
	Volume Worn, 10^{-3} mm^3	0.814	1.32	2.34	5.09
	Ave. Friction Coefficient	0.084	0.060	0.054	0.046
Boronizing	Wear Scar Width, mm	0.172	0.222	0.265	0.328
	Volume Worn, 10^{-3} mm^3	1.26	2.75	4.67	8.80
	Ave. Friction Coefficient	0.073	0.047	0.046	0.043
Hardened	Wear Scar Width, mm	0.156	0.183	0.203	0.273
	Volume Worn, 10^{-3} mm^3	0.949	1.54	2.09	5.09
	Ave. Friction Coefficient	0.068	0.059	0.056	0.045

Plots showing the width of the wear scar and volume worn with time are given in Fig. 4.12 and Fig. 4.13, respectively. From the figures, it is evident that steady-state wear rates are achieved after about one hour. After this initial run-in period, the wear rates remain constant for all the surface treatments. In these tests, the boronizing showed the largest initial wear rate. The wear rates for all the surface treatments tested were approximately the same after the first hour. Thus, the hypothesis that the difference in the total wear rate is primarily due to the first hour of sliding was correct.

4.4.4 Effect of the Environment

All the results discussed above were obtained by testing the various surface treatments in a R134a-polyolester oil mixture. For comparison purposes, the surface treatments were also tested in the same lubricant but without the refrigerant, using air or argon as the test chamber atmosphere. The results from these tests are summarized in Table 4.6 and given in Fig. 4.14. The duration of these tests was one hour and the maximum contact pressure was 150 ksi. The TiN coating was not tested because no measurable wear could be obtained in one hour.

Results from a previous study conducted on the same contacts [1] have shown that the amount of wear for hardened pins tested in a base version of polyolester oil is approximately the same, or even slightly higher than the wear obtained with pins tested in a mixture of R134a and the same lubricant. The results given in Table 4.6 show the same trend. In the presence of air, the wear tended to increase. This increase was more pronounced for the liquid nitrided and boronized specimens, and less pronounced for the ion nitrided and hardened specimens. In order to check whether the presence of oxygen is the reason for this behavior, tests in an argon atmosphere were conducted as well. The wear on both pin and plate specimens for these tests were similar to the wear obtained in R134a environment. Thus, an oxidizing environment may be detrimental for the contact and oil under study.

The surface of the cast iron plates, for tests conducted in refrigerant and air environments, was studied as well. The appearance and the depth of the wear scar were approximately the same for the two environments. There was, however, a difference in the color of the wear scars. With plates tested in R134a or argon, the wear scar was silver in color, while the presence of air produced a yellowish wear scar, probably due to oxidation. Pictures of the wear scar on the plate, for the two environments tested, are given in Fig. 4.15.

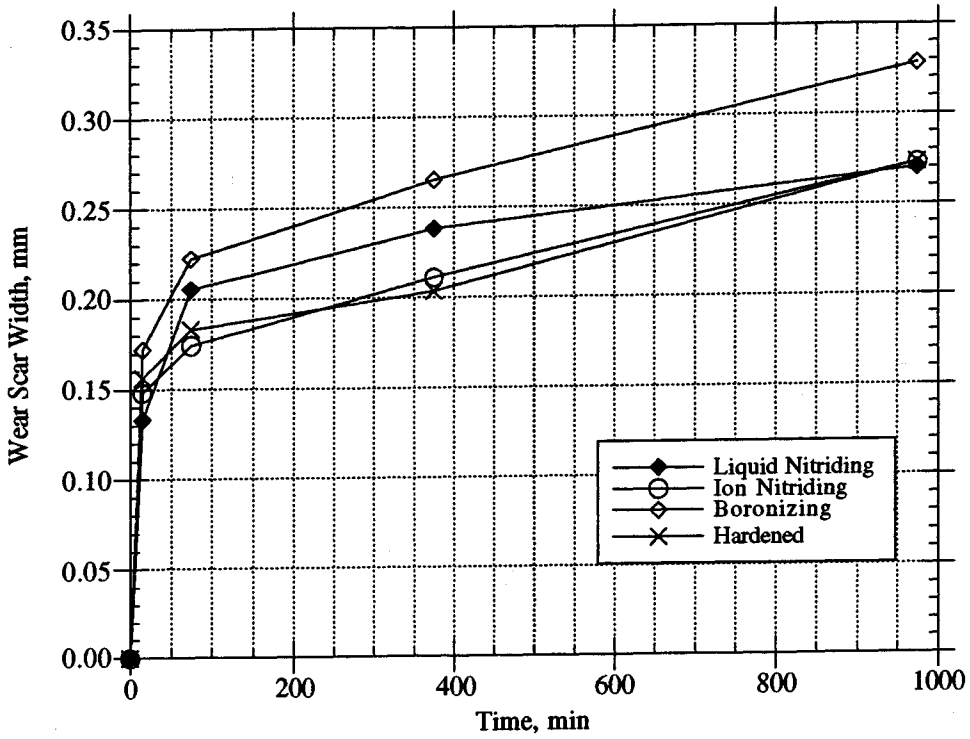

Fig. 4.12 - Pin Wear Scar Width as a Function of Time for Various Surface Treatments

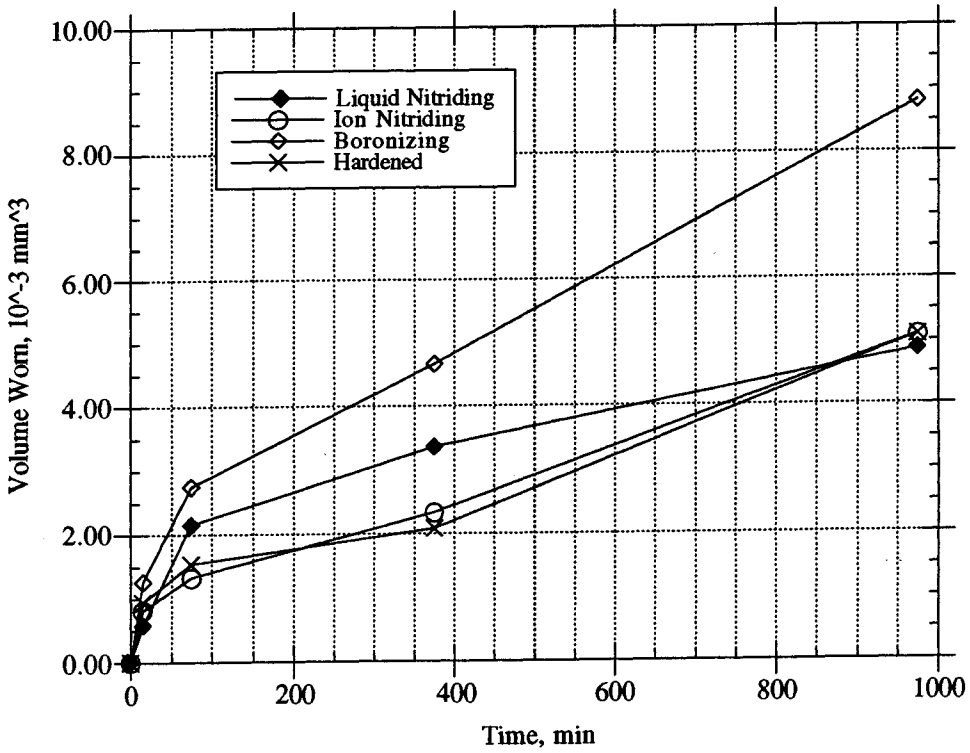

Fig. 4.13 - Pin Volume Worn as a Function of Time for Various Surface Treatments

Table 4.6 - Effect of Test Environment on Pin Wear for Various Surface Treatments

Surface Treatment	Pin Wear Scar Width, mm		
	R134a + Base Polyolester Oil	Air + Base Polyolester Oil	Argon + Base Polyolester Oil
Liquid Nitriding	0.205	0.273	0.215
Ion Nitriding	0.174	0.172	---
Boronizing	0.222	0.312	0.218
Hardened	0.183	0.187	---

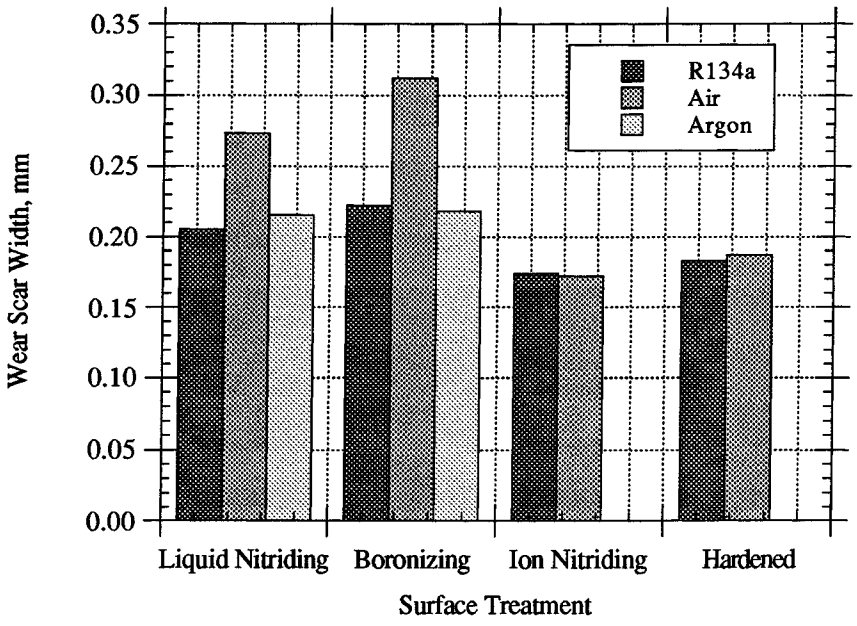

Fig. 4.14 - Effect of Test Environment on Pin Wear for Various Surface Treatments

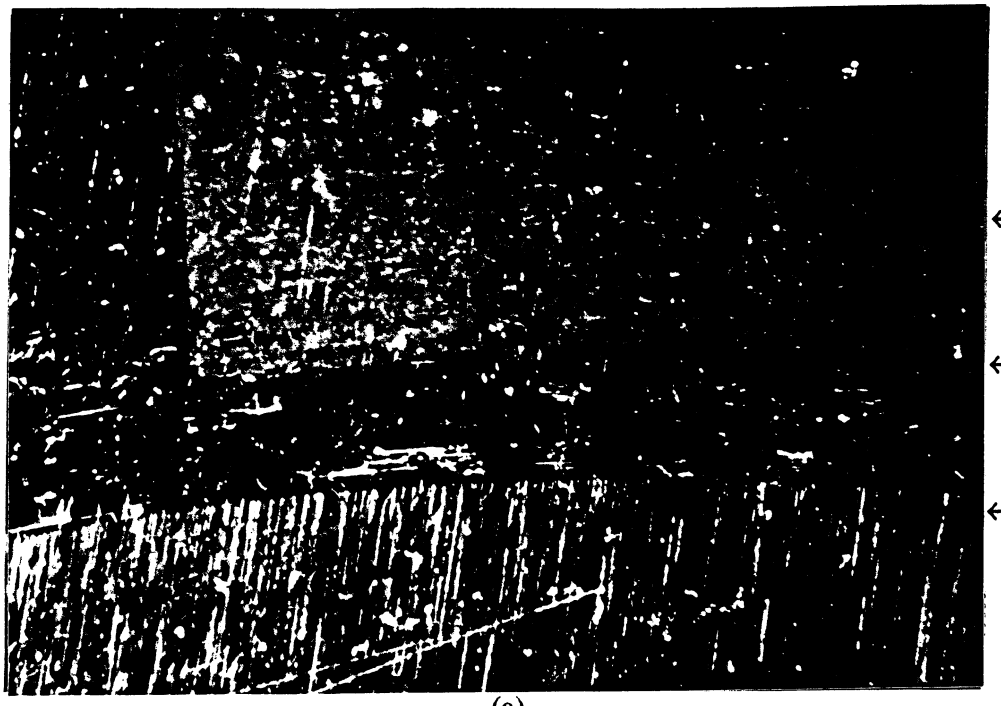

(a)

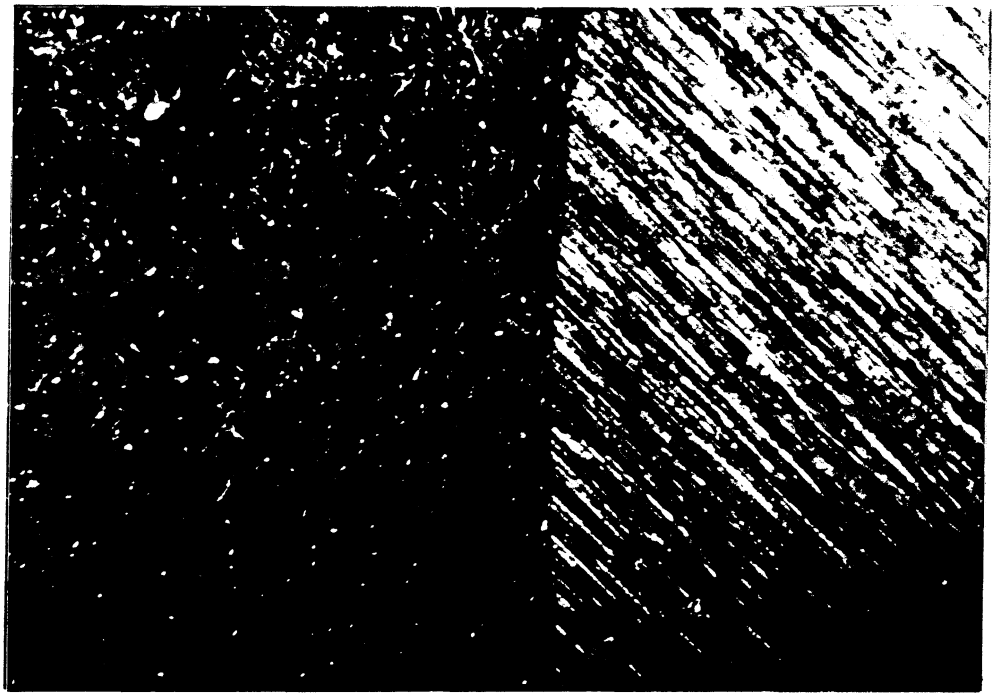

(b)

Fig. 4.15 - Wear Scars on the Gray Cast Iron Plates Tested in different Environments. (a) Virgin Surface at the Bottom of the Picture, (b) Virgin Surafce at the Right of the picture. Contact Pressure = 150 ksi. Test Duration = 1 hour. Pin Surface Treatment: Liquid Nitriding. Lubricant: Polyolester Oil.

4.5 Summary of the Results

The results from the friction and wear tests conducted on various M2 tool steel surface treatments can be summarized as follows:

• The diffusion processes, namely the liquid nitriding, ion nitriding, and boronizing do not seem to offer any tribological advantages over hardened M2 tool steel under the conditions studied.

• The gas nitriding process, regardless of the case thickness, is not suitable for M2 steel because it produces a very brittle case, which cracks and chips-off under concentrated load.

• The TiN coating deposited by a CVD process provides an order of magnitude lower wear than the other surface treatments considered.

• Coefficient of friction and wear depth on the mating surface is higher with the TiN coating than with the other surface treatments. This is due to the presence of very hard asperities with sharp edges on the surface of the coated specimen which abrade the mating surface. A CVD or PVD process which provides a smooth surface should be used for better friction and wear results.

• Heat treatment in an inert atmosphere should be performed after the boronizing process, if any improvement of the wear resistance is desired.

• When a base version of polyolester oil is used as a lubricant, the wear of both mating surfaces is lower in an R134a refrigerant environment than in air.

4.6 References

1. **Davis B., and Cusano C.**, The Tribological Evaluation of Compressor Contacts Lubricated by Oil-Refrigerant Mixtures, ACRC TR-19, May 1992.

2. **Sato S., Komine K., and Machida T.**, Breaking-in Mechanism of the sliding Surface in a Hermetic Rotary Compressor Employing an Ion-Nitrided Crankshaft, Proceedings of the 1992 International Compressor Engineering Conference at Purdue, ed. Hamilton J., Vol. II, 1992, pp. 489-496.

3. **ASM International**, ASM Handbook. Tenth Edition, Vol. 4: Surface Treatments.

4. **Budinski K. G.** Surface Treatments for Wear Resistance, Reston Publishing Co. Inc., Reston, 1979.

5. **Hoyle G.**, High Speed Steels, Butterworth & Co. Ltd., London, 1988.

6. **Palmer F. R., and Luerssen G. V.**, Tool Steel Simplified, The Carpenter Steel Co., Atlanta, 1960.

7 **Roberts G. A., and Cary R. A.**, Tool Steels, American Society for Metals, 1980.

8 **Wilson R.**, Metallurgy and Heat Treatment of Tool Steels, McGraw-Hill Book Co. Ltd., London, 1975

9. **ASM International**, ASM Handbook. Tenth Edition, Vol. 1: Properties and Selection: Irons, Steels, and High Performance Alloys.

10. **Child H. C.**, Effect of Thermo Chemical Treatments on the Mechanical Properties of Tool Steel, *Materials and Design*, 1983 **4** (1), pp. 716-723.

11. **Habig K. H., and Chatterjee-Fischert**, Wear Behaviour of Boride Layers on Allowed Steels, *Tribology International,* 1981, **14** (4), pp. 209-215.

CHAPTER 5

Data Acquisition

Friction and wear tests are usually characterized by a considerable variation of the friction coefficient throughout the test. Change in the wear rate is also possible. There are also a number of other factors that influence the tribological processes at the interface. Some of the most easily measurable of these factors include: temperature, load, sliding velocity and type of motion. To monitor all these parameters a complex data acquisition and control system is necessary.

5.1 Hardware

The hardware that was used in this study for data acquisition and control consists of a microprocessor controlled tribometer, a data acquisition and control board, a computer, and some auxiliary devices such as limit switches, a safety control board, and cable connections. The computer and the data acquisition board serve two different tribometers: a high pressure tribometer (used in this study) and a high temperature tribometer. The computer and the board can serve other test facilities as well, such as oscilloscopes, motor control boards, etc.

5.1.1 Tribometer

The tribometer used in this study is a complex test facility. It is capable of providing a wide range of contact loads (5 to 1000 lbf), angular velocities (0 to 2000 rpm), environmental temperatures (10 to 275 °F), and environmental pressures (50 μm vacuum to 250 psig). Either constant or oscillatory loads and velocities with variable wave form, amplitude and frequency can be applied. Test temperatures can also be controlled with a system of heaters and circulating fluids. A complete description of the high pressure tribometer is given by Davis [1, 2].

All tribometer functions are controlled by a microprocessor. It monitors all test parameters and maintains the conditions of the test in the preset desirable ranges. These conditions can be either manually set on the tribometer control panel, or externally set via a computer controlled board.

The tribometer output is directed to three different devices. The first is the tribometer LCD display where current values of all test parameters are displayed. The second is a standard 25 pin serial RS-232 input/output port, and the third one is a high level electrical output for all important variables. The data acquisition and control system is still

under development. The work on the data acquisition part of the system has been already completed. The data acquisition board reads signals from tribometers high level output connector. The computer control of the tribometer microprocessor is still under development. For this purpose, a standard RS-232 port will be used. At present, all test conditions are set manually from the tribometers keyboard.

The variables read from the tribometers output port are the axial and frictional forces, the frictional torque, and four temperature signals (taken at different locations).

5.1.2 Data Acquisition Board

The board used for data acquisition is the National Instruments AT-MIO-16F-5. It is a high-performance multifunction analog, digital and timing input/output (I/O) board for the PC. The AT-MIO-16F-5 has a 5 μsec, 12-bit sampling analog to digital converter (ADC), 16 single-ended or 8 differential channels, programmable gains of 0.5, 1, 2, 5, 10, 20, 50, and 100, a guaranteed maximum rate of at least 200 ksamples/sec, 8 digital I/O lines able to sink up to 24 mA of current, capability for waveform generation, two analog output channels, and internal timer.

5.1.3 Board Configuration

The board configuration used is the same as the factory setting, i.e. a base I/O address of 220 hex, DMA Channel 6 and Channel 7, and interrupt level 10. Hence no changes to the positions of the jumpers A5 through A9 on the board have been made. If an additional board or some other hardware device is connected to the computer in the future, changes, in the board configuration may be necessary. More information on the base address selection and board hardware configuration is given in AT-MIO-16F-5 User Manual [3].

5.1.4 Analog Input Configuration

The analog input section of the AT-MIO-16F-5 is fully software-configurable. The analog input configuration depends on the particular application. The proper input mode, polarity, and input range have to be chosen for each input signal in order to provide safe and accurate operation of the board. Each of the analog input categories are described in more detail below.

5.1.4.1 Input Mode

The AT-MIO-16F-5 offers three different input modes: non-referenced single-ended (NRSE) input, referenced single-ended (RSE) input, and differential (DIFF) input. The

single-ended input configuration uses 16 channels. The DIFF input configuration uses 8 channels. Both the RSE and the DIFF modes are used for data acquisition from the tribometer. RSE allows greater number of channels (16) and is the mode that is used when both the high pressure and high temperature tribometers are connected to the board. The signals in this case are more susceptible to external noise and allow lower accuracy of the readings. If less than nine channels are necessary, then the DIFF mode will produce the best results. Software for both modes have been developed. In addition to using different software with the different modes, choosing a particular mode leads to changes in the input channel connections as well. The input modes are described in Table 5.1.

Table 5.1 - Input Mode Configurations Available for the AT-MIO-16F-5

Configuration	Description
DIFF	Differential configuration. Provides 8 differential inputs with the negative (-) input of the instrumentation amplifier tied to the multiplexer output of Channels 8 through 15.
RSE	Referenced Single-Ended configuration. Provides 16 single-ended inputs with the negative (-) input of the instrumentation amplifier referenced to analog ground
NRSE	Non-Referenced Single-Ended configuration. Provides 16 single-ended inputs with the negative (-) input of the instrumentation amplifier tied to AISENSE connector (see Fig. 5.2) and *not* connected to ground

The input mode selected depends on the type of signal source. The differential mode should always be used if the signal to noise ratio is low, or when the connecting cable exceeds 15 ft. It is also preferred in all cases when the number of input channels is less than nine. When both tribometers are connected, 16 input channels are necessary. Therefore, a RSE single-ended mode was chosen as the normal operating mode for the board. The differential mode was used only to verify the accuracy of the input signals in RSE mode.

In the AT-MIO-16F-5 User Manual, the NRSE mode is recommended for the case when the board and the signal generating device (the tribometer in this case) share the same building power supply mains, or the same ground reference. Therefore, this was the mode that was tried first. The readings on the computer display (i.e. the signals acquired by the

board) in this mode were off by almost a volt. This condition was unacceptable because it would lead to errors of about 20% on the average. The reason for these inaccurate readings was due to a ground voltage difference between the power outlet used for the computer and the one used for the tribometer. Hence the RSE mode was chosen even though it is recommended only for isolated signal sources. The readings with this mode of operation were correct. To verify the accuracy, the same signals were read with a DIFF input mode. The readings were essentially the same. The only difference was the greater amount of noise in the RSE compared to the DIFF mode. This noise, however did not pose any problems for the data processing and interpretation. Most of this noise, as it was found later, was intrinsic to the tribometer output signals and had nothing to do with the input mode.

5.1.4.2 Input Polarity and Input Range

The AT-MIO-16F-5 has two polarities: unipolar input and bipolar input. Unipolar input means that the input voltage range is between 0 and V_{ref} where V_{ref} is some positive reference voltage. Bipolar input means that the input voltage range is between $-V_{ref}$ and $+V_{ref}$. The tribometer output has signals that are both unipolar and bipolar. Temperature signals for example are unipolar, while forces torque and positions are bipolar. Since only one of these modes can be active for a particular data acquisition setting, the bipolar input was chosen for the analog input configuration.

The AT-MIO-16F-5 has one input range of 10 V. An input range of 20 V is achieved by using the gain of 0.5. Software-programmable gain on the AT-MIO-16F-5 increases overall flexibility by matching input signal ranges to those accommodated by the analog to digital converter (ADC) of the board. The AT-MIO-16F-5 has gains of 0.5, 1, 2, 5, 10, 20, 50, and 100, and is well suited to a wide variety of signal levels. With the proper gain setting, the full resolution of the ADC can be used to measure the input signal. A schematics of the AT-MIO-16F-5 instrumentation amplifier is given in Fig. 5.1. The overall input range and precision, depending on the polarity and gain chosen are given in Table 5.2.

Gain of 0.5 is used for the force and torque signals, and gain of 1.0 is used for the temperature signals. The default gain setting in the software program is 0.5 in order to protect the board from damage. The board gains are independent from the gains on the tribometer amplifier. They are, however, related.

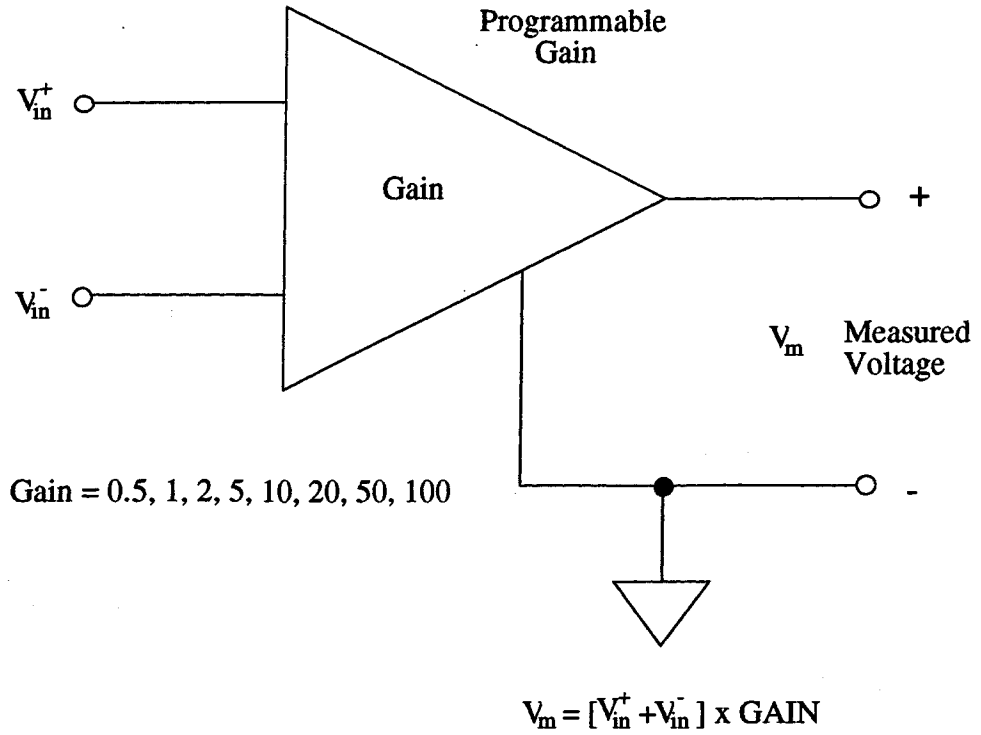

Fig. 5.1 - AT-MIO-16F-5 Instrumentation Amplifier

Table 5.2 - Actual Range and Measurement Precision With the Polarity and Gain Chosen

Range / Polarity	Gain	Actual Input Range	Precision
0 to +10 V	0.5	0 to +20.0 V†	4.88 mV
Unipolar	1.0	0 to +10.0 V	2.44 mV
	2.0	0 to +5.0 V	1.22 mV
	5.0	0 to +2.0 V	488.00 µV
	10.0	0 to +1.0 V	244.00 µV
	20.0	0 to +0.5 V	122.00 µV
	50.0	0 to +0.2 V	48.80 µV
	100.0	0 to + 100 mV	24.40 µV
-5 to +5 V	0.5	-10.00 to +10.00 V	4.88 mV
Bipolar	1.0	-5.00 to +5.00 V	2.44 mV
	2.0	-2.50 to +2.50 V	1.22 mV
	5.0	-1.00 to +1.00 V	488.00 µV
	10.0	-0.50 to +0.50 V	244.00 µV
	20.0	-0.25 to +0.25 V	122.00 µV
	50.0	-100 to +100 mV	48.80 µV
	100.0	-50 to +50 mV	24.40 µV

† 0 to +20 V is the effective range. Signals greater than +12 V will saturate the internal components and result in inaccurate data

If a small gain is selected on the tribometer amplifier, then the output signal will be higher, and lower gain on the board should be selected as well. Adjusting both gains can produce the maximum possible accuracy. It is not desirable, however, to constantly change the board gains, because in case of an error the board may be damaged. Therefore, the board gain settings were fixed and were kept the same for all amplifier output signals.

5.1.4.3 Signal Connections

The AT-MIO-16F-5 I/O connector is shown in Fig. 5.2. It is a 50 pin connector. Pins 1 and 2 are the grounds for the analog input signals. Pins 3 through 18 are assigned to the 16 analog input channels. The channel numbers do not correspond to the pin numbers. The correspondence between the channel and the pin numbers is given in Table 5.3

Table 5.3 - Channel Numbers and Their Corresponding Pin Numbers on the I/O Connector

Channel	0	1	2	3	4	5	6	7	8	9	10	11	12	13	14	15
Pin	3	5	7	9	11	13	15	17	4	6	8	10	12	14	16	18

Pin 19 is designated as AISENSE, and is used instead of pins 1 and 2 with the NRSE mode. Pins 25 through 32 are the digital I/O channels and pins 24, and 33 are the digital grounds, respectively. For these data acquisition arrangement, pins 25 through 33 are used to control the overload relays. The rest of the pins are not used. It is possible that some connections may be made when the control system is completed.

The analog input signals are led through two separate cables to the output ports of the high temperature and high pressure tribometers. At the side of the tribometers, the cables are connected to 25-pin connectors, and at the board ends to 9-pin connectors. Pin numbers for both the 25-pin and 9-pin connectors are given in Fig. 5.2.

5.1.5 Overload Relays

The overload relays protect the tribometer from damage in case of an overload. The axial force, the frictional forces, and the torque on the motor are continuously monitored throughout the test. If any of these variables exceeds some preset value, a signal is generated by the computer. This signal is then sent through the AT-MIO-16F-5 digital I/O port to the overload relays. The latter are activated and the tribometers motors for the load and the rotation are turned off. Two of the relays control the two motors while the other two control the heaters. The heaters will be turned off if certain temperature levels are exceeded.

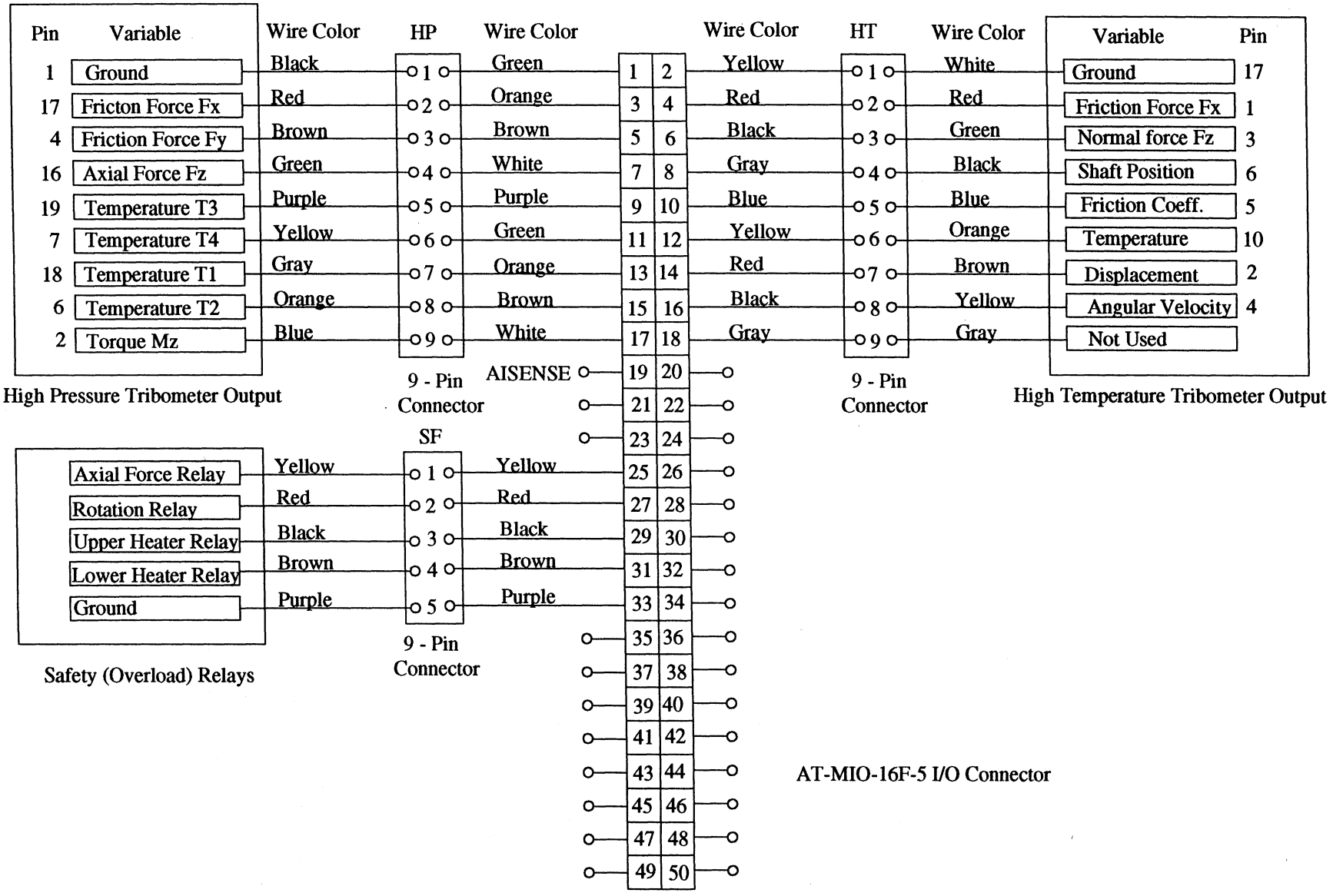

Fig. 5.2 - Signal Connections

The relays are 6311 buffered, non-inverting type with a standard TTL input that can be directly connected to the AT-MIO-16F-5 I/O digital port without any signal amplification. The relays can control circuits of up to 3.5 A and 60 V DC. A schematic of a 6311 relay is given in Fig. 5.3

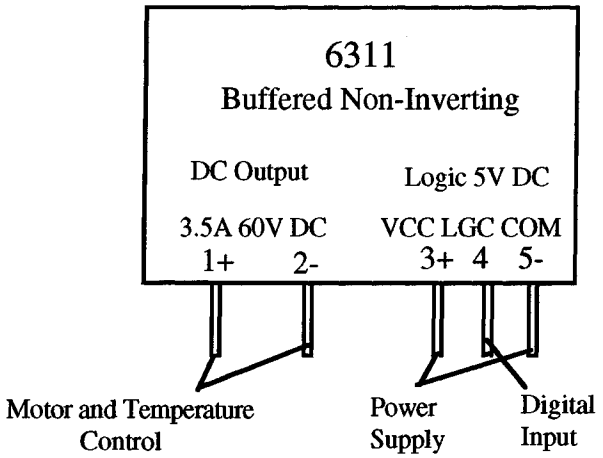

Fig. 5.3 - Schematics of a 6311 Relay

These relays can also be used for motion control. The selection between unidirectional or oscillatory motion, direction of travel, mode of operation, and other modes that require digital control can be performed by installing more relays. For force and speed control, an analogous output signal is required. The AT-MIO-16F-5 has a capability for two channel analogous output. The analog output, however, is a low power signal, and cannot be directly used for motor control. A signal amplifier is necessary.

5.2 Software

5.2.1 The LabWindows Environment

The data acquisition software was developed in the National Instruments LabWindows Environment. LabWindows is a set of software tools for developing, instrumentating, testing, and data acquisition applications in Microsoft C, QuickC, BASIC, or QuickBASIC. LabWindows components are listed below:

- Standard libraries for GPIB and RS-232 communication, file I/O, data formatting, data analysis and graphics.
- A standard library for displaying and controlling a graphical user interface.
- A library of functions for National Instruments plug-in data acquisition boards.

• A set of instrument drivers containing high-level functions for controlling specific instruments.

• An interactive development program.

• An interactive utility for compiling and linking of program applications.

• VXI and an Advanced Analysis Libraries.

It is possible to develop applications both inside and outside the LabWindows interactive development program. The data acquisition program that was used for this study was developed in QuickC and entirely within the LabWindows interactive program. Then it was compiled and linked, using a QuickC compiler and linker, in order to produce a stand-alone directly executable program. More information about the LabWindows environment is given in the National Instruments LabWindows Manuals [4].

5.2.2 Data Acquisition Program

The data acquisition system for obtaining and processing tribological data has several important features:

1. Independent data acquisition from both tribometers that are connected to the AT-MIO-16F-5 board.

Tests on either tribometer can start, stop, and reset independently at the same time. The data acquisition rate is kept constant and equal to the maximum that the board can accommodate. When one of the tribometers is not used, the program automatically recalculates the number of data points acquired per channel such that optimal data acquisition rates and data processing speeds are maintained.

2. Various data acquisition rates.

Three data acquisition rates are used for the different input signals. Signals that do not change fast with time are scanned less frequently than the fast changing signals. The data acquisition rates for various tribometers' signals are given in Table 5.4.

3. Real time display of tribological data.

Friction coefficient, temperatures, friction and axial forces are continuously displayed in the form of a strip chart on the computer screen. The points displayed on the screen are the average values of all the points acquired in one second. Thus, new points are added to the strip chart every second. Every strip chart is automatically scrolled when the whole visible part of the chart is filled. The number of points simultaneously visible on the screen can be adjusted depending on the test duration. The y-axes (various scales are used for the different variables) scales can be changed as well. These adjustments are possible at any time, even when a data acquisition is in progress.

In addition to the real time chart records, the program displays on the screen the time elapsed since the start of the test, average values of certain variables from the beginning of the test, and some other relevant information such as data acquisition error conditions, overload conditions, and numeric values for all variables plotted on the strip charts.

Table 5.4 - Data Acquisition Rates for Various Signals

Data Acquisition Rate	Channels	Variables
Fast Rate 500 points per second per channel	0	Normal Force Fx (HP)
	1	Friction Force Fy (HP)
	2	Friction Force Fz (HP)
	7	Friction Torque Mz (HP)
	8	Normal Force Fx (HT)
	9	Friction Force Fx (HT)
Medium Rate 300 points per second per channel	10	Shaft Position (HT)
	11	Friction Coeff. (HT)
	14	Angular Velocity (HT)
Slow Rate 1 point per second per channel	3	Temperature T3 (HP)
	4	Temperature T4 (HP)
	5	Temperature T1 (HP)
	6	Temperature T2 (HP)
	12	Temperature (HT)
	13	Vertical Displacement (HT)
HP = High Pressure Tribometer; HT = High Temperature Tribometer		

4. Double buffered data acquisition.

The data acquisition process is continuously running in the background while at the same time, data processing, error and interrupt checking and display of data on the screen run in the foreground. With the double buffered data acquisition system much faster data acquisition is achieved.

5. Data Processing

With the data acquisition rates given above, a large number of data points are generated throughout the test. Most of the tests are from one to three hours long. Some longer tests, with durations up to 24 hours, have been conducted as well. It is impossible and probably useless to record and save all these data points. Therefore, all data point

acquired in one second are averaged and only the average value is recorded. The averaging process, depending on the number of points acquired per channel per second, may take a longer time than the data acquisition process. If this is the case, the program automatically adjusts the data acquisition rate such that both processes take approximately the same time. In addition to the averaging, conversion of voltages to engineering units and scaling of the data are performed.

By averaging, possible important information between averaged points is lost. If such information is required, some modifications to the program have to be made. Such modifications are currently in progress.

6. Data Recording

The computer program saves all the average values of the variables to a file. This process runs continuously in the foreground, and therefore, should be as fast as possible. Hence, data are written to a temporary binary file. When the test is over, the program automatically translates the binary file into a text file, and saves it under the same name as the test ID number with the extension .dat. This file can further be read by any text editor, spreadsheet program, or processed in some other way.

7. Hard Copies

The program has its own module for producing a hard copy of the data records. This module loads the desired text file and produces a graphical display on the screen. This plot can be printed on the attached printer, or plotter. The hard copy module is disabled while data acquisition is in progress.

8. Control and Safety Features

Forces, torques, and temperatures are constantly monitored. If some of these variables exceeds a preset limit, a special safety module will be activated. This module will generate an output signal which will be sent to the safety relays. The same module can be used to stop a test after a certain period of time.

The program is divided in several modules. Each of these is structured as a separate function (subroutine), and is independent of the other modules. These program modules are:

- Data acquisition module. Acquires, processes, plots, and saves data to a binary file. This is the major program module. It is divided into several sub modules which take care of the separate processes listed above.
- Setup module. Sets gains, scales, scanning rates, and assigns channels to variables. There are two such modules, one for the high pressure and the other for the high temperature tribometers.
- Hard copy module. Reads data from a text file and produces a hard copy.

• Translation module. Converts binary to text files.

• Stand-by module. Acquires data and displays mean numerical values on the screen It does not plot, or process data. Low data acquisition rate is only used in this module. It is active when the data acquisition module is not active. It is used to provide information for the initial settings, and to check the data acquisition before the test.

• Main program module. This is the body of the main program. All other modules are called as functions from this module. It controls the starts, stops and resets of the data acquisition module.

Each of these modules can be directly transferred and used in another program, if necessary. They do not share a common block of global variables, and, therefore, are to a great extend, autonomous program blocks.

5.3 References

1. **Davis B., Sheiretov T., and Cusano C.**, Tribological Evaluation of Contacts Lubricated by Oil-Refrigerant Mixtures, Proceedings of the 1992 International Compressor Engineering Conference at Purdue, ed. **Hamilton J.**, Vol. II, Purdue University, West Lafayette, IN, USA, 1992, pp. 477-487

2. **Davis B., and Cusano C.**, The Tribological Evaluation of Compressor Contacts Lubricated by Oil-Refrigerant Mixtures, ACRC-TR-19, May, 1992.

3. **National Instruments**, AT-MIO-16F-5 User Manual, April 1991.

4. **National Instruments**, LabWindows User Manual, April 1991.